

Diagnostic Imaging, Interventional Treatment of Brainstem Lesions and Electrophysiologic Diagnostics

2

Contents

2.1	Neuroradiology	38	2.3.2.3	Interpretation of Findings	68
2.1.1	Conventional Native Diagnostics	38	2.3.2.4	Conclusion	69
2.1.2	Computed Tomography	39	2.3.3	Early Acoustic Evoked Potentials	70
2.1.2.1	Principles and Techniques	39	2.3.3.1	Anatomic and Physiologic Principles	70
2.1.2.2	CT in Investigations of the Brainstem	39	2.3.3.2	Application	70
2.1.2.3	Risks	40		Stimulation	70
2.1.3	Magnetic Resonance Imaging	40		Recording	71
2.1.3.1	Principles and Techniques	40	2.3.3.3	Physiologic Variability of EAEP and	
2.1.3.2	MRI Investigations of the Brainstem	42		Abnormal Findings	71
2.1.3.3	Specialized Methods	45	2.3.3.4	Evaluation	71
2.1.3.4	Risks	46		Central Lesions	72
2.1.4	Angiography and Endovascular Interventions	47		Multiple Sclerosis	72
2.1.4.1	Diagnostic Angiography	47		Brainstem Ischemia/Bleeding	74
2.1.4.2	Endovascular Interventions	49		Brain Death	74
	Recanalization	49	2.3.4	Vestibulocollic Reflex	75
	Embolization	51	2.3.4.1	Anatomic and Physiologic Principles	75
			2.3.4.2	Application	75
2.2	Ultrasound Diagnostics	54	2.3.4.3	Evaluation and Reference Values	75
2.2.1	Vascular Ultrasound	54	2.3.4.4	Interpretation	76
2.2.1.1	Anatomic Principles	54	2.3.5	Exteroceptive Suppression of Masticatory	
2.2.1.2	Principles and Techniques	54		Muscle Activity	76
	Continuous Wave (cw) Doppler	54	2.3.5.1	Anatomic and Physiologic Principles	76
	Pulsed Doppler Sonography			Afferences of Exteroceptive Suppression	76
	(Pulsed Wave Doppler, pw Doppler)	55		Interconnection of ES1	77
	Color Duplex Sonography	55		Interconnection of ES2	78
2.2.1.3	Ultrasound Signal Enhancers	55	2.3.5.2	Clinical Application	78
2.2.1.4	Reference Values	56		Stimulation	78
2.2.1.5	Stenosis Criteria	56		Recording	78
2.2.1.6	Clinical Application	57	2.3.5.3	Evaluation	78
	Brainstem Infarction/TIA	57	2.3.5.4	Reference Values/Normal Variants and Pathologic	
	Basilar Artery Thrombosis	58		ES Criteria	78
	Subclavian Steal Syndrome or Subclavian Steal		2.3.5.5	Interpretation of Findings	79
	Phenomenon	58	2.3.6	Somatosensory Evoked Potentials	81
	Rotational Vertebral Artery Occlusion	58	2.3.6.1	Anatomic and Physiologic Principles	81
2.2.2	B-Mode Sonography of the Brainstem	59	2.3.6.2	Application	81
2.2.2.1	Principles and Techniques	59		Stimulation	81
2.2.2.2	Clinical Application	60		Recording	82
	Early Diagnosis of Idiopathic Parkinson's Disease	60	2.3.6.3	Evaluation	82
	Differential Diagnosis of Parkinson Syndromes	61		The Generator Question and the Interconnection	
	Diagnosis of Affective Disturbances	61		of SEPs	82
2.3	Electrophysiologic Diagnostics	61		Far-Field Potentials	82
2.3.1	Blink Reflex	61	2.3.6.4	Interpretation of Findings	83
2.3.1.1	Anatomic and Physiologic Principles	61	2.3.6.5	Brainstem Lesions	83
2.3.1.2	Clinical Application	62		Brain Death	84
2.3.1.3	Interpretation of Findings	63	2.3.7	Transcranial Magnetic Stimulation	84
2.3.2	Masseter Reflex	65	2.3.7.1	Anatomic and Physiologic Principles	84
2.3.2.1	Anatomic Principles	65	2.3.7.2	Application	85
2.3.2.2	Clinical Application and Normal Values	66		Corticofacial Projections	85
				Corticolingual Projections	85
			2.3.7.3	Evaluation	85
				TMS of Corticofacial Projections	85
				TMS of Corticolingual Projections	86

2.3.7.4	Interpretation of Findings	86	Central Lesions	89
	Brainstem Ischemia Prognostic Significance of MEPs	86	Brainstem Ischemia/Hemorrhage	89
	Topodiagnostic Significance of MEPs	87	2.3.9 Recording of Eye Movements	90
	Multiple Sclerosis	87	2.3.9.1 Direct Current Recording	90
	Amyotrophic Lateral Sclerosis	87	2.3.9.2 Infrared Reflective Oculography	90
	Hereditary Spastic Spinal Paralysis	87	2.3.9.3 Videoculography	91
2.3.8	Laser Evoked Potentials	88	2.3.9.4 Scleral Search Coil Technique	92
2.3.8.1	Anatomic and Physiologic Principles	88	2.3.10 Other Electrophysiologic Methods for the Investigation of Brainstem Reflexes	92
2.3.8.2	Application	88	2.3.10.1 Stapedius Reflex	92
	Stimulation	88	2.3.10.2 Trigemino-Cervical Reflex	93
	Recording	88	2.3.10.3 Trigemino-Hypoglossal Silent Period	93
2.3.8.3	Evaluation	89	Literature	95
2.3.8.4	Interpretation of Findings	89		

2.1 Neuroradiology

Peter Stoeter and Stephan Boor

2.1.1 Conventional Native Diagnostics

Conventional native diagnostics of the skull no longer has an important role in disorders of the brainstem today, and conventional tomography has been completely abandoned for reasons of radiation protection. A similar situation exists with a view to special images of the skull base and the petrous bones (in projections according to Schüller and Stenvers), which have been replaced with thin section computed tomography (CT) scans that have a significantly higher detail resolution. Survey radiographs of the skull in two planes and a radiograph of the back of the head obtained in half-axial projection with the tube tilted toward the vertex are occasionally recommended after craniocerebral trauma and shotgun wounds, or for the detection of other metallic foreign bodies. The finding of fractures of the skull cap or skull base can serve as an indicator of violent assault. If not done at the time of the primary diagnosis, a CT scan is indicated at the latest on detection of a fracture on the plain radiograph, in particular in the presence of space-occupying bleeding.

At the craniocervical junction, the search for a fracture of the upper cervical spine is important in trauma patients; in particular unstable fractures of the atlas or dens and luxations with ligament lesions after injury to the spinal cord and the caudal part of the medulla oblongata have to be identified, while a secondary lesion in these structures as a result of incautious manipulation must be prevented. This also applies to instabilities due to other causes, e.g. odontoid bone or rheumatoid arthritis. Radiographic functional studies in forward and backward tilt under fluoroscopy have to be carried out for the assessment of cervical spine stability (Fig. 2.1), whereby the differentiation from the physiologic mobility of the upper cervical vertebrae is not readily achieved, particularly in children.

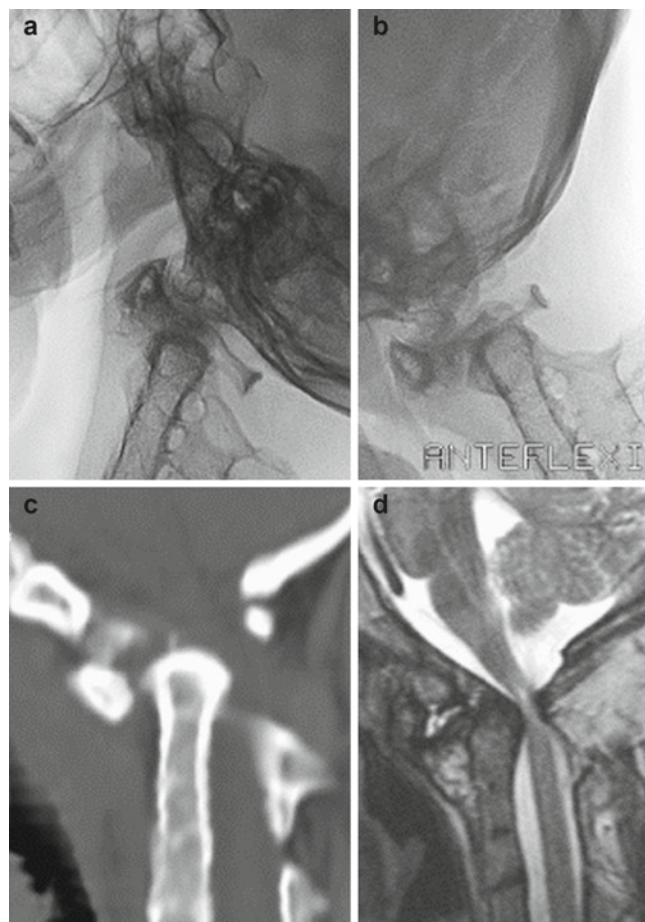


Fig. 2.1 Craniocervical dysplasia. Plain radiograph in backward (a) and forward tilt (b) CT in sagittal reconstruction (c) T2-weighted MRI (d) shortening of the clivus, separate disposition of the dens process as odontoid bone with pseudoarthrosis and anterolisthesis (including atlas and occiput) vis-à-vis the dens, resulting in severe stenosis between the upwardly displaced posterior arch of the atlas and the posterior border of the second cervical vertebral body and dens with malacia (bright signal on T2-weighting) in the caudal part of the medulla oblongata. Only slight increase in forward slippage on forward tilt (comp. a and b). Synostosis C2–5

Further indications for plain radiographs are cranial anomalies (premature suture synostosis), general disorders of the skull cap and skull base as, e.g. Paget's disease, or suspected metastases. Constrictions of the foramina of the skull base can lead to cranial nerve lesions. Constitutional or acquired constrictions at the craniocervical junction, like a basilar impression (upward displacement of the dens into the foramen magnum with resulting depression of the medulla oblongata), or achondroplasia (shortening of clivus with constriction of foramen magnum) can already be identified on the survey radiograph. Overall, however, the information provided by native diagnostics regarding brainstem involvement is limited compared to multislice diagnostic modalities.

2.1.2 Computed Tomography

2.1.2.1 Principles and Techniques

In computed tomography (CT), which – like conventional native diagnostics – is based on x-ray absorption, the x-ray film is replaced by a detector system for the measurement of x-ray absorption. The patient is positioned on the examination table and moved longitudinally, i.e. in very precise small steps or nowadays continuously, through the measurement unit (gantry). The x-ray tube and detector ring are mounted opposite each other in the gantry. In units of the third and fourth generation they rotate continuously around the part of the body to be imaged at a speed of 0.3–3 revolutions per second. The emitted radiation beam is pulsed and collimated in a fan-shaped fashion onto the slice of interest. Modern units enable the measurement of slice thicknesses from 0.5 to 10 mm. The individual detectors transform – as scintillation crystals or ionization chambers – the received radiation into electric signals, from which the image processor calculates the attenuation values of the x-rayed volume elements (voxels).

In newer CT units with continuous rotation, the tube voltage is provided by slip rings, which obviates the need for repositioning of the cables. The examination table moves continuously through the gantry while a spiral scan of the object to be examined is conducted and a volume data set is acquired. The resulting data set can be used to reconstruct single slices of varying thickness. Multidetector systems enable the simultaneous acquisition of multiple (currently up to 640) slices of a specified width. By means of “folded rear projection” relative x-ray attenuation values of the individual voxels can be calculated from the measured detector voltage and correlated to the absorption values of water (0) and air (–1,000) as Hounsfield units (HU). The “density” of gray matter thus ranges at 45 HU, and that of white matter at 35 HU. Because the human eye can differentiate only approximately 20 grayscales, the width and

position of the viewing window have to be accurately adjusted to the contrast area to be differentiated. Conversely, all values above or below the window width are shown as “white” or “black” without further differentiation. Spatial resolution is also low in the presence of slight density differences, ranging only from about 2 to 3 mm, so that pathways and nuclei in the brainstem are poorly differentiated from each other, even when a narrow window width is used. However, in high contrast areas as, e.g. in the visualization of bony petrosal structures, spatial resolutions of up to 0.35 mm can be achieved with special reconstruction algorithms.

Further section planes can be reconstructed from the data sets. With the commonly used 512 matrix the slice thickness is substantially greater than the edge length of the image elements (pixels), the resolution of secondary sections in the reconstruction direction has thus far been lower than for direct measurements. With the introduction collimation, units of the latest generation permit the measurement – or at least the calculation – of isotope voxels, which enables multiplanar reconstruction without quality loss. A further advantage of multiplanar systems, in addition to shorter measurement times, is reduction of partial volume effects and therefore an improved sharpness, resulting from the presence of structures with different densities in one voxel, and their visualization as one unit with proportional weighting.

After intravenous bolus administration of iodized x-ray contrast medium, reconstruction of image elements with maximum intensities, e.g. of vessels using **maximum intensity projection (MIP)**, as well as three-dimensional reconstructions with, e.g. **shaded surface display (SSD)** or **volume rendering technique (VR)**, are also possible. In CT angiography it is important to ensure that the examination of the region of interest is carried out at exactly the moment when the injected contrast medium passes through the arteries or veins.

2.1.2.2 CT in Investigations of the Brainstem

Due to the low spatial resolution in the low contrast area, the diagnostic value of CT in investigations of the brainstem is relatively limited. The primary indication – also in view of the short examination time – is emergency diagnostic imaging, particularly for the demonstration of skull base fractures after trauma, and bleeding in the brainstem or cisterns. Furthermore, calcifications of cavernomas (Fig. 2.2), other vascular malformations or various neoplasms, e.g. ependymomas, can be accurately identified. The majority of brainstem lesions like infarctions or patches of demyelination are rare and can be conclusively shown primarily above the middle of the pons.

In addition to low contrast resolution, this is due to the occurrence of streak artefacts (Hounsfield artefacts) that develop as the result of energetically different x-ray absorption in the bones of the skull base, primarily the petrous bones,

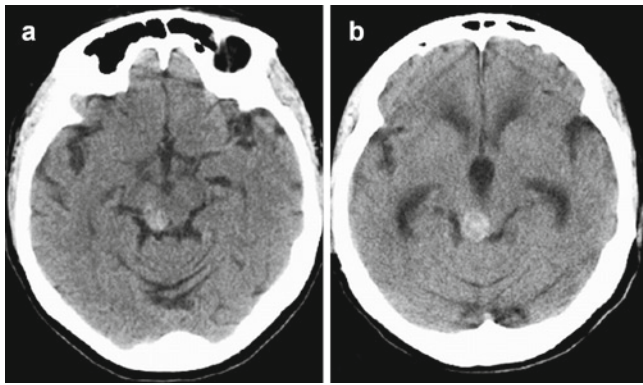


Fig. 2.2 Cavernoma of the lamina quadrigemina. Axial CT at the time of diagnosis (a) and after 8 months (b). Calcifications in the right superior colliculus (a) and enlargement of the hyperdense region due to bleeding with compression of the aqueduct and CSF accumulation (b)

and mask the lower parts of the brainstem. The artifacts can be eliminated only partially with special programs using artefact filters and secondary slice reconstruction from consolidated thin sections. CT perfusion measurements for the differentiation between a nuclear infarct and an undersupplied penumbra do not yet play an important role in brainstem investigations.

However, larger intracerebral and extracerebral tumors as well as other infratentorial space occupying masses like cysts and malformations at the craniocervical junction which may lead to CSF accumulation, can also be visualized on CT. The indication for the investigation may be valid in emergency patients with a suspected increase in intracranial pressure. When magnetic resonance imaging (MRI) can, for different reasons, not be done in patients with a suspected tumor, intravenous contrast medium has to be administered to visualize some intrinsic tumors, e.g. astrocytomas and medulloblastomas – blood–brain barrier disorders and conditions that have high vascular density (e.g. von Hippel-Lindau tumor/Hemangioblastoma or vascular malformations) can be better differentiated from the surrounding structures by contrast enhancement.

This also applies to abscesses originating from the petrous bone, which may lead to clouding of pneumatization cells and osteolytic destructions. Other destructions of the skull base, e.g. metastases, chordomas, chondromas or sarcomas, which may be a cause of brainstem compression are also well visualized on CT scans. Enlargements of the internal acoustic meatus (IAC) are indicators of schwannomas, although a negative CT finding alone is not sufficient for the exclusion of this lesion. In cases where MRI is contraindicated, **CT cisternography** after intrathecal contrast medium injection should be carried out, comparable to the application of this procedure for a suspected cyst, to clarify communication with the subarachnoid space.

CT angiography for brainstem imaging is further used to visualize

- Vascular stenoses or vascular occlusions – particularly when a basilar artery occlusion is suspected
- Arterial aneurysms (demonstration at 90% sensitivity as of a diameter of 5 mm) (Dammert et al. 2004)
- Central cerebral veins or sinus thromboses

The availability of modern units has rendered CT angiography coequal to MR angiography. As in MR angiography, the use of multislice CT scanners enables visualization of the entire supra-aortal vascular region.

2.1.2.3 Risks

In accordance with the X-Ray Ordinance for Radiation Protection, any x-ray application must be approved by specialists and is subject to strict regulations, in particular with regard to pregnant women. In the region of the head, the eye lens is especially sensitive to x-ray exposure and should, whenever possible, be protected from the beam path by tilting of the gantry. In spiral technique applications, an x-ray exposure of the eye lens to 70 mGy simulated petrous bone investigation; (Giacomuzzi et al. 2001) may be assumed when multislice spiral CT is used; the required dose of 0.5–2 Gy (MacLennan and Hadley 1995) for cataract induction is therefore highly unlikely to be exceeded, even after repeated CT scans. The use of x-ray contrast media is also subject to specific requirements: special care has to be taken in the presence of known allergies (possible administration of H_1 and H_2 blockers), disturbance of kidney function with creatinine levels above 1.5 mg/dL (sufficient water intake and administration of acetylcysteine), increased thyroid hormone levels, or decreased basal TSH (poss. perchlorate blockade), and pathologic serum proteins, as in multiple myeloma. The occurrence of allergic reactions is expected in up to 3% of patients, even in those without a prior history of allergies. However, the allergic reactions only rarely (below 0.04%) lead to a severe circulatory shock if non-ionic contrast media are used. Where indicated, and in the absence of a kidney function disturbance, an iodine-containing contrast medium can be replaced with a gadolinium-containing contrast medium. Patients with cardiac insufficiency have to be monitored for a short-term increase in intravascular blood volume after contrast medium injection.

2.1.3 Magnetic Resonance Imaging

2.1.3.1 Principles and Techniques

Magnetic resonance imaging (MRI) is based on electromagnetic waves generated by rotation of the positive proton load (spins). The MRI scanner uses a powerful magnetic field

(0.2–3 T in clinical applications) to align the spins parallel and antiparallel to the main magnetic field. The rotation speed or Larmor frequency is dependent upon the strength of the magnetic field and ranges at 42.5 MHz for 1 T. There is a slight surplus of parallel aligned spins due to ambient heat, which leads to the generation of a magnetic moment in the direction of the main magnetic field, although this can not yet be measured in itself. The additionally applied energy in the form of a high frequency pulse, which has to be in resonance with the Larmor frequency, causes additional spins to be tilted in the antiparallel direction, while the rotation (**precession**) of the spins about the direction of the main field is synchronized or brought “in sync.” This leads to the brief generation of a magnetic moment, which rotates in a plane perpendicular to the main field and generates the initially mentioned electromagnetic waves. These are received by a coil, which functions like an antenna and can be used for image calculation (Lauterbur 1973).

The energy exchange with the surrounding protons and minute local differences in magnetic field strength lead to rapid dephasing of precession of the individual spins and therefore to signal loss. This **spin-spin relaxation** is characterized by T2-time and occurs at a significantly slower rate in pure water than in the presence of macromolecules. The image signal from tissues with a high water content is therefore maintained also after a longer latency of above 100 ms, while tissues with a low water content do not emit a signal at this time point due to spin dephasing (T2-weighting: CSF bright, cortex gray, spinal cord dark gray). However, dephasing caused by inhomogeneous magnetic field effects can be reverted with the application of an additional high frequency pulse, which effects a reversal in the rotational direction of the spin, and an “echo” of the initial signal is formed. The described pulse consisting of an excitation and inversion (180°-) pulse sequence is described as **spin echo- (SE-) sequence**.

The energy release to the surrounding protons, the “lattice,” causes the direction of additional spins generated by the high frequency pulse to be switched into the antiparallel direction, and the magnetic moment rotating in the perpendicular plane will decay with time. Concurrently, the original moment is restored parallel to the main field. This **spin-lattice relaxation** is described by the T1-time and is markedly (up to tenfold) slower than the spin-spin relaxation. If a second excitation pulse is applied at an earlier time point, the more slowly relaxing tissues with a high water content will not yet have recovered full “longitudinal magnetization” oriented toward the field, and only a small surplus of foldable parallel aligned spins is available. As a result, the signal received from these tissues is weaker than that from tissues with shorter T1 time (T1 weighting: CSF dark, cortex gray, spinal cord light grey).

If the influence of both T1- and T2-times on the image signal (short echo and long repetition times) is suppressed by means of the selection of respective sequence parameters,

the number of available protons is the decisive factor regarding the image signal (proton weighting: cortex brighter than spinal cord, CSF dark).

Spatial encoding is achieved with MRI by superimposing three gradient fields above the main field. This enables the modification of the local magnetic fields in all three spatial dimensions, so that each voxel receives a specific field and therefore also a specific resonance condition. Special, time limited connections between these fields further permits variation of the rotation frequency of the spins at the time of the echo, to change their phase, and to enable their application for spatial encoding.

Due to the small size of the brainstem, the images should have the highest spatial resolution possible, i.e. maximal matrix and thin slice thicknesses. Since the image signal of a voxel depends upon its size, imaging of the brainstem requires either a greater number of measurements (repetitions) or greater field strengths. With the application of several parallel-connected coils the measurement times are shortened and the threat of motion artifacts can be significantly reduced.

Spatial resolution can be enhanced with the use of three-dimensional techniques. Particularly suitable for T2 weighting is the **constructive interference in steady state (CISS)** sequence, which allows measurement of slice thicknesses below 1 mm. As a result of the especially long echo times virtually all structures outside the CSF-containing cisterns are visualized as dark areas. The vessels and cranial nerves coursing in the cisterns can be viewed in high resolution images, as can virtual endoscopy procedures (Boor et al. 2000; Fig. 2.3) and the labyrinth in the petrous bone, while intensity differences in the brainstem as, e.g. patches of demyelination or fresh infarcts versus normal structures are almost impossible to differentiate. The CISS sequence is therefore used mostly to differentiate between a neurovascular compression or a cisternal space-occupying or for petrous bone diagnostic imaging. Epidermoids, which are also almost impossible to differentiate from the CSF-signal, can be shown as mildly (in comparison with CSF) hypointensive space-occupying masses with this modality.

T1 weighted sequences are also capable of further enhancing spatial resolution with the measurement of a three-dimensional volume data set, which provides a high signal-to-noise ratio. For reasons of time, the refocusing pulse is not applied here and a (weaker) echo is generated with the application of gradient fields, although this reacts with considerably higher sensitivity to magnetic field inhomogeneities (**gradient echo sequence**). At the concurrent prolongation of echo time (T2* weighting), the demonstration of fresh bleedings and paramagnetic blood degradation products (ferritin), e.g. older bleedings and cavernomas, becomes possible (Fig. 2.4). The described effect of signal attenuation due to magnetic field disturbances can be used advantageously in imaging perfusion measurements, where

Fig. 2.3 Acoustic neurinoma. High-resolution MRI (CISS) in T2-weighting (a) and respective calculation of virtual endoscopy (b). Mass at the entrance to the internal acoustic meatus right, and normal course of the statoacoustic nerve left in cerebellopontine angle cistern. View of the lower surface of the tumor and the AICA, viewed as if through an endoscope located more caudally in the parapontine cistern

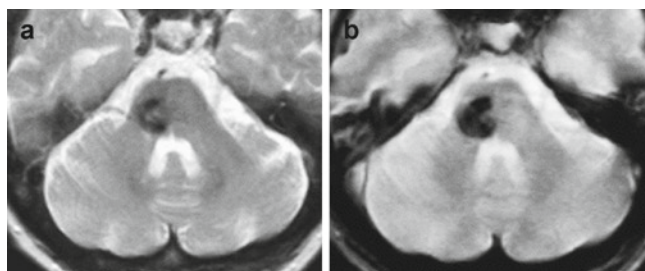
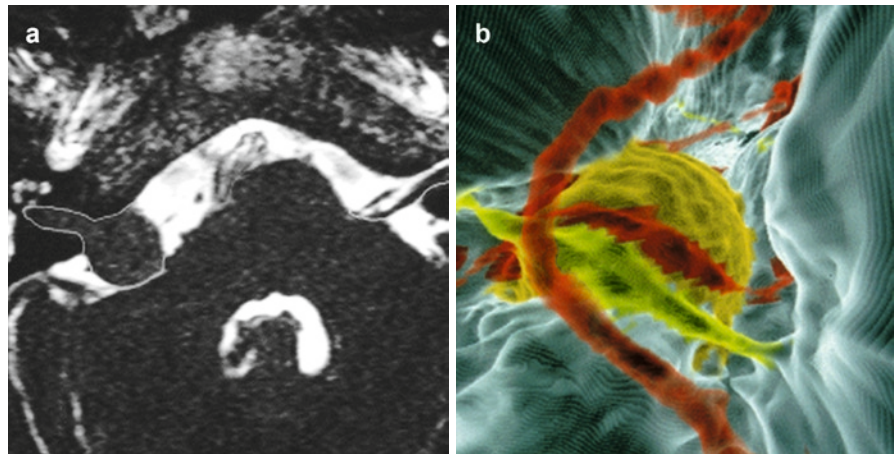


Fig. 2.4 Pontine cavernoma. MRI in T2 weighting (a) and T2* weighting (b). Signal reduction due to iron deposit (old bleeding) is markedly greater in the T2* weighted sequence, which is substantially more sensitive to susceptibility disturbances

signal degradation as a result of repeated measurements can be observed during the passage of the contrast agent bolus. However, this technique, which has an important role in the diagnosis of supratentorial infarcts and tumors, is not as frequently used in brainstem imaging.

The T1 weighted signal of stationary spins can be suppressed by reducing the time interval between two excitations (**repetition time**), so that in particular successive spins flowing into the excited slice produce a signal (**time-of-flight [TOF] angiography** for imaging of vessels). Venous overlay can be reduced by presaturation of the sinus above the convexity. Contrast agent infusion enables both suppression of artifacts due to turbulent flow and contrasting of veins (**contrast enhanced MRA [CE-MRA]**). Comparable to CT-angiography (CTA), the reconstruction of the course of the vessels can be accomplished with postprocessing programs in MRA. Both methods of MR angiography are used to show vascular stenoses and malformations (angiomas, aneurysms; Fig. 2.5), in addition to imaging of neurovascular compressions. For special questions regarding the venous system, the use of TOF-MRA has proven to be of advantage, primarily for intracranial segments, due to the higher spatial resolution, while the examination of a large area is enabled by CE-MRA, making this the more suitable method for the extracranial segments.

A further method for MR tomographic flow measurement – used in particular in investigating CSF-flow at the craniocervical junction, in the cisterns and in the aqueduct – consists of imaging with phase contrast images by means of a two-dimensional steady state free precession sequence at velocity encoding of 7–10 cm/s in the direction of the z axis. The CSF flow leads to a phase shift that is proportional to the flow velocity and therefore quantifiable (Fig. 2.6). However, these investigations are time consuming due to required synchronization with cardiac movements (ECG triggering).

Diffusion imaging employs brief applications of strong gradients before and after a 180° pulse, causing only signals of stationary spins to be completely rephased, while spins of diffusing protons produce a weaker signal due to their exposure to gradients of varying strengths as a result of a change in their spatial orientation before and after reversal of the rotational direction. Areas with diffusion disturbances like infarcts and occasionally also fresh patches of demyelination are therefore viewed with high signal in these images (Fig. 2.7). These lesions are characterized by high signal in both diffusion weighting and T2 weighting sequences, therefore the T2 effect has to be calculated as well as the apparent diffusion coefficient (ADC). Diffusion disturbances are viewed as dark areas on these ADC maps.

2.1.3.2 MRI Investigations of the Brainstem

MRI is superior to other imaging modalities in imaging the form and tissue structure of the brainstem, and thus makes a major contribution to differential diagnosis. To be discussed in this chapter are primarily the technique used for the investigation and the brainstem anatomy, while examples of pathologic findings are presented in the respective specialized chapters.

All cranial nerves in the cisterns can be shown and differentiated from adjacent vessels on both T1 and T2 weighted sequences. While the robust trigeminal nerve can also be

Fig. 2.5 Aneurysm of the basilar artery tip. MR angiography (TOF sequence) (a) with MIP reconstruction (b) conventional vertebral DSA left (c) and 3D rotational angiography (d). The aneurysmal sack exits from the basilar artery tip and both P1 segments of the posterior cerebral arteries. The branches supplying the thalamus are visualized on DSA only

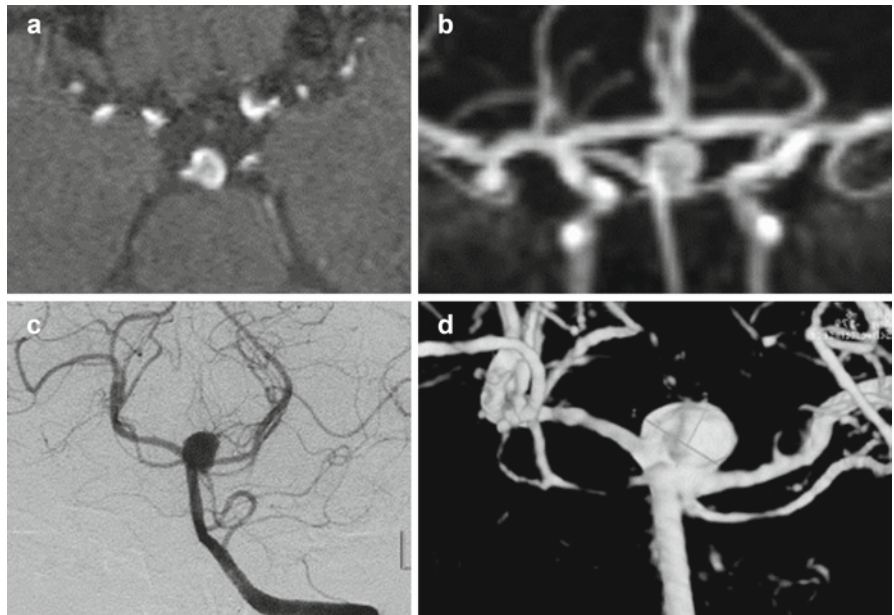


Fig. 2.6 Chiari-II (Arnold–Chiari) malformation. MRI in T1 weighting (a), phase contrast image of CSF flow during systole (b), and diastole (c). Descent of the entire brainstem and cerebellar vermis, which extends together with the cerebellar tonsils through the foramen magnum into the spinal canal, with compression of the medulla oblongata and blockade of retromedullary CSF flow. Premedullary CSF flow is still demonstrable, systolic in caudal (dark), and diastolic in cranial (bright) direction

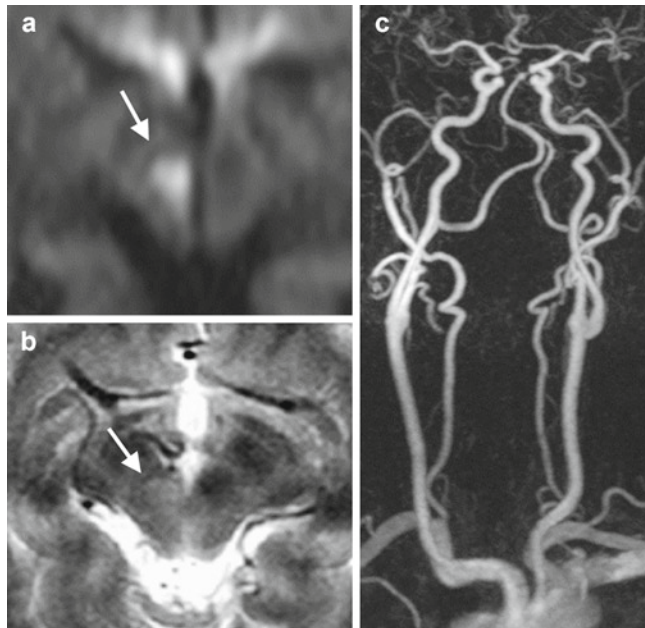
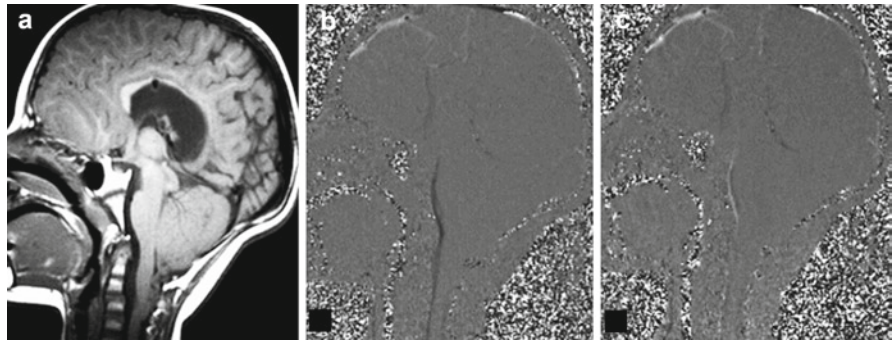


Fig. 2.7 Fresh midbrain infarction. MRI in T2 weighting (a) diffusion weighting (b) and CE MRA (c). While the paramedian infarction (arrows) is visualized primarily as a bright diffusion barrier in DWI, the T2 image shows only slight signal enhancement. CE MRA of the supratentorial vessels does not demonstrate any relevant stenosis

identified on survey scans, this is the case for more delicate nerves like the trochlear or abducens nerve only when a sufficiently high spatial resolution is achieved with CISS or gradient echo sequences. Regarding the vestibulocochlear nerve and the facial nerve, the four bundles of the superior and inferior vestibular nerves, the auditory nerve and the facial nerve in the internal auditory meatus can be differentiated in sagittal sections, while conclusive differentiation between the glossopharyngeal nerve and the vagus is generally not possible. Form, location and size of the individual brainstem segments can be assessed without difficulty. This also applies to the fourth ventricle, and here in particular to the rhomboid fossa, the aqueduct, and the cerebellar peduncles. The internal structure of the brainstem is characterized by close interweavement of pathways and nuclei, which can be very well differentiated with the use of proton weighted sequences and diffusion tensor imaging (see Specialized methods) (Fig. 2.8). In proton weighted images the pathways and nuclei display varying degrees of brightness, depending on their proton content. Diffusion weighting visualizes the different courses of pathways by giving preference to the diffusion parallel to the pathway (**signal reduction**) or by reducing the diffusion perpendicular to it (**signal enhancement**).

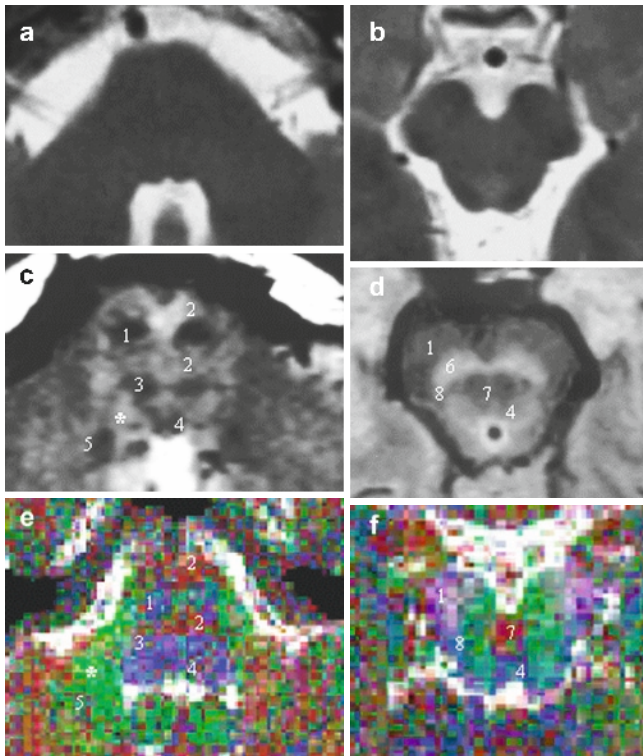


Fig. 2.8 Normal MRI anatomy of brainstem pathways. T2 weighting (a, b), proton density weighting (b, e, f) color coded DTI maps (c, f). Axial sections through the lower part of the pons (a, c, e) and the midbrain (b, d, f). 1 Pontine base with corticospinal tract (pyramidal pathway) and 2 pontocerebellar tract (middle cerebellar peduncle), 3 pontine tegmentum with tegmental tract, 4 medial longitudinal fascicle, 5 spinocerebellar tract (lower cerebellar peduncle), asterisk: lateral part of the reticular formation with vestibular nuclei, 6 substantia nigra, 7 crossing of cerebellar efferents (cerebellorubrothalamic tract), 8 medial lemniscus, color coding on DTI color maps, red: trajectories in right-left direction, green: trajectories in AP direction, blue: ascending and descending trajectories

Sections through the upper part of the medulla oblongata permit identification of the long pathways, e.g. the pyramidal pathway ventrally, the medial lemniscus in the center, and the olive and the ascending pain and cerebellar pathways laterally. Located in the dorsal part of the medulla, i.e. in the floor or exit of the fourth ventricle, is the medial longitudinal fascicle, as well as the primary nuclei of the cranial nerves IX–XII. The corticospinal tracts and the cerebellar afferents coursing in a lateral direction are visualized in the base of the pons and can be differentiated from the more dorsally located pontine tegmentum with the medial and lateral lemnisci, the central tegmental tract, and the medial longitudinal fascicle. Visualized in the sections through the midbrain are the descending pathways in the cerebral crus, as well as the substantia nigra with several markedly enlarged Virchow–Robin spaces in the T2 image, where the relatively bright crossing of the cerebellar efferents, and the more rostrally located red nucleus, the lamina quadrigemina and the periaqueductal gray can also be identified. Pathologic processes of the

brainstem associated with severe morphological changes as, e.g. complex malformations (Chiari malformation, Dandy–Walker complex, Joubert syndrome), tumors of the brainstem and adjacent structures, as well as obstructions of the CSF passage with resulting hydrocephalus can be identified without difficulty. Pronounced stenoses or occlusions of the aqueduct, e.g. after inflammations, typically appear as a trumpet-shaped enlargement of the rostral segment of the aqueduct, which is located anterior to the occlusion. These can often already be identified in T2 weighted images due to the absence of a flow signal (no flow-related signal decay). Under these conditions the phase-weighted sequences described above are particularly suitable for flow imaging. Furthermore, atrophies due to system degeneration, i.e. olivopontocerebellar atrophy (OPCA) or pseudobulbar paralysis can be identified based on apparent loss of substance in the medulla, pons and/or midbrain (mesencephalic sagittal diameter below 14 mm). Intracerebral lesions of the brain substance like infarcts and patches of demyelination require the use of at least T2 weighted sequences with high resolution (512 MB matrix or a narrow field of view) and thin slicing (slice thickness 2–3 mm). Wallerian degeneration of brainstem pathways can also be shown with this procedure, as well as toxic or metabolic damage to pathways, as in pontine myelinolysis, or the rare occurrence of olivary pseudohypertrophy following central tegmental tract lesions. The evaluation of proton weighted images is not readily accomplished in the brainstem, due to the close anatomic relationship of the gray matter to the white matter; this is in contrast to the cerebrum where edemas and gliomas can be well identified using this weighting. As mentioned above, exact anatomic knowledge of brainstem structures is a prerequisite for the differentiation of circumscribed lesions of pathways and nuclei in proton weighted images. Furthermore, fluid attenuated inversion recovery (FLAIR) sequence, which provides valuable supratentorial information, also does not yield a contrast-rich image of small brainstem lesions.

In the presence of acute vascular processes, in particular of ischemic infarctions, diffusion weighted sequences should be taken to ensure that small lesions are not missed, and can be differentiated from possibly existing older ones (Fitzek et al. 1998). Infarcts lead to the breakdown of cell metabolism and ion pumps. This results in development of intracellular edema with compression of the extracellular space, the location with the most prolonged and therefore MRI-relevant water diffusion. A diffusion obstacle is created as a result of cellular swelling and the interruption of the active proton transport through the membrane. As diffusion leads to signal loss in MRI images, the nuclear infarcts with diminished diffusion appear early and are characterized by high signal intensity, while signal enhancement in the T2 weighted image, which is dependent on the water content, occurs after several hours or days. MRI is therefore superior by far to CT,

particularly for the early diagnosis of brainstem infarcts. Although brainstem bleedings are also visualized on MRI in the acute stage as space-occupying masses – and with signal inhomogeneities in the diffusion image – they can be better shown with a latency of several days, due to the pronounced increase in signal intensity on T1 and T2 weighting over time. Ferritin deposits can be identified even later but particularly well in T2* weighted images, whereby cavernomas exhibit a typical “mulberry-shaped” arrangement of dark borders and a bright center. These deposits are absent in teleangiectasies and in developmental venous anomalies (DVA). For the investigation of space-occupying masses, a gadolinium-containing MR contrast medium is generally administered to display disturbances of the blood brain barrier as, e.g. gliomas or abscesses. A contrast material should also be injected for lesions whose origin can not be conclusively identified (ischemic, traumatic, or degenerative) in order to detect the presence of a blood–brain-barrier disturbance and thus to enable the diagnosis of an acute occurrence and/or spread of a process. This is of particular importance in multiple sclerosis when a acute episode of the disease is suspected, as well in the also well localized acute disseminated encephalomyelitis (ADEM), where all lesions are at a similar stage of development and therefore capable of uniform contrast medium uptake in the acute stage. Other inflammatory processes – sarcoidosis, borreliosis, tuberculomas and other encephalitides (e.g. listeriosis) – as well as neoplastic infiltrations in the cisterns and the substance of the brainstem are further visualized as circumscribed areas with enhancement (Fig. 2.9). Acute Wernicke’s encephalopathy due to vitamin B1 deficiency is also characterized by blood–brain-barrier disturbances, typically in the central gray matter of the midbrain and the hypothalamus.

Contrast medium is also given to detect the above-mentioned vascular malformations, although primarily for the

performance of MR angiography. While the contrast medium free TOF method provides better spatial resolution, it occasionally is rendered less diagnostic by turbulence caused by artifacts and is dependent upon flow velocity. Contrast medium is given in patients with arteriovenous malformations mostly to image venous drainage, while the arterial feeders are better captured on TOF angiography. This also applies to showing neurovascular compressions like trigeminal neuralgia, as well as to other cranial nerve disturbances, e.g. vascular compression of the vestibulocochlear nerve with concomitant attacks of vertigo. In addition to the abovementioned CISS sequences, TOF angiographies before and after contrast medium application are used here, to enable the differentiation between arterial and venous vessels in close proximity to the nerves.

Contrast enhanced MR angiography (CE-MRA) is used to show the entire supraaortic region. Compared with contrast medium free angiography, which provides a higher resolution, CE MRA offers the advantage, that turbulence artifacts can be reliably differentiated from genuine constrictions. The demonstration of therapy relevant stenoses and occlusions on CE-MRA can be accomplished with a high degree of certainty, so that conventional digital subtracted angiography in the vertebrobasilar region is used in exceptional circumstances and exclusively for diagnostic reasons. This also applies to TOF-MR angiography for the detection of aneurysms. A high reliability rate can be achieved with this modality for aneurysms of 3 mm in diameter and above (Hirai et al. 2005).

2.1.3.3 Specialized Methods

The following specialized methods are used for investigations by MRI imaging:

- Cerebral activation
- Diffusion tensor imaging (DTI)
- Spectroscopy

During **cerebral activation** the linkage of neuronal activity and brain perfusion leads to vasodilation with a latency of a few seconds. This produces both an increase in perfusion and oxygenated and therefore diamagnetic hemoglobin content. Both effects lead to a small increase in signal intensity, although this is only slightly higher than the basic noise of the image signals. The statistic significance therefore has to be demonstrated based on the correlation between repeated activations and signal development. Brainstem activations can thus be demonstrated with horizontal and vertical gaze direction nystagmus at different levels (pons or mesencephalon). In patients, this method has so far been applied for the preoperative diagnosis of cerebral processes (motor and speech activation).

Diffusion tensor imaging (DTI) represents a further development of diffusion weighting. Since the diffusion of

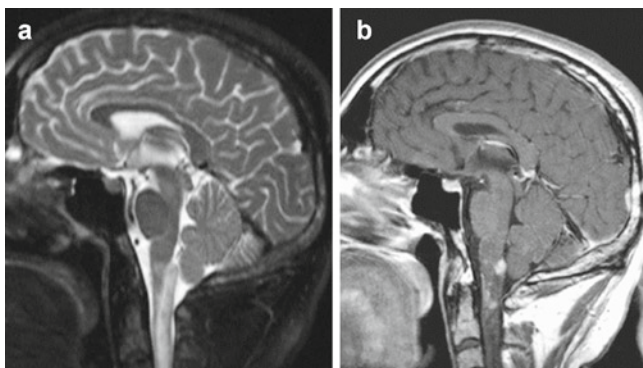


Fig. 2.9 Infiltration of basal cisterns and brainstem in lymphatic leukaemia. Sagittal section in T2 weighting (a) and T1 weighting following contrast medium application (b). Marked signal (T2) enhancement (edema) in the medulla oblongata with circumscribed barrier disturbance (contrast agent leakage), extra- and intracerebral

water molecules is always isotropic in water, but restricted in tissue by cell borders, and particularly by axon sheaths (anisotropic diffusion), the degree of anisotropy and the principal diffusion direction can be determined with gradient applications in different directions, and the measurement of a nine component diffusion tensor.

The degree of the averaged diffusion direction and anisotropy serves as a parameter for intact nerve tract function. The courses of the main nerve tracts can be reconstructed from the principal characteristic vector of the tensors in the form of direction-coded color maps (Fig. 2.10). In clinical practice this method is used primarily for preoperative imaging of cerebral tumors and vascular malformations. The purpose of

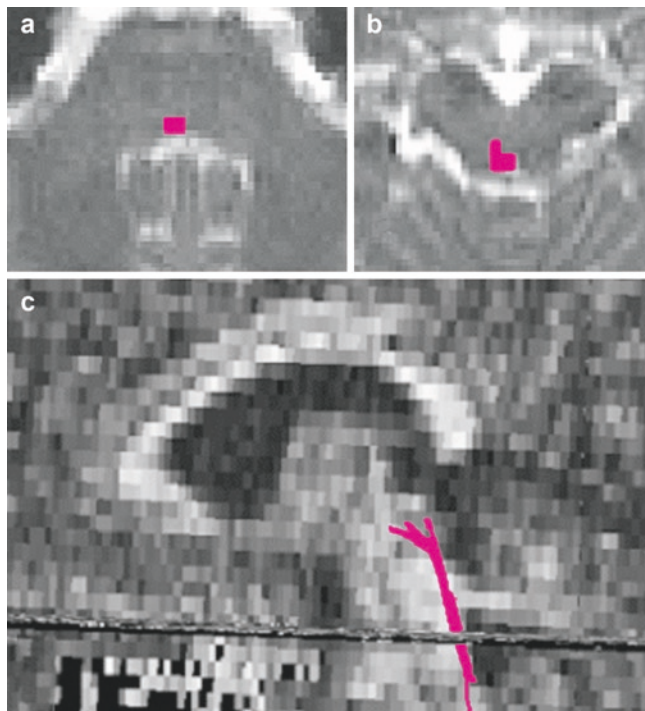


Fig. 2.10 Trajectories of the right medial longitudinal fasciculus calculated from DTI data sets in axial (a, b) and sagittal cross-section (c)

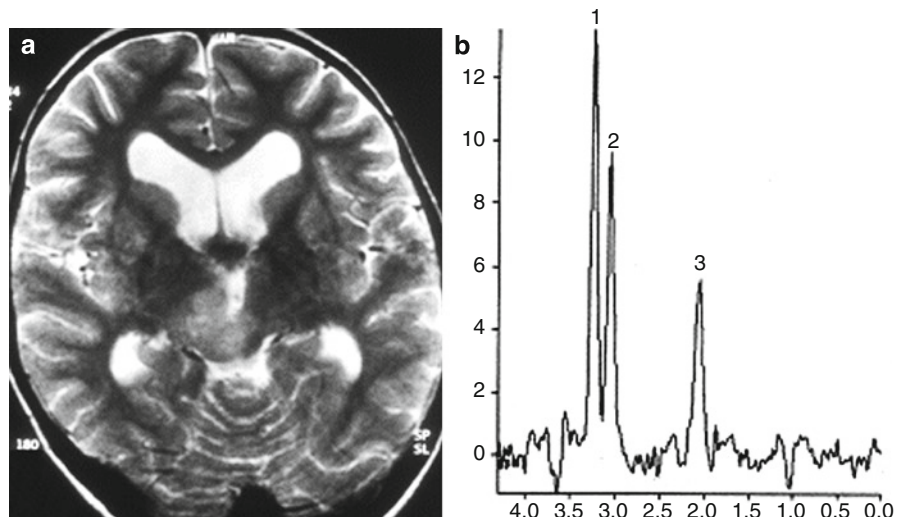
the depiction of pyramidal pathways or optic radiation, and transfer of the trajectories to neuronavigation systems is to avoid injury of these pathways in the course of surgical interventions. This method can also show the corticospinal projections that traverse the pontine base.

The signal of protons from water molecules used for imaging is suppressed during **spectroscopy**, which causes signals of protons from other substances to be visualized. Depending on their molecular environment, these show a slight substance-specific shift in Larmor frequency compared to water. The described frequency shift permits differentiation of three major peaks (choline [CHO] as a marker for membrane reconstruction, creatinin [Cr] as an indicator of energy metabolism, and *N*-acetyl aspartate [NAA] as an osmolyte). In the presence of tumors and depending on the tumor grade, there is an increase in the choline level compared with the creatinin level, and a decrease in the level of *N*-acetyl aspartate (Fig. 2.11). A lactate peak might be observed in acute inflammations and demyelinations. Other products of metabolism as, e.g. amino acids or acetates in abscesses may, in some instances, be shown on spectroscopy. This method is nevertheless rarely used in clinical brainstem diagnostic tests, because the small measurement volume required here necessitates a long examination time.

2.1.3.4 Risks

Apart from slight tissue warming and the occurrence of photopsias at high magnetic field strengths (3 T), no MR-specific side effects have been shown in tissue, on condition that specific absorption rates (SAR) are given consideration. The indication for MRI examinations should, however, be particularly strict in pregnant women – especially in the second part of pregnancy – because the fetus reacts with increased movement to the acoustic noise due to the rapid switching on and off of the magnetic field gradients.

Fig. 2.11 Thalamus and brainstem glioma: T2 weighted section through the lamina quadrigemina (a) and proton spectroscopy (b). Right-paramedian, in T2 signal-intensive space-occupying lesion in medial part of the thalamus and the superior quadrigeminal bodies, with pronounced increase in the choline peak (1), a slightly decreased creatinin (2) and markedly decreased *N*-acetyl-aspartate (NAA) peak (3)



While MRI does not generally represent a health hazard, the situation is completely reversed in the presence of ferromagnetic foreign material in the body, e.g. iron or steel remnants (shell fragments, splinters after accidents, old implants), that may heat up and cause injury to the vessels or nerves as a result of displacement. This applies in particular to old aneurysm clips and intraorbital metal fragments. Metallic paints used in tattoos can also cause burns. Damage may further result from the antenna effect of metal wires inside and outside the body that are used as electrophysiologic leads (e.g. ECG cables and electrodes). Whenever possible, these should be replaced with light guides. Especially patients with pacemakers are at a high risk for burns and subsequent scarring, as well as for arrhythmias.

In this context MRI is rarely indicated only in patients with specially designed pacemaker devices or with a vital indication, and under adherence to appropriate safety precautions (among others the presence of a reanimation team with cardiologic competence) (Loewy et al.2004). Although other metals, including platinum or tantalum are not paramagnetic, artifacts frequently appear. Substantial signal loss and major image distortions are also caused by dental braces. To a lesser degree these events may also result from body piercing and make-up, especially from eye shadow containing active magnetic substances.

Another, not insignificant risk is posed by the presence of ferromagnetic objects (gurneys, wheelchairs, surgical instruments, gas bottles) in the examination unit, if these are pulled into the scanner with a great expenditure of energy and transported while being exposed to increasing magnetic field strength in the vicinity of the magnet. Monitoring of the patient in the scanner is also difficult. A MR compatible device for the measurement of vital parameters is not always available, so that particular attention must be paid to the occurrence of epileptic episodes, or cardiovascular and respiratory disturbances as well as sudden emesis, which may develop in brainstem processes. A similar problem may arise during chemical sedation which may be indicated in agitated patients, e.g. small children. Gadolinium-containing contrast agents are better tolerated than the contrast media used in x-ray radiography, since the volumes are smaller and no iodine is injected. Although allergic reactions are also rarer, they may nevertheless be life-threatening. The use of unbound gadolinium may lead to nephrogenic systemic fibrosis in patients with severe renal impairment, and an accurate diagnosis is imperative in these cases.

2.1.4 Angiography and Endovascular Interventions

2.1.4.1 Diagnostic Angiography

Conventional angiography requires technical skill as well as experience and is, as an invasive procedure, associated with

a complication rate. In the presence of an exclusively diagnostic indication it is therefore increasingly replaced by Doppler sonography and CT or MR angiography. Conventional angiography provides a high spatial resolution and enables the depiction of blood flow phases in chronological order, therefore this “gold standard” cannot be completely abolished. Selective vertebral angiography is required for visualization of the vertebrobasilar vascular system and can, especially in younger patients, be performed without technical difficulties. The Seldinger technique with insertion of the catheter via the femoral artery is employed for this procedure. The use of the subtraction technique permits the elimination of bone densities and leads to a significant improvement in image quality, especially in the posterior cranial fossa where the overlying petrous bones can be dispersed. It is carried out in form of digital subtracted angiography (DSA), if possible with a biplane x-ray unit. By the use of selective catheter placement in a vertebral artery, this procedure enables reduction of the contrast medium volume to a few milliliters, at an iodine content of 250 mg/mL compared to injection into the subclavian artery. A 3D-technique for angiography has become available, equipped with a C-arm unit that rotates around the head of the patient placed in the isocenter. With this procedure, complete angiograms at intervals of only few angular degrees are possible. The obtained data sets are used for three-dimensional reconstructions of the cervical and intracranial vessels which provide details of particular value in the diagnosis and therapy of aneurysms (free projections of the aneurysm head, exact measurement). Indirect techniques like countercurrent angiography of the brachial artery with the injection of 30 mL of contrast medium using high pressure, and contrast medium injection via a central venous catheter have been largely abandoned, as they do not offer any advantages over sectional image angiography with regard to image quality. Direct puncture of the vertebral artery is contraindicated due to the high risk of complications associated with intramural contrast medium injection. In the arterial phase of angiography, the origin of the vertebral artery from the subclavian artery is slightly constricted, also under normal conditions.

Visualized in the further path of the vessel are the V1-segment up to its entry into the transverse foramen of the sixth cervical vertebra, the V2-segment in the homonymous “canal,” the arch of the atlas (V3-segment) between the second cervical vertebra and the foramen magnum, and finally the V4-segment until it unites with the contralateral vessel.

From its cervical part, the vertebral artery sends muscle branches which anastomose with the other cervical arteries, principally with the external occipital artery. In the presence of embolizations in this region, these anastomoses have to be regarded as possibly “dangerous.” From the V4 section two meningeal branches supplying the dura mater originate extracranially, while the posterior inferior cerebellar artery (PICA) originates at a different level from an intradural location and divides, after a variable, loop-shaped course along the

medulla oblongata, into two branches which supply blood to the basal parts of the vermis of the cerebellum and the cerebellar hemispheres. Small branches originating from the intracranial vertebral artery cross the lateral medullary fossa to supply the lateral medullary tegmentum and dorsal lateral base.

The anterior spinal artery also originates from the V4 segment in a mostly asymmetrical fashion. Conversely, the anterior inferior cerebellar artery (AICA) branches off the proximal section of the basilar artery in the prepontine cistern and supplies the medial portions of the cerebellum; it also characterized by a vicarious relationship with the PICA and the more distally arising middle cerebellar artery. Angiographic depiction of the latter, as well as of the pontine branches, is possible only if the vessels are dilated due to the abnormally rapid rate of blood flow associated with arteriovenous malformations or fistulae, otherwise the vessels are too small to demonstrate.

The superior cerebellar artery (SCA) arises in the distal segment of the basilar artery, frequently divided into two branches on one side. The cisternal segment of the artery winds around the midbrain and supplies the surface of the cerebellum, sending one branch to the superior vermis, one marginal hemispheric branch to the lateral fissure, and additional branches to the cerebellar convexity. At its tip, the basilar artery divides into the posterior cerebral arteries which proceed parallel to the superior cerebellar artery in the ambient cistern, i.e. rostral to the oculomotor nerve that travels in an anterior direction between these two arteries. The cisternal posterior segments (P1 and P2) are individually variably connected with the carotid siphon via the posterior communicating arteries and are therefore of critical importance for the basal collateral circulation (cerebral arterial circle [circle of Willis]). The thalamic perforating branches, as well as the medial posterior choroidal artery which proceeds to the plexus of the third ventricle, arise from the cisternal segment and require particular attention in the presence of basilar tip aneurysms.

Increased vascular filling in the posterior cranial fossa occurs after an arterial phase of approximately 3 s and a long capillary phase of 2 s, a period during which vascular staining is observed only in pathological cases. The anterior and posterior veins of the cerebellar surface draining into the great cerebral vein (vein of Galen) and the tentorial sinus can be differentiated, as well as, in some instances, the veins draining into the transverse and sigmoid sinuses. Perimesencephalic and prepontine veins are further visualized, and parapontine imaging of the vein of Dandy draining into the superior petrosal sinus is accomplished. In addition to the blood flowing through the jugular foramen into the bulb of the internal jugular vein, which also receives blood from the inferior petrosal sinuses and occasionally from the occipital sinus, the occipital emissaries participate, as a variation, in the drainage of the intracranial space. Vascular drainage is further achieved via

the basilar plexus located intradurally on the clivus, and via veins in the neighborhood of the foramen magnum travelling to the internal vertebral venous plexus. The basilar venous plexus may also be responsible for prognostically benign perimesencephalic subarachnoid hemorrhage (SAH), in this case an aneurysm is generally not detected.

The **indication for diagnostic angiography** of the vessels of the posterior cranial fossa is currently made in compliance with strict guidelines. While patients with malformations and tumors of the posterior cranial fossa previously also underwent angiography for the visualization of tumor vessels, or to at least enable the identification of the tumor location on the basis of the demonstrated arterial or venous displacement, today these examinations are carried out primarily in preparation for endovascular interventions. They become possible under certain prerequisites in the presence of vascular processes with stenoses and occlusions of the vertebral or basilar arteries. An investigation of the subclavian artery is further indicated when subclavian steal syndrome is suspected, as well as in cases of vascular malformations, primarily aneurysms, arteriovenous angiomas and dural AV fistulas. On occasion, conventional angiography is required for the preoperative identification of venous anomalies in the neighborhood of brainstem cavernomas, or of venous or sinus occlusions if CT angiography does not provide conclusive findings. Further indications include the confirmation of vasculitis, a disease which, comparable to degenerative vascular processes, is associated with arterial stenoses, although these may appear to be less punched out and can be accompanied by vascular dilatation. Angiography is also performed when intra-arterial treatment (thrombolysis or mechanical extraction of thrombi is considered as is discussed further below).

Safety measures to be considered regarding the application of contrast media, especially in patients with a history of allergic reactions, have already been discussed in the section on computed tomography. The specific **risk for neurologic complications** associated with diagnostic cranial vessel angiography remains unchanged and ranges from 0.5% to 1%, despite the use of modern non-ionic contrast media with reduced osmolality and the technological improvements of catheters and guide wires (Willinsky et al. 2003).

In addition to pareses, ataxias and eye movement disturbances represent the most severe complications in the vertebrobasilar system. The causes of these events may be small infarctions induced by embolic mechanisms that can be shown with diffusion weighted MRI in up to 20% of purely diagnostic angiographies, but remain in most cases clinically silent. The incidence of these lesions can be markedly reduced by using air bubble filters and heparinization of the contrast medium, as well as flush solution (Bendszus et al. 2004).

Transient amnesia and cortical blindness may develop following infusion of larger contrast agent volumes in patients with the respective disposition, although these events

usually occur only after one or two successive injections. These complications have been interpreted as posterior encephalopathy on the basis of typical MR findings (Saigal et al. 2004).

Radiation exposure is dependent upon the duration of angiography, and particularly on the screening time during cerebral interventions. The effective dose value for single interventions varies from 1.5 to 16 mSv, and may be in excess of 40 mSv for multiple procedures (Livingstone et al. 2003).

2.1.4.2 Endovascular Interventions

Recanalization

Recanalization is performed for vertebrobasilar stenoses and occlusions. These usually develop either as the result of a vascular wall lesion of atheromatous or inflammatory origin with localized thrombosis, or can be of atrial origin emboli due to dysrhythmia, septum defect, or generalized clotting disorders. The most common sites include the already relatively narrow origin of the vertebral artery from the subclavian artery, the intracranial V4 segment, as well as the entire course of the artery. The cervical vertebral segment may also very rarely be constricted from outside by osteophytes of the cervical vertebral joints. The symptoms, e.g. vertigo, can be provoked by certain neck or head positions.

Vascular compression may also be caused by **tumors** like meningiomas or tumors of the base of the skull at the craniocervical junction. Further causes involving both the vertebral and carotid arteries include **dissections** with bleeding within the vascular wall, e.g. following whiplash injury or chiropractic maneuvers; they may also occur spontaneously in vascular wall disorders, e.g. fibromuscular dysplasia. A distinctive feature of this distribution area is the **subclavian steal syndrome**. It develops as a result of retrograde vertebral artery blood flow in response to high-grade proximal subclavian artery stenosis or occlusion.

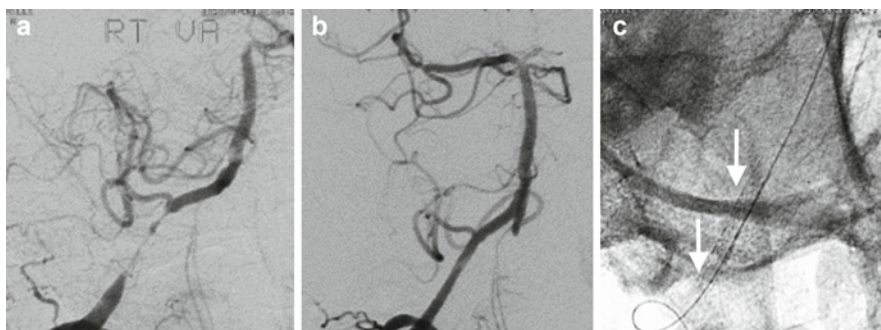
For the detection of vascular stenoses or occlusions, including those in the vertebrobasilar region, **Doppler sonography** represents the method of choice, followed by CTA or MRA techniques. Only when these do not provide a satisfactory confirmation of the tentative diagnosis, or if conflicting clinical findings are reported, can invasive conventional angiography be applied for diagnostic purposes. In the presence of proximal vascular processes, the origins of the vertebral arteries on both sides may be so severely narrowed that even short-term occlusions resulting from catheter insertion on one side are not tolerated. With a view to the possible development of brainstem ischemia, selective catheterization should be dispensed with for safety reasons, and the depiction of the vertebral artery should be attempted by means of a survey angiography of the subclavian artery, a

possibility to improve the quality in these cases is the simultaneous compression of the respective brachial artery manually or during blood pressure reading. Although this does not provide a high-contrast image, it is generally satisfactory to permit a conclusive diagnosis. In the setting of proximal vertebral artery occlusion, the depiction of the collateral supply via cervical branches of the subclavian artery – the ascending or the deep cervical artery – as well as of superior cervical anastomoses with the occipital artery may be required.

Endovascular therapy for stenoses of the vessels responsible for blood supply to the brain was introduced in the 1980s. While this initially involved widening of stenoses at the carotid bifurcation and in the proximal section of the subclavian artery in the presence of a steal syndrome (Kachel et al. 1991), these interventions were later also successfully performed at the origin of the vertebral arteries and, more recently, also along the extracranial and intracranial course of the vertebral and basilar arteries. The therapeutic intervention is initiated by introducing a guide catheter over which a micro guidewire and a microcatheter can be advanced through the stenosis. After an exchange-maneuver, a balloon catheter is then passed over the microwire and inflated to dilate the stenosis. Subclavian artery occlusions can also be recanalized in this manner, provided a guidewire is successfully advanced through the occluded passage from the proximal or distal lumen of the vessel (after puncture of the brachial artery). The inflated balloon does, however, not only push atheromatous plaque into the vascular wall, but may also cause dissections and thus the risk of distal emboli affecting the entire vertebrobasilar system if they develop in the subclavian artery. Acute thrombosis of the dilated vascular segments represents a further, albeit rare complication. The administration of platelet aggregation inhibitors (acetylsalicylic acid, clopidogrel) before and after the intervention is therefore indispensable. With the use of these agents, subclavian artery interventions, also without additional stent applications, were reportedly associated with the recurrence of vascular occlusions in only 10% of cases over a 5-year postinterventional period.

The prognosis for vertebral artery origin stenoses and intracranial artery stenoses after dilatation alone was less favorable, so that stenting was increasingly required to provide vascular wall support. In contrast to coil closure of aneurysms, where the stent serves to prevent coil loop prolapse into the parent vessel and wall stress in the artery is lower, stenoses have to be widened and patency of the lumen must be maintained. For this reason, primarily balloon-tipped models are mainly used for stenosis dilatation (Fig. 2.12). Vascular dilatation can be carried out after predilatation or concurrently with stent placement. Stents with a great radial force have to be employed in vertebral artery origin stenoses, similar to those used for renal artery origin stenoses, in order to ensure sustainable success. In the further course of the vertebral artery, specifically in the intracranial segment,

Fig. 2.12 Dilatation/stenting for intracranial vertebral artery stenosis persisting under anticoagulation therapy. Vertebral artery angiography (a) before and (b) after stent application in the subtracted image, native image (c) with stent (arrows)



high-flexibility stents have to be used to avoid injury to the vascular wall during placement. Self-expanding stents for use in the intracranial territory are available today, although in some instances redilatation may be required.

The risk for occlusion of the small arteries arising from intracranial segments of the vertebral and basilar arteries is apparently less high than initially assumed, due to the rare occurrence of ischemic complications in the area adjacent to the stent. This also applies to “overstenting” at the origin of larger vessels like the cerebellar arteries, which remain patent in the vast majority. The risk for complications associated with the intervention itself (ischemia, stent thromboses, bleeding) has been shown to range 9–15% (Weber et al. 2005; Kurre et al. 2010). Recurrences observed for coronary arteries unfortunately also occur in the cerebrovascular system. Six months after dilatation and stent therapy the incidence rate of intracranial residual stenoses ranged at 30%, while a rate of more than 40% was reported for extracranial residual stenoses, which were most frequently observed at the origin of the vertebral artery. These lesions were resymptomatic in more than a third of cases (SSYLVA Study Investigators 2004). The therapy of vertebral artery origin stenoses may therefore be started by dilatation without stent placement and the intervention can be repeated should restenosis occur. A staged procedure has recently been proposed for therapy of intracranial stenoses where dilatation and stenting is performed at intervals of several weeks. Overall, stent-assisted dilatation for arteries supplying blood to the brain is an area undergoing continuing development of materials and application techniques, and therefore does not enable a concluding statement at this time. An evidence-based advantage of invasive therapy over conservative treatment has not been demonstrated in the available literature.

The indication for stent-assisted dilatation of stenoses must thus be carefully considered. With respect to subclavian artery interventions it should be limited to patients with symptomatic steal syndrome, and in the presence of vertebral artery origin stenoses to patients with bilateral constrictions and ischemic symptoms persisting under anticoagulation therapy. The latter also applies to intracranial vertebral and basilar artery stenoses where collateralization via the posterior communicating artery does not infrequently occur.

Regarding the performance of **acute dissections**, reserve is also essential in judging the indication for interventional vessel dilatation, to prevent vascular wall bleeding from being pressed out with the subsequent danger of embolizations into distal regions. The thorough pre- and postinterventional therapy with thrombocyte aggregation inhibitors is indispensable for any stent application.

A different situation is encountered in patients with **acute occlusion of both vertebral arteries, or of the basilar artery** due to the very poor prognosis for the spontaneous course, where the omission of lysis is known to result in a mortality rate of 40%, as well as in the need for constant care in two thirds of survivors (Schonewille et al. 2005, 2009). While embolism represents the most common cause in the distal basilar segment, in the proximal segment pre-existing stenosis with subsequent thrombosis may be the causative factor. The occlusion should be removed as early as possible due to the otherwise poor prognosis, whereby the local procedure has been the preferred measure for over 20 years compared with systemic lysis. Similar to supratentorial acute infarction, basilar or vertebral artery occlusions always represent a medical emergency. In the absence of a conclusive Doppler sonography finding, the diagnosis of vascular occlusion can be confirmed by CT or MR angiography. In contrast to middle cerebral artery trunk occlusion, the time limit to fibrinolysis has not been definitely defined and depends on the clinical condition: a rapid, invasive procedure in the presence of progressing symptoms, but reserve in patients with symptoms of several hours or prolonged infarctions. All other contraindications to lysis therapy, comprising bleedings, injuries, or prior surgical interventions, must self-evidently be observed. The optimal therapeutic procedure for this entity is still under intense discussion (Schonewille et al. 2009; Schulte-Altdorneburg et al. 2009), the BASICS registry opened that field again. The intravenous versus the intraarterial use (with or without a bridging concept) of thrombolytic drugs is recommendable, the superiority of one of the concepts has not been thoroughly investigated.

Intra-arterial lysis is performed via microcatheter with the infusion of urokinase (upto 1,000,000 IU) or recombinant tissue plasminogen activator (rT-PA upto 100 mg). Alternatively,

glycoprotein IIb–IIIa inhibitors can be used. In thrombolytic therapy, the tip of a microcatheter is either advanced to the proximal end of the thrombus or the embolus, or moved past this within the vascular lumen with the help of a guiding catheter; lysis is then achieved on slow catheter withdrawal. Despite the application of high doses, recanalization of the arteries can be expected in only 44–80% of cases, depending upon the volume of the thrombus and the time interval to onset of lysis. In addition, there is the danger of embolizations into the superior cerebellar and the posterior cerebral arteries.

Mechanical thrombus removal is therefore frequently attempted, although with unpredictable success. Applied are wire loops, wire spirals and wire baskets for the retraction of an embolus, mechanical destruction using ultrasound or negative pressure (water jet pump effect), as well as “simple” aspiration via microcatheter, which is considered to be relatively effective, in particular in combination with preceding partial lysis (Fig. 2.13). The effectiveness of recent developments like mechanical thrombus fragmentation, brush-type microwires, and temporary stent insertion for acute therapy remains to be shown. Because proximal occlusions frequently occur in combination with stenoses, additional dilatation with stent application is recommended in these patients. A similar procedure is also possible for distal occlusions if lysis or mechanical thrombectomy is unsuccessful after a period of time.

However, the paucity of currently available data does not permit a definitive statement on the success of this procedure. Critical prognostic factors include the patient’s clinical condition, and the latency to vascular recanalization (Eckert et al. 2002). For each intervention, additional bridging to the onset of therapy is possible with systemic administration of r-TPA or eventually glycoprotein IIb–IIIa inhibitors, and additional postinterventional heparinization over a minimum period of 24 h is requisite. Since platelet aggregation inhibitors further have to be given when stents are used, the anticoagulation regimen needs to be tailored to individual needs, to avoid provocation of intracranial bleeding.

The reported survival rates for these invasive procedures currently range from 30% to 60%, while comparative independence was found in more than 50% of survivors (Pfefferkorn et al. 2005). The results of additional studies have to become available to ascertain if the results obtained

with this procedure are also improved according to evidence-based criteria over those obtained in patients undergoing conservative therapy or systemic lysis.

Embolization

Embolization is a therapeutic option for the treatment of vertebrobasilar aneurysms, arteriovenous angiomas and dural arteriovenous fistulas comparable to conditions in the “anterior” circulation. Two different types of aneurysms are observed in the posterior cranial fossa: berry-shaped aneurysms that classically develop at the junction of vessels where they form a saccular pouch, and fusiform aneurysms formed along the wall of the vessel as the result of a vascular wall disorder (degenerative, inflammatory, or after dissection). In the majority of cases, the first type leads to typical subarachnoid hemorrhage (SAH), or may be an incidental finding, while the second type is more frequently associated with symptoms of brain stem or cranial nerve compression and potential SAH.

Berry aneurysms of the vertebrobasilar system occur primarily at the tip of the basilar artery, with the aneurysm neck being located between the two posterior cerebral arteries, or between the posterior cerebral artery and the superior cerebellar artery, but less frequently at the origin of the PICA. They are rarely found at the origin of the AICA, or along the course of the basilar artery, the posterior cerebral artery, or the cerebellar arteries. Although they may occur in conjunction with arteriovenous angiomas. The incidence of vertebrobasilar aneurysm bleeding is markedly higher (1.8% p.a.) than in the anterior circulation, so that their therapy, including that of incidentally found aneurysms, is indicated for all sizes (Vindlacheruvu et al. 2005). After the occurrence of bleeding, emergency treatment should be commenced, due to the possibility of rebleeding, which places the patient at increased risk.

Out of two competing therapeutic options, i.e. neurosurgical **clipping** of the aneurysm neck and endovascular **coiling** of the aneurysm sack, endovascular intervention in the posterior circulation has gained a certain advantage over clipping, because of the difficult surgical access to the principal

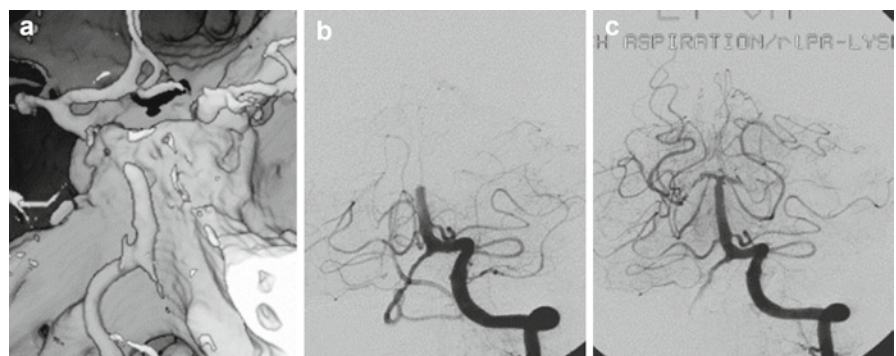


Fig. 2.13 Recanalization of an acute distal basilar artery occlusion. CTA (a) and DSA before (b) and after (c) recanalization. After only partially successful lysis with 10 mg rTPA, the residual (suspected embolic) material was aspirated via vertebral artery catheter. Residual posterior cerebral artery stenosis, *right*, and occlusion due to floated off emboli, *left*

locations. In the absence of very pronounced atherosclerotic changes in the vertebral artery, an aneurysm at the origin of the PICA, or at the tip of the basilar artery can be accessed via the endovascular route without major difficulties by experienced hands. Provided the aneurysm neck is small, a microcatheter is advanced to the site of the aneurysm and the aneurysm sack is occluded with detachable spiral coils (Fig. 2.14). Differently shaped coils consisting of platinum wires formed in the shape of a double helix are available for this procedure. The coils may be made of untreated metal, be coated with a hydrogel matrix, Dacron threads, or vasoactive substances. Separation of the coil from the delivery wire, which is retrieved later, can be achieved by electrolytic, thermic, or mechanical means.

Coil occlusion is, however, more difficult to accomplish in wide-necked aneurysms, where the aneurysm neck can be occluded with a temporary balloon during coiling to avoid coil protrusion into the parent vessel (**remodeling technique**). An assistive stent can also be used for this purpose, and is a suitable device with great flexibility but relatively low thrust force that has been available for a number of years. The disadvantage of this method in an acute patient is the need for anticoagulation, which is mandatory after stent application but requires complete aneurysmal occlusion and leads to difficulties in

the performance of subsequent procedures, e.g. the insertion of intraventricular drainage. The choice of the appropriate treatment option therefore needs to be agreed on in each individual patient by the neurosurgeon and the neuroradiologist. Reliable data on the benefit of one of these approaches over the other in the posterior fossa, in contrast to the vessels in the anterior circulation, was not shown by the results of the ISAT study (Molyneux et al. 2002), due to the small number of patients with vertebrobasilar aneurysms included in the study.

The decisive factor for the success of aneurysm coiling is the size, shape of the aneurysm sack and the configuration of the aneurysm neck. On average, therapeutic effective (sub) total occlusion can be expected in 80% of cases. The periprocedural complication rate of incidental aneurysms, without consideration of sequelae after bleeding, ranges below 5%. Coil compaction or widening of the aneurysm neck may lead to recurrence (~15%). Angiographic follow-up studies are therefore recommended after 6 months and 2 years; at these time points a re-coiling (Fig. 2.15) may be performed (Berkefeld et al. 2004). Recurrent bleeding occurred in 1% of

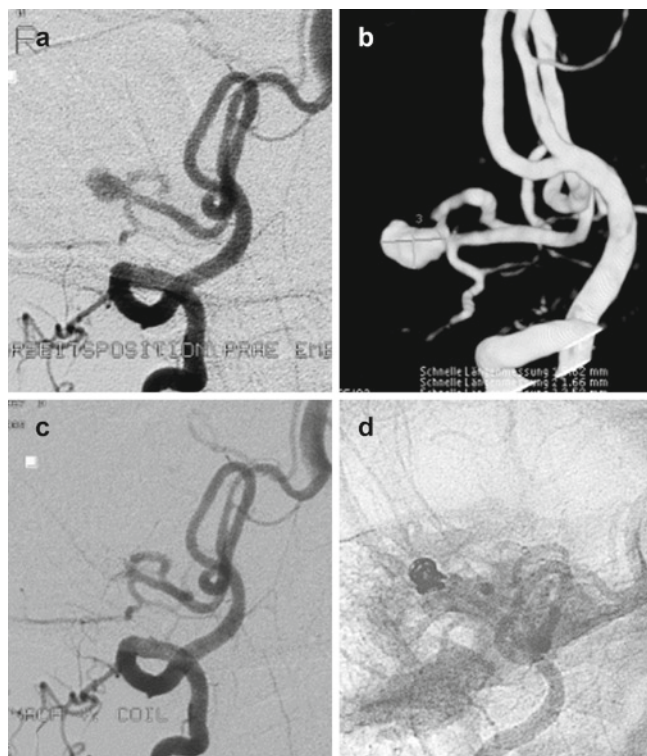


Fig. 2.14 Coil occlusion of a distal posterior inferior cerebellar artery aneurysm following acute subarachnoidal bleeding. DSA and 3D angiography (a, b) prior to and after (c) coiling of the aneurysm with visualization of the coil packet in the unsubtracted image (d)

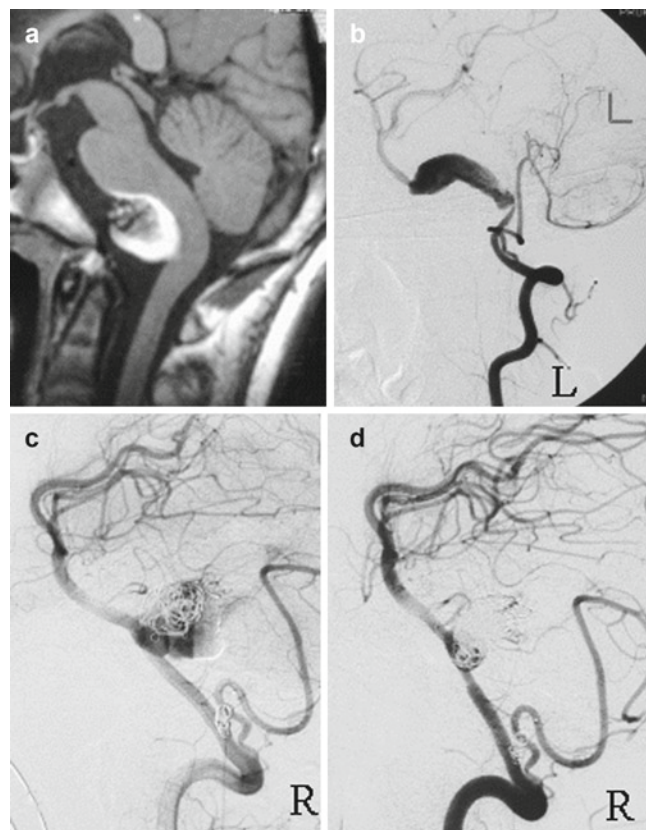


Fig. 2.15 Coil occlusion of a fusiform vertebral artery aneurysm left with brainstem compression. MRI with partially thrombosed aneurysm before intervention (a), vertebral DSA left before coil occlusion (b) and vertebral DSA right before a second intervention with recanalization and widening of aneurysm (c). After stent application via the vertebral artery right, and repeat coil occlusion of the distal aneurysmal segment (d)

cases during the first 12 months after coil occlusion, but developed less often after clipping. The findings of the ISAT study (Molyneux et al. 2002) showed a significant and durable better clinical result – at least in the anterior circulation – after the endovascular procedure than after neurosurgical clipping.

Fusiform aneurysms of the vertebral or basilar arteries can lead to life-threatening brainstem compressions. The prognosis is also very poor in patients with vasodilatation developing after a dissection with intracranial bleeding. If an additional circumscribed saccular dilatation is present in the fusiform dilated segment, this can be treated with a neurosurgical or endovascular approach (using stenting and coils as in saccular aneurysms). Although coiling does not remove the space-occupying mass, it can reduce pulsations and thus lead to an improvement of symptoms. Occlusion of the entire dilated segment with clipping or coiling (trapping) represents a therapeutic alternative. In this setting, a balloon occlusion test has to be carried out prior to clipping/coiling to ensure that the described occlusion will be tolerated. Another alternative is occlusion of one or even both vertebral arteries in the V4 segment to achieve a change in flow dynamics (although its form can not be accurately predicted) in an attempt to effect (partial) embolization of the aneurysmal lumen.

The prerequisite for this procedure is, once again, adequate collateralization of the basilar artery via the cerebral arterial circle. Closed-wall stents (covered stents), very fine-meshed stents (flow-remodelling stents) and multiple telescoped intracranial stents are capable of blood flow modelling that enables extensive reconstruction of the original vascular lumen and thus offers further therapeutic options. Techniques like that were previously limited by the unsatisfactory flexibility of previously available stents (Saatci et al. 2004).

Only 5–20% of cerebral **arteriovenous angiomas** or **malformations (AVM)** are found at an infratentorial location, with only 25% of these being situated in the brainstem. They may occur as part of a general “angiomatosis,” e.g. Osler’s disease, or Wyburn-Mason syndrome. They can become manifest most frequently in the form of bleedings and less often with neurologic deficits. Whether the tendency to hemorrhages is increased compared to the supratentorial location is controversially discussed.

The precarious location renders both neurosurgical and endovascular interventions difficult, because not only misembolization into non-target arteries, but also perinidal edema and hemorrhages may occur after successful embolization.

If an occlusion of the respective segment is nevertheless indicated in patients with rebleeding or progression of symptoms, and in view of the fact that the size of brainstem AVMs is generally in the favorable range of below 10 mm,

stereotactic radiation represents the therapy of choice. However, the finding that post-therapeutic perinidal gliosis and rebleeding may occur until the time of definitive obliteration of the vessel after a period of up to 3 years has to be accepted. Successful embolization of brainstem AVMs has been reported in a small series of patients, in whom the usual procedure (injection of a *N*-butyl-cyanoacrylate [NBCA]-lipiodol mixture into the nidus via microcatheter) was performed without significant complications, although complete obliteration was achieved in only one out of six patients (Liu et al. 2003). On principle, embolization is a factor which requires consideration in the decision on the therapeutic concept for brainstem AVMs.

Comparable to pial AVMs, **dural arteriovenous fistulae (DAVF)** can cause bleeding and neurologic deficits, the latter developing as a result of venous reflux leading to edema and subsequent gliosis. DAVFs of the posterior cranial fossa are supplied by branches of the external occipital artery, the ascending pharyngeal artery, the medial and posterior meningeal arteries, as well as by the internal carotid artery (tentorial artery), that drain primarily into the sigmoid and transverse sinuses. In uncomplicated cases they may cause pulse-synchronous bruits in the ear. In cases of orthograde drainage (Borden Type I) there is no absolute need for therapy. In the presence of additional sinus stenoses, retrograde drainage into the cranial veins may develop (Borden Type II); this may further be observed in lesions located on the border of the tentorium. There may also be direct shunt drainage into the leptomeningeal veins (Borden Type III), which are then frequently characterized by circumscribed stenoses and widening (Szikora 2004). As space-occupying masses, the latter can cause brainstem and cranial nerve compression. Involvement of the cranial nerves is often associated with subarachnoidal or intracerebral bleedings, so that shunt occlusion must always be attempted when cranial nerves are involved.

While a short-term improvement may be observed following transarterial embolization with particles, NBCA or Onyx[®], the ramified vascular network can only less often be completely occluded with this therapeutic measure. Because the actual fistula points are mostly confined to a circumscribed region of the drainage vein, this region can be coil occluded via a transvenous approach, which enables complete obliteration of the fistula. Prior to this intervention it has to be angiographically confirmed that no other cranial veins drain into the segment designated for occlusion. This is of particular importance for fistula drainage into the transverse or sigmoid sinuses, whose occlusion could otherwise lead to bleeding due to passive hyperemia.

Available alternatives to the endovascular approach in the therapy of DAVFs or incomplete fistula obliteration include neurosurgical interventions, e.g. “skeletalization” of a sinus, or stereotactic radiation.

2.2 Ultrasound Diagnostics

Martin Eicke and Uwe Walter

Ultrasonic diagnostic procedures of the brainstem have undergone continuous development over the past 20 years. The possibility of non-invasive identification of intracranial vertebrobasilar stenoses was first opened with the introduction of transcranial Doppler sonography in the mid-1980s. The advent of color duplex systems in the early 1990s saw the beginning of the age of accurate anatomic localization of intracranial vessels. The further development of duplex systems finally enabled transcending the boundaries of “classical” vascular ultrasound and placing image-morphologic aspects in the foreground of scientific research.

The potential of this method has not yet been exhausted, in particular with regard to the therapeutic possibilities for extrapyramidal system diseases.

The following chapter therefore discusses both the aspects of vascular ultrasound as the currently well established standard procedure and the possibilities of intracranial morphologic B-mode image diagnostics.

2.2.1 Vascular Ultrasound

2.2.1.1 Anatomic Principles

Extracranial course: The origin of the vertebral artery (V0) is the preferred site of atherosclerotic plaque formation in this vessel and the entire posterior circulation. Endothelial rupture due to the physiologic presence of shearing forces and turbulences develops particularly frequently in this region and may lead to emboligenic stenoses in the further course. The hemodynamic risk of proximal stenosis or occlusion is relatively low, as extensive anastomoses usually provide sufficient distal vessel refilling via the contralateral vertebral artery or branches of the external carotid artery. The vertebral artery then travels craniad, anterior to the scalene muscle (prevertebral segment, V1) and enters the costotransverse foramen at the level of the sixth vertebra (transverse segment, V2). Distal to the foramen of the axis it initially curves at a 90° angle lateralward and runs again upward; after issuing from the foramen in the transverse process of the atlas the vessel bends backward at a right angle (V3). It finally curves medially and crosses the atlas via the vertebral artery sulcus (atlas segment, atlas loop); in this region the vessel is also predisposed to atherosclerotic changes and trauma, due to its pronounced tortuosity. The vertebral artery then pierces the posterior atlantooccipital membrane as well as the dura mater and continues in a rostral direction in the intracranial subarachnoid space (intracranial segment, V4).

Intracranial course: The intracranial location of the vertebral arteries varies considerably, as significant side shifting may develop. The basilar artery arises at the confluence of the vertebral arteries and is approximately 30 mm long and 3 mm in diameter. In the majority of individuals the vessel courses rostrally in the midline, but in 10–20% of individuals extensive deviations to the right or left may be observed.

2.2.1.2 Principles and Techniques

Three different system types are used in vertebrobasilar diagnostics:

- Continuous wave (cw) doppler
- Pulsed doppler sonography
- Color duplex sonography

Continuous Wave (cw) Doppler

This instrument evaluates the so-called Doppler shift, the frequency differences between the emitted and the reflected signal. According to the Doppler equation, this frequency difference is dependent on the relative speed of the reflector in relation to the probe on the one hand, and the emitted output frequency on the other hand. Frequency shifts resulting at the usual output frequency of 4 MHz and physiologic flow velocities of 10–200 cm/s, extend from 0.2 to 16 kHz, and are therefore within the audible frequency range of the human ear.

The advantages offered by these instruments are that they are easy to handle, reasonably priced, and offer excellent sensitivity. Depth localization is not possible. Conversion of the frequency shift (kHz) to velocity values is not admissible in the presence of an unknown insonation angle.

Examination technique: In particular segments V0 and V3 are amenable to examination with cw Doppler sonography. With the transducer held medial and caudal, V0 is imaged approximately 3 cm above the clavicle. The vertebral artery can be differentiated from other vessels in this region (particularly the common carotid artery, thyrocervical trunk) by the strong reverse Doppler effect on intermittent compression in the region of the atlas loop.

Optimal visualization of V3 below the mastoid can be achieved with the patient’s head turned slightly to the contralateral side. In contrast to the internal carotid artery, the vertebral artery can typically be depicted with the flow towards the transducer as well as, with slight tilting of the transducer, away from it. While extracranial vessels like the occipital artery can be compressed by applying pressure to the vessel with the transducer tip, which leads to the loss of the Doppler signal, this is generally not possible (except in very slim patients) on insonation of the vertebral artery.

Pulsed Wave Doppler Sonography (pw Doppler)

Pw Doppler devices offer the additional option of depth allocation. Selective presetting of a time window of interest between transmission and reception enables analysis of the reflected signal from a specified depth window. One advantage among others is that a vessel can be followed along its course deep into the tissue. In vertebrobasilar ultrasound this procedure is particularly appropriate for V4/basilar artery examinations with the use of a low frequency 2 MHz transducer capable of deep penetration.

Examination technique: The patient should be in a sitting (or supine) position and lower the chin as far as possible to the chest. The transducer is placed in the midline, approximately 3 cm below the occipital tubercle. On slight turning of the transducer, the right and left vertebral arteries can generally be differentiated at a depth of 60–70 mm, due to the availability of different spectral frequencies and pulsilities. The vessels can frequently be imaged with bidirectional flow to a depth of 65 mm (atlas loop), and at greater depths only with flow away from the transducer. The vertebral arteries can serve as guide vessels to the basilar artery. In the evaluation, consideration must be given to the fact that the identification of the exact transition zone of the vertebral arteries and the basilar artery by means of pw Doppler can be made only with great reservations. Findings reported in the literature vary, depending on the application pressure, from 70 to 110 mm (!) (von Büdingen and Staudachet 1987; Ringelstein et al. 1990).

It is therefore indispensable that a minimum depth of 100 mm is reached for secure identification of the proximal basilar artery. Complete visualization of the basilar artery to its division into the posterior cerebral arteries (tip of basilar artery) is possible in maximally 70% of cases, owing to deterioration of the signal-to-noise ratio. (von Büdingen and Staudachet 1987). A conversion of the frequency shift (Hz) into flow velocity is usually preferred by most sonographers on insonation of V4/basilar artery. The basis for this is the assumption that the insonation angle may be $<30^\circ$ and can therefore be disregarded.

Color Duplex Sonography

In the performance of color duplex sonography color coded sonographic flow velocity information is superimposed onto the morphologic information provided by the B-mode image. Furthermore, a spectral Doppler image (pw mode) can be derived from the vessel segment of interest using the B-mode image. Because the vascular band can be identified along its course and at its location in the tissue by means of the B-mode image, it is possible to perform an angle correction, which enables conversion of the measured frequency shift (Hz) into physiologic flow velocity data (cm/s). In section V3, the differentiation between an

atherosclerotic lesion and a dissection can be made in individual patients. However, the vertebral artery is located deeper in the tissue along its entire course than the carotid artery, so that the image quality is poorer due to signal attenuation and can not compete with the resolution obtained for the carotid arteries. Duplex sonography can, on principle, be used for all of the described vessel segments. It further enables examination of the V1 and V2 segments.

Examination technique: In a first step, the distal common carotid artery is visualized inclusive of its bifurcation. The transducer head is then tilted so that the ultrasound beam is directed laterally, in order to image the dorsolaterally located vertebral artery. It is normally readily identifiable between the vertebrae (acoustic shadow), by means of color coding and is located directly below the vertebral vein. From here it is possible to advance segment by segment to caudal or cranial.

While optimal visualization of segments V0–V3 is accomplished at a frequency of 5 MHz, a 2–2.5 MHz transducer must be used for imaging of V4/basilar artery due to its location at a greater depth. Scanning with this transducer does not provide information on plaque morphology. A disadvantage of color duplex sonography is the frequently inadequate visualization of deeper basilar artery segments due to its moderate color sensitivity. To compensate this effect, the additional application of an ultrasound signal enhancer is frequently required.

2.2.1.3 Ultrasound Signal Enhancers

The relatively great depth and small diameters of the vessels to be examined are factors that diminish the diagnostic power of ultrasound in a large number of patients.

Ultrasound enhancers are particles capable of enhancing the signal by 10–30 dB after entering the circulation. Currently available substances for signal enhancement consist of two components: gas and an encapsulating outer shell. The presence of the gas is crucial for signal enhancement, while the shell “only” serves to stabilize the bubble. When the sound beam reaches the interface between the liquid and the gas, the different high impedance triggers a strong reflection, which leads to signal enhancement at the receiver. The substances for signal enhancement are able to pass through the capillary bed and, as a rule, enable better visualization of the vascular system over a period of 3–5 min. The substances with current regulatory approval are shown in Table 2.1.

Levovist® (legally approved in Germany, Italy, France and Spain) is contraindicated in patients with galactose (not lactose!) intolerance.

Due to three reported deaths of patients with cardiopathies, SonoVue® (EMA approved; FDA approval applied) is contraindicated in patients with acute coronary syndrome and clinical instability.

Table 2.1 Ultrasound contrast agents with current regulatory approval for use in (transcranial) signal enhancement

Signal enhancer (Trade name)	Gas	Outer shell	Approval
Levovist® 4 mg	Galactose-air microparticles	Palmitic acid	D, E, F, I
SonoVue®	Sulphur hexafluoride	Phospholipids	EUR, Asia FDA approval (12/2010)

The application of signal enhancing substances in the vertebrobasilar system is expedient in the absence of visualization of the V4 segments and the basilar artery. Visualization of the V4 segments is achieved in most patients with these substances; an average improvement in the penetration depth of about 1 cm to a maximum of 10 cm has been reported for the basilar artery. The tip of the basilar artery is, however, usually not reached (Brunner-Beeg and von Reutern 1999; Iglseder et al. 2000).

2.2.1.4 Reference Values

“Reference values” are overall less reliable than in the anterior circulation, because the vertebrobasilar system is characterized by a wide inter- and intraindividual range of flow velocities. Furthermore, pronounced caliber differences are often found when making a bilateral comparison, so that the direct bilateral comparison is of lesser importance here than, e.g. in assessing the carotid arteries.

Pulsatility is lower, the more cranial the examination of the vessels is performed: a typical finding for vessels with pronounced downstream parenchymal perfusion.

The presence of vertebral artery hypoplasia (2–4%) represents a physiologic variation from the norm. The average diameter of this vessel is 3.81 ± 0.46 mm (Bartels et al. 1991) in the V2 segment, so that hypoplasia is defined as a vessel with diameter of <2.5 mm. Typical in hypoplasia is a change in the Doppler spectrum in terms of a resistance profile, due to the fact that the hypoplastic vessel does not connect to the basilar artery which supplies the brain. This finding should not be confused with a pathologic resistance profile in vascular occlusion. In these cases the vessel diameter is not reduced.

2.2.1.5 Stenosis Criteria

One of the **primary (direct) stenosis criteria** is an increase in flow velocity in the region of the stenosis, where the highest values are measured immediately poststenotically, in the so-called jet. The presence of a stenosis $>95\%$ and subsequent decreased flow volume, lead to a reduction in flow velocity, which may be characterized by pseudonormal values. A

Table 2.2 Stenosis criteria in the V4/basilar artery territory (according to Widder et al. 1999)

Finding	Criteria	Flow velocity (cm/s)
Definitive finding of stenosis	Maximum systolic value <i>and/or</i> Mean value	≥ 120 ≥ 70
High suspicion of stenosis	Maximum systolic value <i>and/or</i> Mean value <i>and/or</i> Significant flow disturbance	≥ 100 ≥ 60

serviceable categorization was proposed by Widder for the region of the V4 segment and the basilar artery (see Table 2.2).

A more differentiated allocation of stenoses to appropriate grades on the basis of primary stenosis criteria, analogous to the procedure for the internal carotid artery, is difficult; it is not essential in clinical practice. No results of studies demonstrating the need for making the choice of the therapeutic procedure contingent upon the allocation to a precise stenosis grade have been published thus far.

Secondary stenosis criteria comprise changes in the flow profile, which are verifiable as indirect results of a major flow obstacle:

- **Prestenotically**, reduced diastolic flow velocities in terms of a resistance profile serve as indicators of a distally located high-grade stenosis. In particular the detection of diastolic zero flow provides objective evidence of a downstream severe, high-grade stenosis or vascular occlusion. Hypoplasia must, however, be excludable in the B mode image. Differentiation between a distal occlusion and severe high-grade stenosis is frequently not possible (Fig. 2.16a).
- **Poststenotically**, reduced pulsatility with a relatively high diastolic flow velocity at a markedly reduced systolic flow velocity is an indicator of a major flow obstacle (Fig. 2.16b).

Tertiary stenosis criteria provide evidence of collateral vessels which are demonstrable only in the presence of high-grade stenoses. It has to be taken into consideration that in the presence of a unilateral vertebral artery occlusion/high grade stenosis, the contralateral vessel functions as the collateral vessel and may be physiologically characterized by a corresponding long-segment (slight to moderate) increase in flow velocity. Proximal vertebral artery occlusions are generally well collateralized by external vertebral artery anastomoses in segments V2–V4, which usually enable the demonstration of a return to normal flow conditions as early as in the V4 segment. In high-grade proximal basilar artery stenosis/occlusion or bilateral vertebral artery occlusion, retrograde filling of the basilar artery via the posterior communicating artery may occur in particular cases (thereby enhancing survival of the patient).

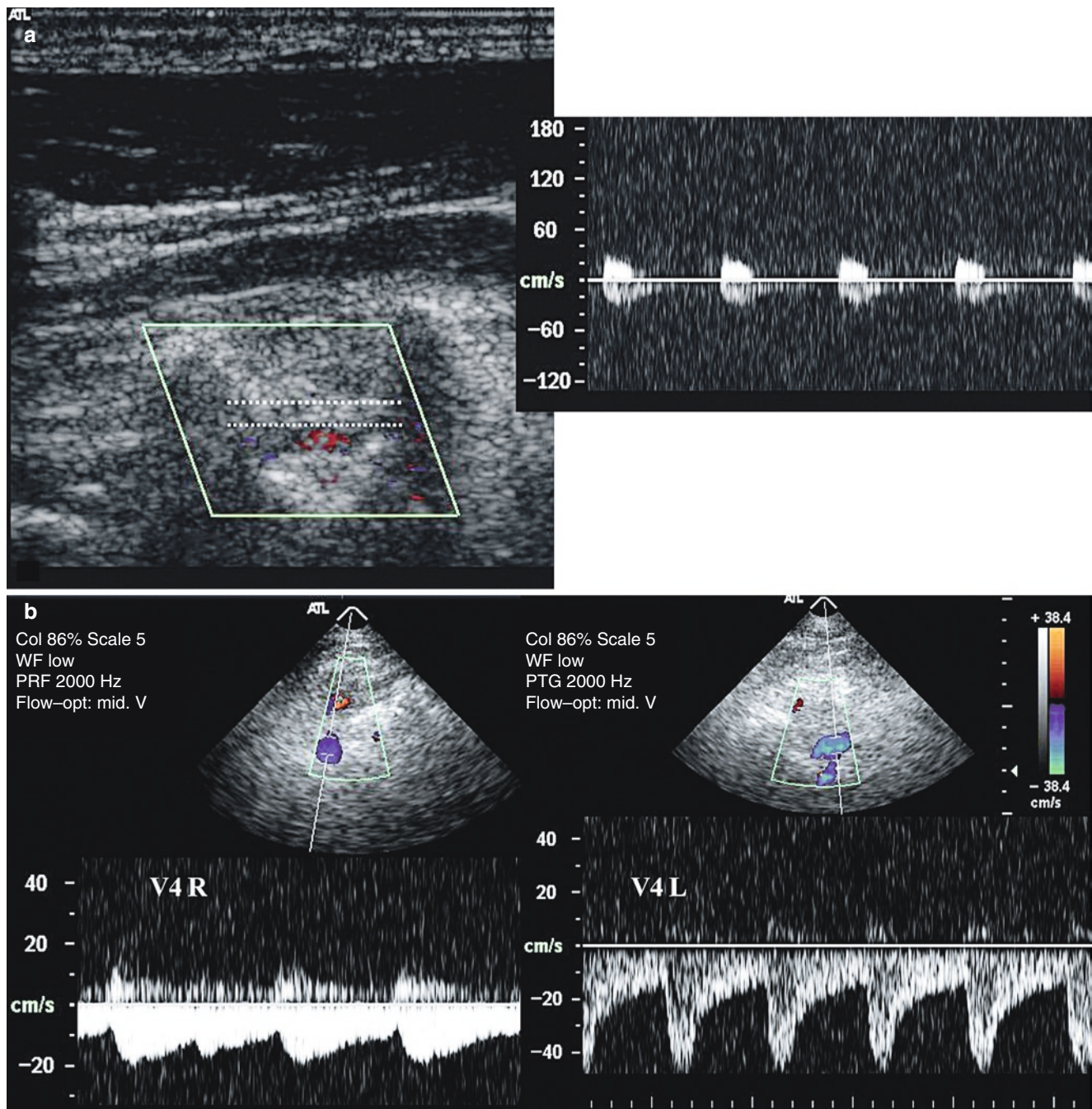


Fig. 2.16 (a) Vertebral artery dissection (V2). The dissection membrane is represented in the B mode image, the remaining lumen is narrowed. Diastolic flow (resistance signal) is absent prestenotically.

(b) Transcranial insonation of the same patient: color duplex shows post-stenotic flow in the left V4 segment normal right V4 segment. Confluence of the vertebral arteries and the proximal basilar artery are visualized

2.2.1.6 Clinical Application

Brainstem Infarction/TIA

The documentation guidelines issued by the German Society of Ultrasound in Medicine (DEGUM) and the American Institute of Ultrasound in Medicine (AIUM) call for mandatory visualization and documentation of the V2 segments at each color duplex examination, and respectively of the V3

segments on cw Doppler investigations. The examination of both these segments enables an initial assessment of the presence of a severe proximal or distal flow obstacle. When indicated, the finding has to be supplemented by an examination of the V0/V1 segments. In TCD, independent of the intracranial transtemporal finding, an additional transcranial assessment of the V4/basilar artery segment should be carried out. Results of large randomized studies on the therapeutic consequences of a diagnostically conclusive stenosis are not

available at this time, although interventional therapies may certainly be expected to open up new options for the therapy of recurrent refractory brainstem ischemias. Currently reported data showing a high re-stenosis rate of 47% do, however, not justify routine stent application, or surgical intervention with transposition of the proximal vertebral artery to the common carotid artery.

Basilar Artery Thrombosis

The diagnosis of basilar artery thrombosis is a controversially discussed topic. Due to its non-invasiveness sonography is, on principle, a valuable tool for establishing this diagnosis. Nevertheless, the basilar artery can frequently, at least in the distal segment (basilar tip thrombosis), not be conclusively diagnosed, owing to its location deep in the tissue. Furthermore, flow profiles in the proximal basilar artery without abnormal findings do not permit exclusion of a distal occlusion. Although ultrasound signal enhancers are able to improve the sensitivity of this method significantly, their use does not permit the definite exclusion of a thrombosis. Only in case of bilateral preocclusive flow signals in the vertebral arteries and missing signal of the basilar artery the diagnosis of proximal basilar artery thrombosis can be established with relatively great diagnostic certainty.

Subclavian Steal Syndrome or Subclavian Steal Phenomenon

The patient with subclavian steal syndrome typically complains of non-specific dizziness, in some cases also of loss of consciousness after muscular stress in one arm. Subclavian artery syndrome is a consequence of an occlusion or high-grade stenosis of the subclavian artery or the brachiocephalic trunk. To meet the oxygen requirements in the lower arm, collateralization occurs via the contralateral vertebral artery or, in some instances additionally, via the basilar artery, leading to retrograde flow in the ipsilateral vertebral artery. The identical hemodynamic finding, occurring in an asymptomatic form, is described as a subclavian steal phenomenon.

Examination technique: In addition to occlusion or a stenosis signal of the subclavian artery, the steal syndrome

in the contralateral vertebral artery is characterized by orthograde relatively high flow velocities. In the ipsilateral vertebral artery of a patient with the full clinical picture of subclavian steal syndrome, complete flow reversal can be identified already during rest. Because the flow profile can bear a striking resemblance to a normal flow profile (but: absence of early diastolic aortic valve reversion phenomenon!), attention needs to be paid to the flow direction in performing any routine imaging procedure of the vertebral artery. An initial finding in “incomplete” steal effect consists of systolic deceleration at unchanged diastole. At later stages, pendulous flow with retrograde flow during systole and orthograde flow during diastole are observed.

Subclavian steal syndrome can further be provoked with the **brachial artery ischemia test** (Fig. 2.17): the brachial artery is first compressed – by means of inflation of the pressure cuff to suprasystolic values over 1 min – to cause ischemia in the lower arm. The peripheral arterioles in the arm are thus maximally dilated and compensatory hyperemia is triggered on sudden decompression. This leads to an immediate effect in the ipsilateral vertebral artery in the form of instantaneous retrograde flow in the vessel, or to enhancement of the retrograde flow component. This test can be performed additionally in the basilar artery to assess the effect on this vessel (carotidobasilar overflow).

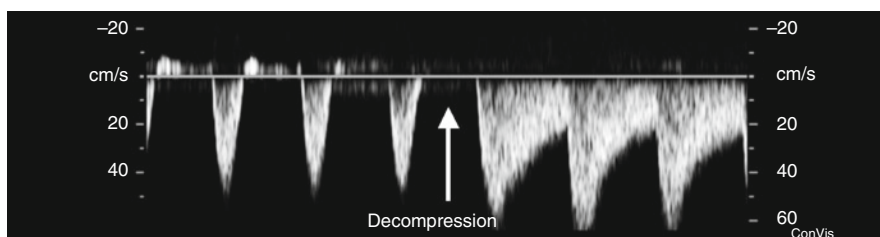
The possibility of dynamic and continuous recording offered by Doppler sonography makes it the method of choice for the diagnosis of steal effect.

Rotational Vertebral Artery Occlusion

A differential diagnosis is proposed in patients complaining of head rotation related vertigo and syncope (Hunter’s stroke) to confirm the suspected presence of rotational vertebral artery occlusion. In particular patients with known unilateral vertebral artery occlusion report that the symptoms are regularly provoked on extreme rotation of their head. Principal causative factors comprise processes in the region of C II/III; degenerative bony structures, ligaments, as well as muscles may compress the vertebral artery on head rotation (Netuka et al. 2005).

Examination technique: Alternatively, cw Doppler may be used to visualize the V3 segment, and the V2 segment may be examined with duplex sonography. During

Fig. 2.17 Subclavian steal effect. Pendulous flow (V2) with systolic deceleration (retrograde flow) and orthograde diastolic flow at ipsilateral subclavian artery stenosis. Complete flow reversal after decompression of the brachial artery



rest the vertebral artery is usually represented without abnormal findings. The patient is then asked to move the head in such a way that the symptoms are elicited. The diagnosis is confirmed in the presence of a change from an unremarkable Doppler signal into a high resistance Doppler signal with disappearing diastole at the concurrent development of clinical symptoms.

2.2.2 B-Mode Sonography of the Brainstem

The use of transcranial B-mode sonography of the brainstem is expedient for particular neurologic and psychiatric disorders, as it is capable – superiorly to conventional MRI – of showing specific changes in the substantia nigra and midbrain raphe. Ground-breaking was the discovery of characteristic findings in Parkinson's disease and depression (Becker et al. 1995a, 1995b). These findings have since been replicated and clinical applications have been defined.

2.2.2.1 Principles and Techniques

Imaging is performed using an optimized ultrasound system with a phased array sector transducer (1.6–2.5 MHz). On principle, the same transducer as that applied for color duplex sonography can be used; a number of different equipment manufacturers have, however, developed special transducers providing higher resolutions for B-mode imaging.

Generally selected **device parameters** include an image depth of 14–16 cm, and a dynamic range of 45–50 dB.

The examination is carried out using the temporal bone window in axial section, with the transducer being placed preauricularly, parallel to the orbitomeatal line. Despite optimization of the image parameters (image brightness, time gain compensation, among others), brainstem assessment is not possible, or possible to a limited extent only, in 5–10% of

patients. During the examination consideration has to be given to the fact that axial image resolution is superior to lateral image resolution. Tissue harmonic imaging (THI mode) is capable of improving resolution, although it is even more strongly dependent on the insonation window; it has, not yet been sufficiently investigated by relevant studies.

In the sectional image the mesencephalon is viewed as a butterfly-shaped hypoechoic structure surrounded by the strongly echogenic cisterns (Fig. 2.18). The echogenicity of the following structures is assessed in this plane: the ipsilateral **substantia nigra** – appearing as a patchy area or as a delicate band, the ipsilateral red nucleus, and the median brainstem raphe. **Hyperechogenicity** denotes an abnormally increased intensity or area of the ultrasound echo compared with a normal finding. The gradation of echogenicity can be done semiquantitatively according to the visual impression or – in particular for the substantia nigra – quantitatively by planimetric measurement of echogenic areas (Fig. 2.19). Because planimetric measurements are device- and transducer-dependent, reference values have to be established in larger normal populations separately for each ultrasound system. A marked increase in substantia nigra hyperechogenicity exists at values above the 90% percentile measured in the normal population, moderate substantia nigra hyperechogenicity is present at values above the 75% percentile (Berg et al. 2001a). On measurement with the Siemens Sonoline Elegra system, substantia nigra areas smaller than 0.20 cm² are classified as normally hyperechogenic, areas ranging from 0.20 to 0.25 cm² are classified as moderately, and areas as of 0.25 cm² as significantly hyperechogenic. Echogenicity of the median raphe is assessed semiquantitatively (Becker et al. 1995b). In normal conditions the raphe nucleus is viewed as a continuous linear structure (Fig. 2.20). Echogenicity is regarded as being moderately reduced when the raphe nucleus is still identifiable, but viewed as a low-echogenic or interrupted band; echogenicity is considered to be significantly reduced when the raphe nucleus – despite good visualization of the nucleus ruber – is not differentiable from the surrounding midbrain parenchyma.

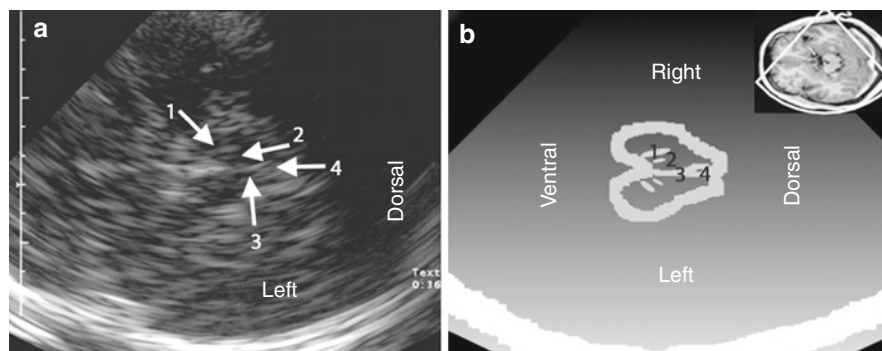


Fig. 2.18 Sonogram of the brain. (a) Axial section at midbrain level. The contralateral cranial bone is readily identified as a bright structure at the lower edge of the image. At the center, the mesencephalon is viewed as a butterfly-shaped hypoechoic structure surrounded by the strongly echogenic basal cisterns. Visualized at increased echogenicity in the midbrain cross section is the substantia nigra bilaterally

(ipsilateral: arrow 1), the nucleus ruber bilaterally (ipsilateral: arrow 2), the median brainstem raphe (arrow 3), as well as the aqueduct (arrow 4). (b) Schematic representation of (a); 1 ipsilateral substantia nigra, 2 ipsilateral red nucleus, 3 brainstem raphe, 4 aqueduct. The image inserted at the top right shows a corresponding MRI image for easier orientation

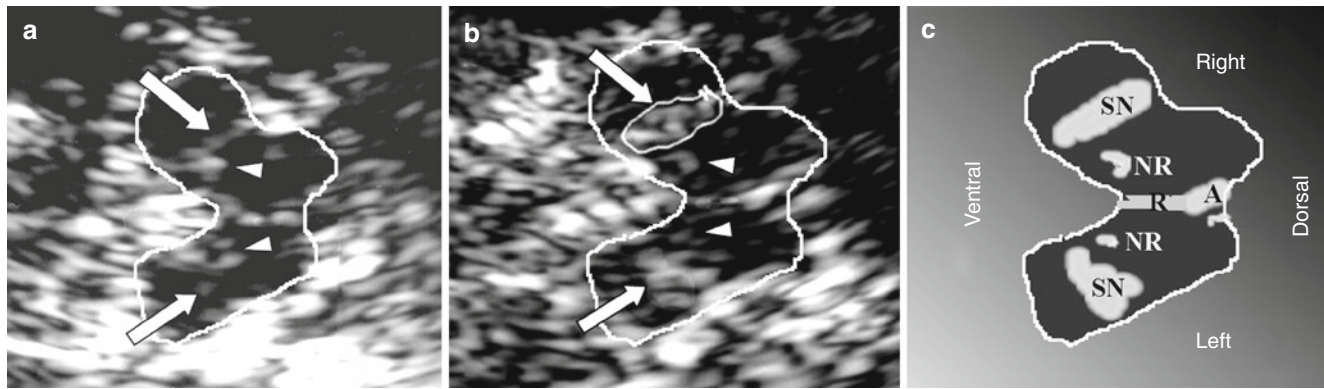


Fig. 2.19 Substantia nigra in axial sonogram of the midbrain. (a) Unremarkable finding: the substantia nigra is viewed as a delicate echogenic band- or patch-shaped structure (arrows). Also readily identifiable is the border echo of the red nucleus bilaterally (arrow heads). (b) Pathologic finding: the substantia nigra is markedly hyperechogenic

bilaterally (arrows). The assessment and planimetric measurement of the surface area is always done ipsilaterally. For this measurement the substantia nigra was traced with the cursor. The red nucleus can be differentiated bilaterally (arrow heads). (c) Schematic representation of (b): SN substantia nigra, NR nucleus ruber, R raphe A aqueduct

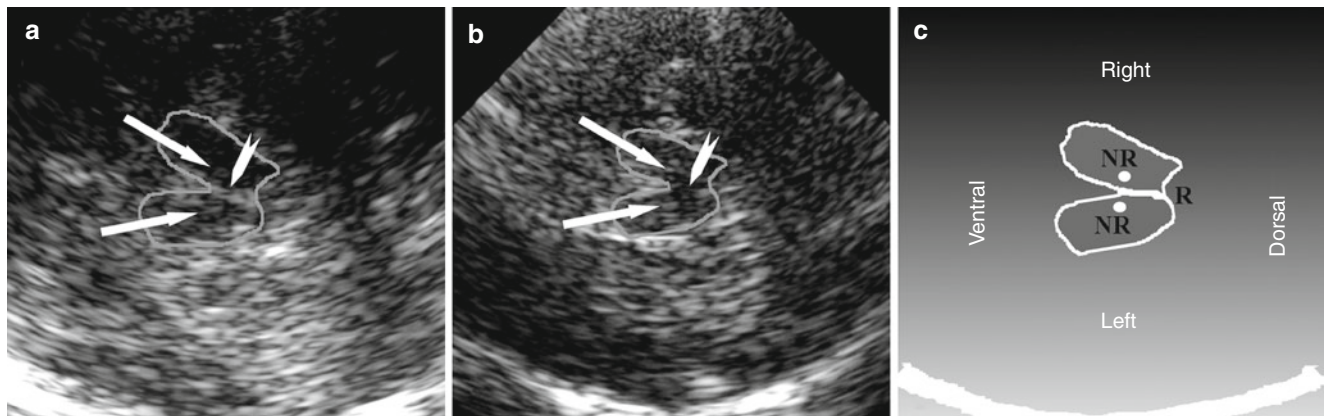


Fig. 2.20 Brainstem raphe in an axial sonogram of the midbrain. (a) Abnormal finding: despite good visualization of the nucleus ruber bilaterally (arrows), the brainstem raphe (arrowhead) is not represented; a significantly reduced echogenicity is noted. (b) Unremarkable finding:

the midbrain raphe (arrowhead) is viewed as a distinctly echogenic, linear, continuous structure (arrow: nucleus ruber). (c) Schematic representation of (b): NR nucleus ruber, R – raphe

2.2.2.2 Clinical Application

Early Diagnosis of Idiopathic Parkinson's Disease

Approximately 95% of patients with idiopathic Parkinson's disease show substantia nigra hyperechogenicity that is pronounced in 73–79%, and moderate in about 20% of cases (Berg et al. 2001b; Walter et al. 2006a). No significant differences in substantia nigra echogenicity were found for the clinical subtypes (akinetic-rigid subtype, equivalent subtype, tremor-dominant subtype). Higher substantia nigra echogenicity is observed primarily contralaterally to the clinically affected side. It remains stable during the clinical course; a more pronounced manifestation correlates with an early onset and slow progression of Parkinson's disease (Schweitzer et al. 2006). The cause of substantia nigra hyperechogenicity may be an (genetically conditioned?) increased iron deposition in

abnormal protein binding. The high frequency of this finding in relatives of Parkinson patients speaks in favor of a genetic influence.

Marked substantia nigra hyperechogenicity is also found in 10% of healthy adults, and at a similar incidence for successive decades of life up to age 80 years (Berg et al. 1999b). This finding correlates with results of PET studies in adults of approximately 30 years of age with a pathologic reduction in ^{18}F -dopamine uptake in the caudate nucleus and putamen, with an accumulated incidence of parkinsonism following the administration of high-potency neuroleptics, and in patients older than 60 years without pre-existing extrapyramidal motor disorders, with motor slowing compared to individuals with normal substantia nigra echogenicity (Berg et al. 2001a). These findings suggest that substantia nigra hyperechogenicity reflects nigrostriatal dopamine system dysfunction already years or decades

before manifestation of a Parkinsonian disorder. The value of brainstem sonography for the prediction of later development of a Parkinsonian disorder is currently undergoing investigation by number of prospective studies.

Differential Diagnosis of Parkinson Syndromes

Brainstem sonography supports discrimination between idiopathic Parkinson's disorder and atypical Parkinson syndromes (Walter et al. 2003, 2004a). Normal substantia nigra echogenicity differentiates multiple system atrophy from Parkinson's disease at a specificity greater than 90%. The presence of bilateral marked hyperechogenicity enables differentiation of corticobasilar degeneration from progressive supranuclear palsy. Diagnostic certainty is enhanced by sonography of other structures (lentiform nucleus, third ventricle). The characteristic constellations of findings are shown in Table 2.3.

Diagnosis of Affective Disturbances

Reduced echogenicity of the midbrain raphe was a frequent finding in unipolar depression, and in Parkinson's disorder-related depression (Becker et al. 1995b; Berg et al. 1999a). Correlation was established between reduced raphe echogenicity and signal alteration on MRI in the region of the posterior raphe nucleus, and has been discussed as the expression of a central serotonergic system disturbance. Depressed patients with reduced raphe echogenicity showed a more favorable response to selective serotonin reuptake inhibitor therapy than patients with normal raphe echogenicity (Walter et al. 2006b). Studies are currently underway to determine whether sonography of brainstem raphe represents a useful instrument in the decision on the therapeutic strategy for depressive disorders.

2.3 Electrophysiologic Diagnostics

Jürgen Marx, Frank Thömke, Peter P. Urban, Sandra Bense, and Marianne Dieterich

2.3.1 Blink Reflex

The blink reflex has become the most widely used electrophysiologic test of brainstem function since its first electromyographic recording by Kugelberg (1952). It enables the quantitative assessment of the different components of the human blink response. Following unilateral stimulation of the trigeminal afferents, two successive reflex responses can usually be evoked in surface EMG of the orbicularis oculi muscle: an early component (R1), which is typically observed only ipsilaterally, and a late component, which can be induced ipsilaterally (R2) and contralaterally (R2c) to the site of stimulation (Fig. 2.21). While the R1 component does not have a clinical correlate, the R2 component corresponds to visible eye closure resulting from contraction of the orbicularis oculi muscle. In addition, inconstant recording of a third reflex response can be achieved ipsilaterally and contralaterally with stronger stimulation magnitudes fivefold to sixfold of the sensory threshold (Rossi et al. 1989). However, owing to the poor reproducibility of this response, it has not become an integral part of routine clinical diagnostics.

2.3.1.1 Anatomic and Physiologic Principles

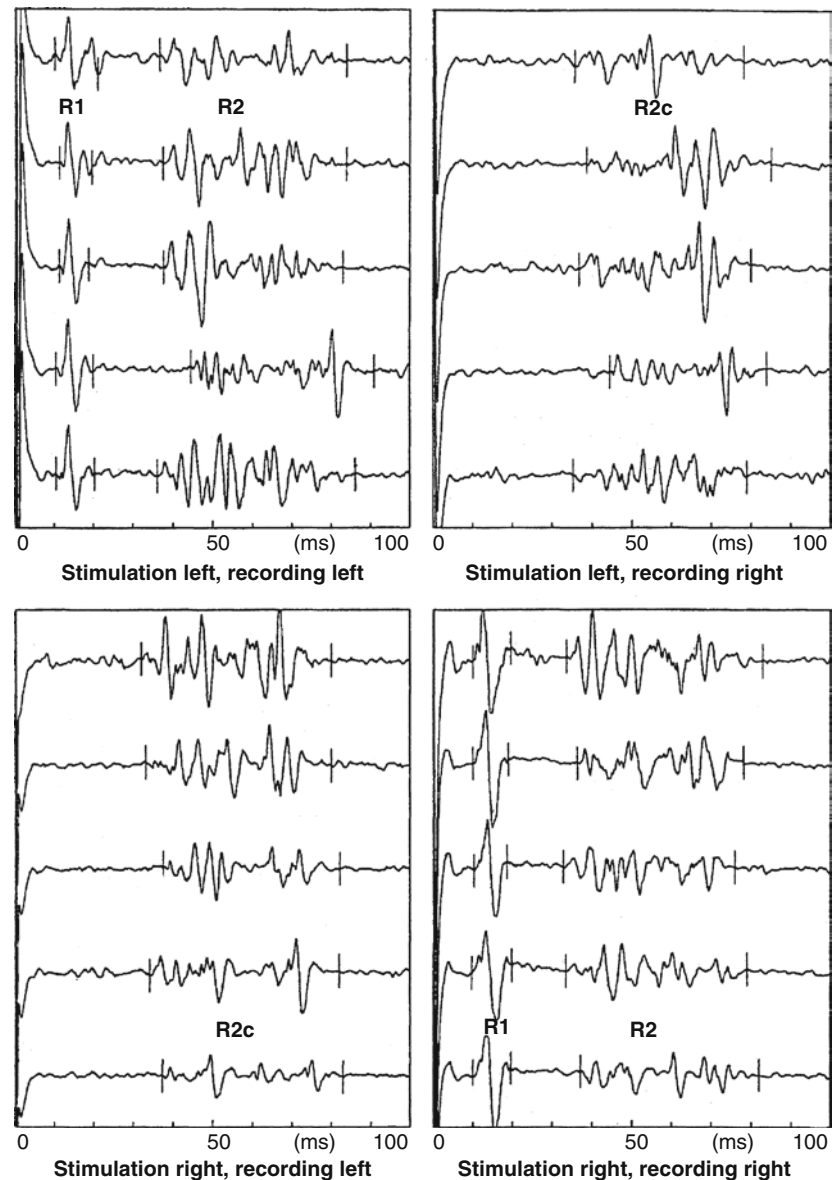
Sensory nociceptive parts of the supraorbital nerve, the first branch of the trigeminal nerve, constitute the peripheral afferents of the blink reflex. The facial nerve is the common efferent of all response components. Different topographic mapping studies have shown the central course of the early R1 component after entry of the trigeminal afferents to extend from the lateral aspect of the mid-pons to the

Table 2.3 Typical sonographic findings for the substantia nigra (SN), the lentiform nucleus, and the third ventricle in healthy persons older than 60 years, and in patients with different clinical pictures

Syndrome	SN hyperechogenic at least unilaterally	SN hyperechogenic bilaterally	Lentiform nucleus hyperechogenic	Third ventricle dilated (>10 mm)
Normal situation	+	(+)	+	(+)
Idiopathic Parkinson's disease	+++	+	+	(+)
Multiple system atrophy	(+)	–	+++	–
Progressive supranuclear gaze paresis	+	–	+++	+++
Corticobasilar degeneration	+++	+++	+++	–
Lewy body dementia	+++	+++	+	(+)

Frequency of abnormal findings in previous studies: – not found in any patient; (+) very rare; + low incidence; ++ frequent finding; +++ demonstrated in the majority of cases

Fig. 2.21 Electromyographic recording of a normal blink reflex obtained separately on either side after the respective supraorbital stimulation



ipsilateral region of the facial nucleus, in particular to the intermediate subnucleus (Marx et al. 2001). The exact course of the R1 reflex arc in the brainstem has been investigated by only a small number of experimental studies (Cruccu et al. 2005). The findings of clinical correlations and electrocoagulation studies in an animal model suggest a strictly ipsilateral dorsomedial pontine course with a close relationship to the principal trigeminal nerve nucleus (Ongerboer de Visser 1983). In humans, the frequent conjoint occurrence of R1-abnormalities and internuclear ophthalmoplegia is in favor of an anatomic proximity of the reflex arc to the medial longitudinal fasciculus.

The bilaterally occurring late R2 response follows a polysynaptic reflex arc. After entry of the trigeminal afferents into the pons, the central fibers are assumed to descend together with the spinal tract of V from the dorsolateral pons to the level of the caudal pole of the hypoglossal nucleus in the medulla oblongata. After partial crossing at

this level, they reascend through the propriobulbar segment of the reticular formation, medial to the spinal nucleus of the trigeminal nerve, bilaterally to the facial nucleus region (Cruccu et al. 2005). The fibers ascending to the ipsilateral facial nucleus may be located more laterally than those coursing to the contralateral nucleus (Tackmann et al. 1982).

The central R2 reflex arc is subject to suprasegmental hemispheric and mesencephalic control.

Both a supratentorial lesion and a disturbance of consciousness can influence the occurrence of the R2 response. The R2 response further habituates after multiple stimulations.

2.3.1.2 Clinical Application

The supraorbital nerve is usually stimulated separately on both sides by means of surface electrodes placed on the



Fig. 2.22 Technique for eliciting the blink reflex on supraorbital stimulation

supraorbital foramen (Fig. 2.22). The stimulation cathode should be positioned above the foramen, with the stimulation anode approximately 2 cm above it and rotated slightly laterally, to avoid transfer of the stimulation current to the contralateral side. If the infraorbital segment of the trigeminal nerve is to be examined, the stimulation cathode is placed on the infraorbital foramen above the exit point of the nerve, and the stimulation anode is positioned about 2 cm below. Stimulation is applied with supramaximal rectangular impulses of 0.1 ms, at an intensity of 3–20 mA. The stimulation strength can be increased until a stable maximal electromyographic response is obtained. The patient's eyes should be closed lightly. The stimuli are applied at interstimulus intervals of at least 10–20 s to avoid habituation of the R2 response (Kimura 1989). The stimulus responses of each orbicular muscle are recorded separately on either side using surface electrodes. The different lead electrode is positioned directly below the lower eyelid, at an approximate mid-position between the inner and outer orbital border, the indifferent electrode is placed in the temporal region at the lateral orbital border. An additional ground electrode can be affixed submentally or to one forearm. Filter limits are usually set at 20 and 3,000 Hz.

Measured are latencies from the trigger signal to initiation of the evoked reflex response. A minimum of five successive reflexes are recorded and evaluated for this purpose.

Applying this technique, supraorbital stimulation evokes an ipsilateral R1 response and bilateral R2 responses in all healthy subjects.

Defined as **pathologic** are

- The absence of individual reflex components
- Absolute latency prolongations above the upper limits of normal
- Side to side latency differences above the upper limits of normal

Pronounced intra- and interindividual amplitude fluctuations are usually not considered in the evaluation.

Table 2.4 Upper limits of normal of blink reflex components published for different patient collectives

Investigator	Component	Absolute latencies (ms)	Side differences (ms)
Kimura (1975)	R1	<13.0	<1.2
	R2	<40.0	<5.0
	R2c	<40.0	<7.0
Hopf et al. (1991)	R1	<12.1	<1.2
	R2	<42.5	<5.0
	R2c	<44.5	<7.0

While an R2 response can always be evoked on infraorbital stimulation, this is not consistently possible for the R1 component. Paired double stimulation with a short interval (<10 ms) exerts facilitating effects on the R1 component, in particular when the R1 component can not be evoked or appears unstable on single stimulation in the presence of a demonstrable R2 component (Kimura 1975). The upper limits of normal are summarized in Table 2.4.

2.3.1.3 Interpretation of Findings

A delay in all reflex components after simultaneous stimulation indicates an **afferent defect** and is observed after a peripheral ophthalmic or trigeminal nerve lesion. A lesion of the afferent type has also been described for intra-axial lateral pons lesions when these also involve the trigeminal entry zone (Hopf et al. 1992).

An **efferent defect** can be shown as unilateral absence or delayed latencies of the orbicularis oculi muscle reflex response, and is typically detected in patients with Bell's palsy (Kimura 1989). In this case the typical pattern develops mostly within 1 week after onset of the paresis. In defect healing with aberrant regeneration, an R1 or R2 response can also be obtained in the mentalis or frontalis muscles, in addition to an orbicularis oculi muscle response. In patients with Guillain-Barré syndrome, Fisher's syndrome or congenital motor, and especially sensory neuropathy, markedly prolonged R1-latencies can be found bilaterally, while this is not the case for the R2 component, a finding that may be accounted for by the wider normal range (Valls-Solé et al. 1990).

The blink reflex primarily represents a highly sensitive method for the demonstration of vascular or inflammatory brainstem lesions affecting the mid- and lower pons, as well as the medulla oblongata (Fig. 2.23). In a study that included 180 patients with brainstem infarctions undergoing diagnostic testing with a variety of electrophysiologic brainstem reflexes and evoked potentials, the blink reflex had a 30% rate of abnormal findings and emerged as the method with the highest sensitivity for verification of clinically suspected brainstem lesions (Cruccu et al. 2005). In patients with transient symptoms or the lack of a confirmed lesion on magnetic resonance imaging, the blink

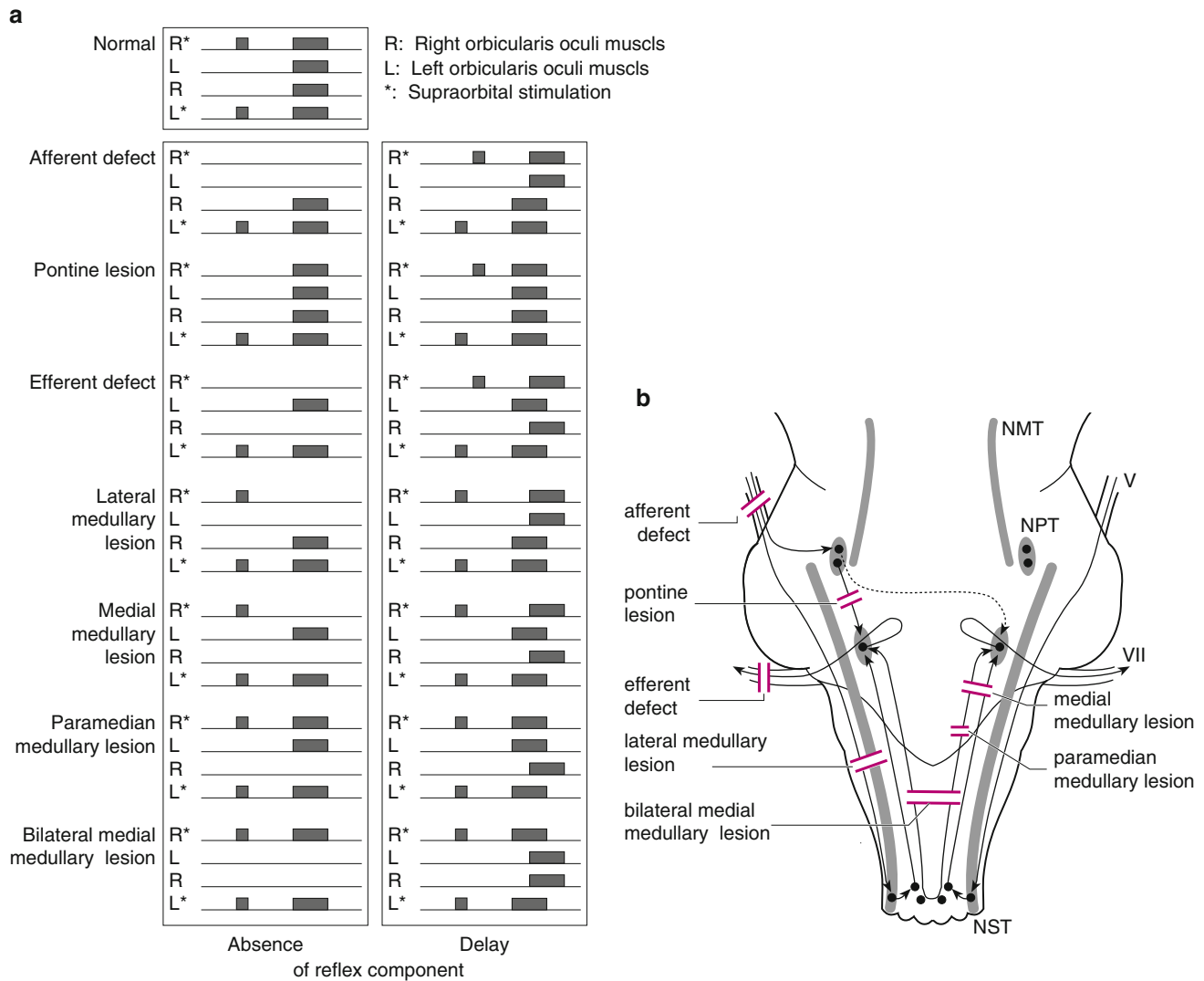


Fig. 2.23 Classical pathologic patterns of the blink (a) reflex and their assignment to the respective brainstem lesions (b). NMT trigeminal motor nucleus, NPT trigeminal principal nucleus, NST trigeminal sensory nucleus, V trigeminal nerve, VI facial nerve

reflex identified a central pathology in a relevant number of cases, which is of crucial importance for the decision on the subsequent therapeutic regimen as, e.g. the initiation of secondary stroke prevention (Marx et al. 2002). In addition, the blink reflex is a valuable tool in the economic follow-up of functional recovery after brainstem lesions.

Topodiagnostic findings of imaging-based correlation studies have suggested a relationship between delays in the R1 component and **ipsilateral pontine pathology** (Cruccu et al. 2005; Fig. 2.24). An isolated R1 pathology – without involvement of the R2 component – is an indication of a **lateral mid-pontine lesion**, although an association with internuclear ophthalmoplegia is frequently found on clinical examination (Hopf et al. 1991).

Different R2 abnormality patterns may develop in the presence of **medullary lesions**. In the majority of patients with a typical lateral or dorsolateral medulla oblongata infarction a loss or delay in the ipsilateral R2 and R2c response is often observed. Following extension of the

lesion medially beyond the spinal tract of V, an ipsilateral R2 and a bilateral R2c loss may develop, which is usually associated with extended or only incompletely remitting clinical symptoms. (Aramideh et al. 1997). A delay in the R2c alone is much more rarely noted and is suggestive of a **contralateral paramedian medullary lesion**. In contrast, a **bilateral medial medullary injury** most often only involves the crossed fibers for the R2c of both sides (Hopf 1994). However, the described constellations of findings often also occur in mixed forms. **Suprasegmental lesions** occurring primarily in the postcentral region are more likely to lead to a delay in the R2 than in the R1 component. In patients in coma due to **supratentorial injury**, the R2 component may initially be lost, while the R1 component is generally maintained until the development of a secondary brainstem lesion. As a rule, both components can be demonstrated in patients with **apallic syndrome**, although they are absent in the brain dead patient (Metha and Seshia 1976).

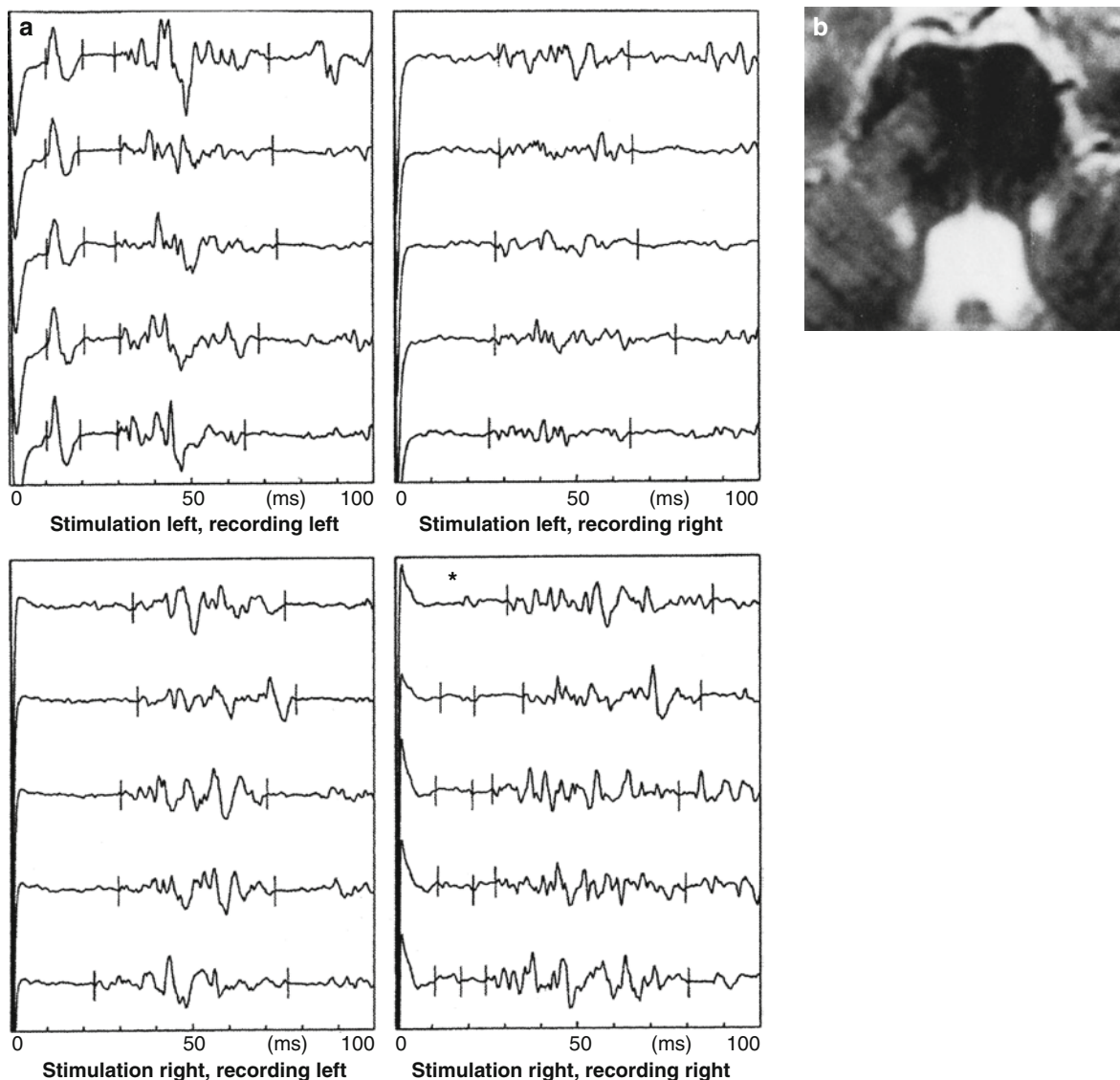


Fig. 2.24 Example of an ipsilaterally absent R1-component (a) in a patient with acute right-pontine brainstem ischemia in the respective T2-weighted MRI (b)

2.3.2 Masseter Reflex

Frank Thömke

2.3.2.1 Anatomic Principles

The masseter reflex is a monosynaptically transmitted monophasic (myotatic) stretch reflex of the masseter muscle. In contrast to all other stretch reflexes, the cell bodies of the afferent neurons are located in the central nervous system, in the mesencephalic nucleus of the trigeminal nerve. Afferents are Ia fibers from the masseter muscle spindles, which run in the masticatory nerve possibly crossing to the sensory root via anastomoses in the Gasserian ganglion, before entering the brainstem at the

level of the mid-pons, and ascend in the mesencephalic tract of the trigeminal nerve to the mesencephalic nucleus of the trigeminal nerve. This nucleus contains the cell bodies of the first-order sensory neurons, which send collaterals down to the motor nucleus of the trigeminal nerve in the lower pons, where monosynaptic transmission to masseter muscle motoneurons takes place. The efferents of the masseter motor neurons in turn course in the motor root of the trigeminal nerve to the mandibular nerve, and finally travel in the masseter nerve before entering the masseter muscle (Fig. 2.25; Hopf 1994; Thömke 2003). According to current knowledge, masseter reflex abnormalities indicate ipsilateral brainstem lesions between the levels of the fifth nerve motor and the third nerve nucleus, provided that trigeminal nerve functions are intact (i.e.,

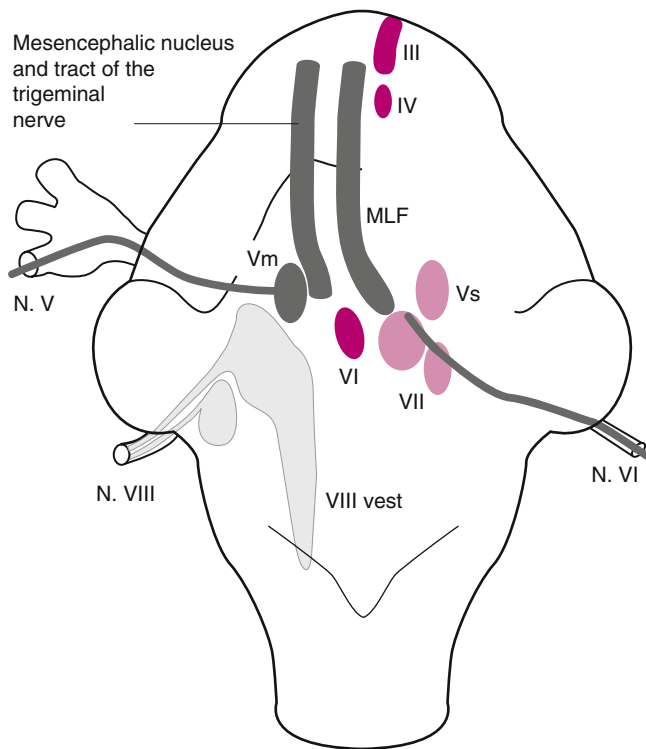


Fig. 2.25 Representation of the central masseter reflex arc and adjacent structures (According to Nieuwenhuys et al. 1989). *MLF* medial longitudinal fascicle; *III* oculomotor nucleus; *IV* trochlear nucleus; *Vs* main sensory trigeminal nucleus; *Vm* motor trigeminal nucleus; *VI* abducens nucleus; *VII* facial nucleus; *VIII* vest: vestibular nucleus; *N. V* trigeminal nerve; *N. VI* abducens nerve; *N. VIII* vestibulocochlear nerve

normal corneal reflex, trigeminal sensory function, and masseter function).

The masseter central reflex arc has a close topographic relationships to numerous brainstem structures. In the pons it is closely related to the vestibular nerve segment adjacent to the vestibular nucleus (and to the medial vestibular nucleus), to the inner knee of the facial nerve, as well as to the proximal segment of the abducens nerve. In the midbrain, the intramesencephalic segments of the trochlear and oculomotor nerves lie in close proximity (Nieuwenhuys et al. 1989; Hopf 1994; Thömke 1999). Between the mid-pons and the third nerve nucleus level there are also close anatomical relationships to the medial longitudinal fasciculus, to descending excitatory projections to the paramedian pontine reticular formation, and to the widely ramified neuronal network involved in the generation of smooth pursuit eye movements.

2.3.2.2 Clinical Application and Normal Values

The masseter reflex is elicited by a brisk tap with a reflex hammer on the patient's jaw, which stretches the masseter muscles on both sides. The examiner places the index finger on the tip of the patient's chin, whose mouth is slightly open, and taps his index finger with the reflex hammer. The

recording is triggered at the moment of the mechanical tap by a signal from a piezo-electric element mounted in the hammer. The reflex is recorded simultaneously on both sides. Recording of the reflex response is primarily performed non-invasively with the use of surface electrodes, that are placed above the muscle belly 25 mm above the margin of the mandible (recording electrode), and over the zygoma at the lateral edge of the orbit (reference electrode) with a bandwidth of 20–2,000 Hz (overview see Thömke 2003). With a more invasive technique signals are recorded by concentric needle electrodes, although this method is not widely used and has thus far been investigated by a very small number of studies only (Yates and Brown 1981; Cruccu et al. 1987).

The reflex responses recorded by surface electrodes are biphasic compound muscle action potentials of the masseter muscle. The latency is the time interval between the impact of the reflex hammer on the tip of the chin and the negative deviation of the compound muscle action potential from baseline, and the amplitude represents the maximal negative deflection of the compound muscle action potential from baseline (Fig. 2.26).

All published studies reported relatively large interindividual differences of latency and amplitude, whereas intraindividual fluctuations on repeated stimulations were only small. There was a wide difference in the number of the recorded reflex responses, which ranged from 3 to 35, and the calculation of latencies has not always been well-defined.

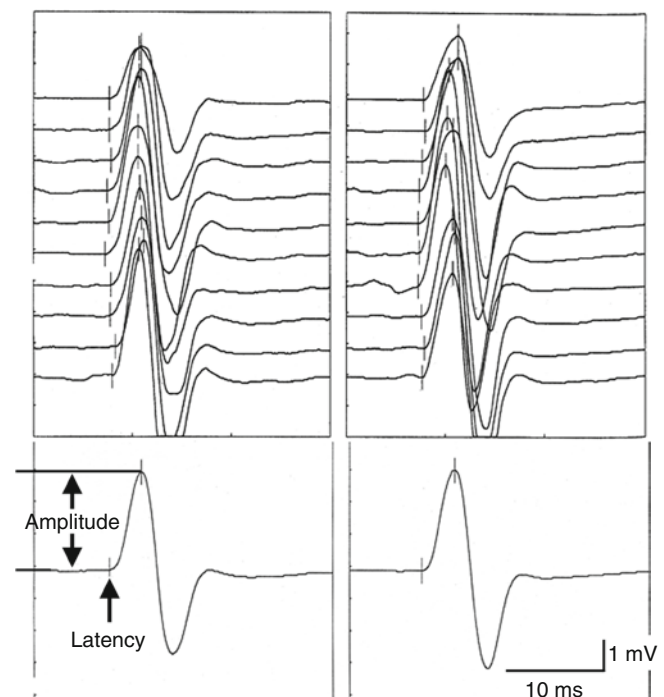


Fig. 2.26 Original registration of a simultaneous masseter reflex recording in a healthy person. The two upper graphs depict the recording of ten successive individual reflex responses; the two lower graphs show the cumulative average curve derived from the individual recordings

Some authors based the evaluation on the shortest among three reflex responses as proposed by (Goodwill 1968). The criterion established by (Ferguson 1978) is an abnormal side difference of more than 0.5 ms based on more than ten reflex responses. In our experience, the mean value calculated from ten successive reflex responses has proven of value. With a good reproducibility of the individual responses, the mean latency of the ten responses is identical to the latency of the cumulative average curve (Fitzek et al. 2001). In a variety of normative collectives investigated with different registration techniques, a certain amount of variability of absolute latencies was observed. However, a side difference in latencies of below 0.5 ms, as well as increasing latencies at increasing age were well reproducible with all registration systems (Table 2.5; Hopf and Gutmann 1990; Krämer et al. 1992; Bremer 1993; Ben Ghezala et al. 1996; Fitzek et al. 2001).

In contrast to the latencies, masseter reflex amplitudes are substantially codetermined by muscular tension, in addition to being characterized by a significantly higher interindividual variability. Furthermore, the amplitudes have not been investigated as extensively as the latencies. Reductions in amplitude from one third up to one half of the higher amplitude have been described as abnormal by different studies (Table 2.6). In one study (Crucchi et al. 1987) even a reduction of one fourth with reference to the higher amplitude was considered to be outside the normal range, i.e. of the mean value plus a 2.5-fold standard deviation. In this study the reflex responses were obtained with concentric needle electrodes, but with surface electrodes in all other studies.

In addition to the delay in the absolute latency, an abnormal side difference has been identified as the most sensitive parameter of pathologic change.

Table 2.5 Normal values of masseter reflex latencies reported by different studies

	Latencies (mean value \pm SD ^a)	Side differences (mean value \pm SD ^a)
Goodwill (1968) <i>n</i> = 86	8.4 \pm 1ms	\leq 1 ms
Kimura et al. (1970) <i>n</i> = 20	7.1 \pm 0.62 ms	0.27 \pm 0.15 ms
Ongerboer de Visser and Goor (1974)	7 ms (20–30 years) (<i>n</i> = 9) 7 ms (31–40 years) (<i>n</i> = 7) 7.4 ms (41–50 years) (<i>n</i> = 10) 7.8 ms (51–60 years) (<i>n</i> = 10) 8.4 ms (61–70 years) (<i>n</i> = 6) 7.8 ms (71–80 years) (<i>n</i> = 4) In another 5 patients aged 71–80 years no reflex response was evoked bilaterally	0.07 \pm 0.15 ms for the entire group
Yates and Brown (1981) <i>n</i> = 21	8.7 \pm 1s	0.1 \pm 0.2 ms
Görömbey et al. (1986) <i>n</i> = 20	6.4 \pm 0.9 ms	0.1 \pm 0.2 ms
Lowitzsch and Marzi (1986) <i>n</i> = 24	7.6 \pm 0.7 ms	0.23 ms
Crucchi et al. (1987a) <i>n</i> = 25	7.2 \pm 0.8 ms	0.11 \pm 0.15 ms
Hopf and Gutmann (1990) <i>n</i> = 58	6.9 \pm 0.4 ms (\leq 40 years) (<i>n</i> = 27) 7.6 \pm 0.5 ms ($>$ 40 years) (<i>n</i> = 31)	0.15 \pm 0.12 ms for the entire group
Bremer (1993) <i>n</i> = 112	6.4 \pm 0.7 ms (\leq 42 years) (<i>n</i> = 29 women) 6.9 \pm 0.5 ms (\leq 42 years) (<i>n</i> = 29 men) 7.3 \pm 0.6 ms ($>$ 42 years) (<i>n</i> = 26 women) 7.5 \pm 0.6 ms ($>$ 42 years) (<i>n</i> = 28 men)	0.17 \pm 0.14 ms for the entire group
Fitzek et al. (2001) <i>n</i> = 105	7.7 \pm 0.6 ms (\leq 50 years) (<i>n</i> = 40 women) 8.1 \pm 0.7 ms (\leq 50 years) (<i>n</i> = 30 men) 8.8 \pm 1 ms ($>$ 50 years) (<i>n</i> = 20 women) 8.8 \pm 0.5 ms ($>$ 50 years) (<i>n</i> = 15 men)	\leq 0.4 ms ^b for the entire group \leq 50 years \leq 0.54 ms ^b for the entire group $>$ 50 years

^aAs far as indicated

^bUpper limit of 95% confidence interval (as the normative collective of Fitzek et al. did not exactly fulfil the normal distribution criteria, the 95% confidence interval was used to determine the upper limit of normal reflex latencies)

Table 2.6 Normative values of masseter reflex amplitudes reported by different studies

	Amplitudes (mean value \pm SD ^a)	Side differences (mean value \pm SD ^a)
Cruccu et al. (1987) <i>n</i> = 25	0.8 \pm 0.6 mV	7% \pm 10%
Hopf and Gutmann (1990) <i>n</i> = 58	2.2 mV (\leq 40 years) (<i>n</i> = 27) 1.9 mV ($>$ 40 years) (<i>n</i> = 31)	17.2% \pm 8.6% ^b 18% \pm 8.8% ^b
Bremer (1993) <i>n</i> = 112	3.2 \pm 1.6 mV (\leq 42 years) (<i>n</i> = 29 women) 2.8 \pm 1.6 mV (\leq 42 years) (<i>n</i> = 29 men) 2.7 \pm 1.9 mV ($>$ 42 years) (<i>n</i> = 26 women) 2.4 \pm 1.3 mV ($>$ 42 years) (<i>n</i> = 28 men)	\leq 48.5% ^{b,c} for all women and men
Fitzek et al. (2001) <i>n</i> = 105	2.0 \pm 0.9 mV (\leq 50 years) (<i>n</i> = 40 women) 1.7 \pm 0.8 mV (\leq 50 years) (<i>n</i> = 30 men) 1.0 \pm 0.5 mV ($>$ 50 years) (<i>n</i> = 20 women) 1.1 \pm 0.6 mV ($>$ 50 years) (<i>n</i> = 15 men)	\leq 33% ^{b,c} (or \leq 0.8 mV) for the entire group \leq 50 years \leq 33% ^{b,c} (or \leq 0.4 mV) for the entire group $>$ 50 years

^aAs far as indicated^bRelating to the side with the higher amplitude^cIndicated in all cases is the upper limit of the 95% confidence interval

The following are regarded as pathologic findings:

- Side differences in latencies from \geq 0.5 ms (Fig. 2.27)
- Unilateral or bilateral latencies outside the age-related normal range, i.e. higher than the respective mean value plus a 2.5-fold standard deviation
- Unilateral or bilateral reflex loss (Fig. 2.28); no reflex responses may occasionally be recorded in healthy patients older than 70 years
- Partial reflex loss, i.e. the absence of four or more reflex responses over ten examinations
- A difference in amplitude of more than 50% with regard to the respective higher amplitude

The single recording of an abnormal masseter reflex can on principle be the expression of an acute or an older, pre-existing lesion. The presence of an acute lesion is regarded as confirmed if one of the following findings is documented in subsequent examinations:

- A unilateral or bilateral reduction (or increase) in latency of 0.8 ms or higher
- A unilateral or bilateral return of a previously absent reflex response (Fig. 2.28)

2.3.2.3 Interpretation of Findings

Suprasegmental, i.e. supratentorial or cerebellar lesions do not have an influence on the masseter reflex (Hopf et al. 2000). However, damage to the peripheral segments of the reflex arc outside the brainstem, i.e. lesions of the third branch of the trigeminal nerve, the mandibular nerve, or masseter muscle pareses are possible causes of an abnormal masseter reflex (Kimura et al. 1970; Ongerboer de Visser and Goor 1974; Ongerboer de Visser and Goor 1974;

Ferguson 1978; Cruccu et al. 1987). In the presence of clinically intact functions of the trigeminal nerve, i.e., normal corneal reflex, normal trigeminal sensory function, normal masseter function, an abnormal masseter reflex indicates ipsilateral brainstem dysfunction between the caudal pons and the rostral midbrain. Overall, the examination of the masseter reflex represents one of the most sensitive electrophysiologic tests for the demonstration of a functionally relevant brainstem dysfunction, which may be attributed to the extensive rostrocaudal course of the central reflex arc.

An abnormal masseter reflex is the most frequently identified abnormal electrophysiologic finding in patients with vertebrobasilar ischemia (Mika-Grüttner et al. 2001; Marx et al. 2002). In addition to the rostrocaudal extension of the central reflex arc, the vascular architecture of the pontomesencephalic brainstem is of crucial importance here. The region of the central masseter reflex arc comprises not only the terminal circulation territory of the long penetrating branches from the basilar artery but also vessels exiting from the lateral and dorsolateral segments of the circumferential branches of the basilar artery (Hassler 1967).

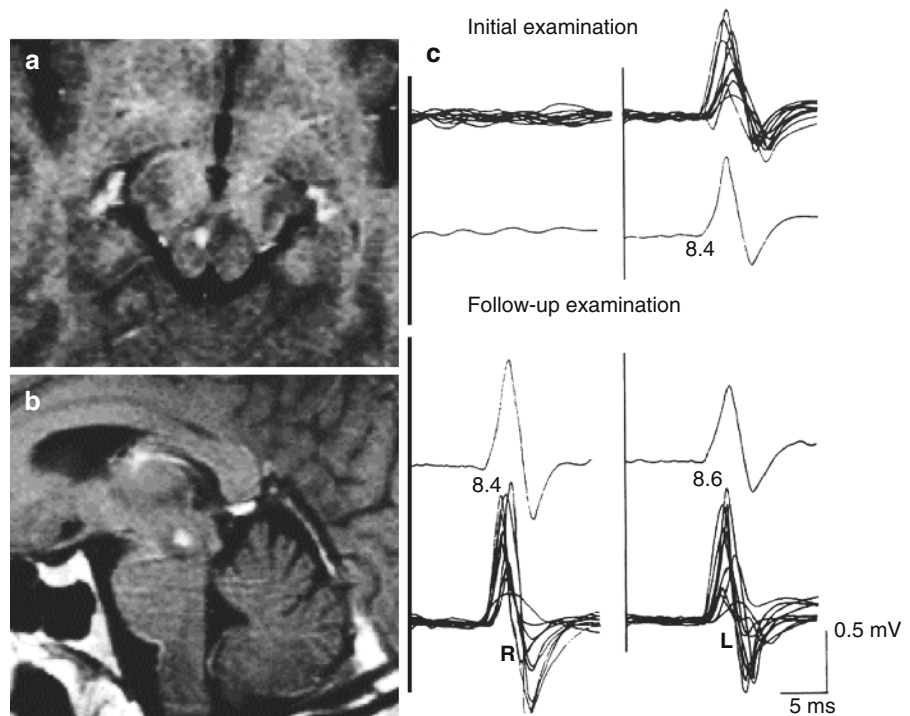
Abnormal masseter reflex findings have been reported in 30–60% of patients with multiple sclerosis, and their incidence may be higher than abnormal findings for the blink reflex or acoustic evoked potentials. Patients with internuclear ophthalmoplegia also frequently show ipsilateral masseter reflex abnormalities (overview Thömke 2003). This may be attributed to the close proximity of the medial longitudinal fascicle to the central reflex arc between the mid-pons and the rostral midbrain, which are at mutual risk for injury from possible primarily ischemic or demyelinating lesions located in this region.

The occurrence of masseter reflex abnormalities in patients with isolated cranial nerve dysfunctions can also be explained by anatomic conditions. The central reflex arc is located in

Fig. 2.27 Patient with dorsolateral infarction of the rostral pons right. MRI (image at *center*); ipsilateral latency-delayed and amplitude-reduced masseter reflex right (*left graph*); at normal elicitation left (*right graph*)



Fig. 2.28 MRI: Patient with circumscribed dorsal mid-brain infarction right. Absence of ipsilateral masseter reflex at normal elicitation left (*upper curves*). Normalization at follow-up (*lower curves*) confirms presence of a current lesion



close proximity to the oculomotor, trochlear, abducens and facial (inner knee of facial nerve) nerves, as well as to the vestibular nerve proximal to the nucleus (and to the medial vestibular nucleus), so that mutual damage to these structures is possible (Thömke and Hopf 1999). In patients with Arnold–Chiari malformations, the masseter reflex has further proven highly useful for the identification of disturbed pontomesencephalic brainstem functions; the sensitivity is here again attributable primarily to the rostrocaudal extension of the central masseter reflex arc (Koehler et al. 2001).

2.3.2.4 Conclusion

The electrophysiologic examination of the masseter reflex is a highly sensitive test for the demonstration of a functionally relevant pontomesencephalic brainstem dysfunction, which continues to be a valuable diagnostic tool. Electrophysiologic diagnostic methods (masseter reflex, blink reflex, electrooculography) are superior to magnetic resonance imaging (MRI)

when only T1 and T2 weighted sequences with slice thicknesses of ≥ 4 mm are prepared (Mika-Grüttner et al. 2002; Thömke et al. 2002). As a result of the markedly improved visualization of the brainstem by means of more recent MRI techniques (e.g. diffusion weighted and fluid attenuated inversion recovery [FLAIR] sequences) and thinner, 2–3 mm thick slices, an increasing number, although not all, functionally relevant brainstem lesions are depicted (Mika-Grüttner et al. 2001, 2002; Marx et al. 2002). MRI identifies morphologic damage, which is frequently, although not always, associated with disturbed function of morphologically damaged structures. In contrast, electrophysiologic examinations detect disturbances of function, that are often due to morphologic damage, but which may also occur in the presence of normal (or only slightly damaged) morphology, i.e. in the absence of MRI-documented lesions. The electrophysiologic examination of the masseter reflex is a widely available, cost-effective, and readily reproducible test that can provide important information on the presence of a relevant brainstem dysfunction and the dynamics of its clinical course.

2.3.3 Early Acoustic Evoked Potentials

Peter P. Urban

2.3.3.1 Anatomic and Physiologic Principles

Early acoustic evoked potentials (EAEP) are viewed as electrical potential fields in response to an auditory stimulus recorded from the scalp or the auditory canal, using electrodes with a latency of up to 10 ms. The anatomic course of the auditory path renders EAEP's suitable for the detection of tegmental brainstem lesions. EAEP's consist of five successive positive (in contrast to conventional upwards plotted) peak potentials (Fig. 2.29).

Wave I originates in the cochlear segment of cranial nerve VIII, presumably near the exit site from its foramen. Wave II is generated in the most proximal part of the cochlear nerve in the region of the cochlear nucleus. Intraoperative tests on the exposed cochlear nerve lend support to the assumption that Wave II is generated by an abrupt change in the conductivity of **cerebrospinal fluid** compared to the cerebral parenchyma at the entrance site to the brainstem at the pontomedullary junction (Martin et al. 1995). The accurate topographic allocation of subsequent waves is, however, less well-defined. The possible origin of wave III may be in the horizontal connections between the cochlear nucleus, the nuclei of the medial and lateral superior olives, and the trapezoid body at the pontine level. The conjectured origin of waves IV and V is in the mesencephalic lateral lemniscus ascending to the inferior colliculus (Markland 1994).

A reliable topographic allocation of the lesion to the right or left side is possible alone for wave I, and can be made with reservations only for wave II. In view of the bilateral projections in the brainstem, changes in waves III, IV and V do not permit a dependable allocation of the lesion to one of the

sides. There are currently a number of indications that these waves in particular do not originate in a neuronal structure, but have multiple generators (Kaga et al. 1997).

2.3.3.2 Application

Stimulation

Stimulation is achieved by clicks, i.e. sounds with a frequency spectrum ranging from 500 to 7,000 Hz, that are generated by a rectangle-shaped electric pulse of 100 μ s transmitted through earphones. Depending on pulse polarity at the earphone membrane, the clicks generate a pressure (condensation click) or suction (rarefaction click) stimulus to the tympanic membrane. Rarefaction clicks frequently lead to larger amplitudes of wave I, and more often produces readily distinguishable waves IV and V. In some settings, rarefaction clicks are therefore used exclusively. The application of condensation clicks lead to larger wave V amplitudes. The alternating application of rarefaction and condensation clicks, or subsequent averaging of the curves reduces the stimulus artefact. The use of alternating clicks alone is advised against because artefacts will also sum up and can thus simulate potentials. In addition, latency differences in individual waves between condensation and rarefaction clicks may cause elimination of the waves due to summation. Furthermore, in some patients a pathologic finding is detected only with the use of one stimulation polarity, while it would have been missed with the application of alternating stimulation, or on stimulation with the other polarity only.

The clicks are applied using a frequency of 10 Hz. The stimulus strength ranges 70 dB HL above the individual auditory threshold, which needs to be determined first; **95 dB HL** should not be exceeded. The stimulus is applied monaurally and the contralateral ear is masked with white noise at a stimulus strength 40 dB HL below that of the click.

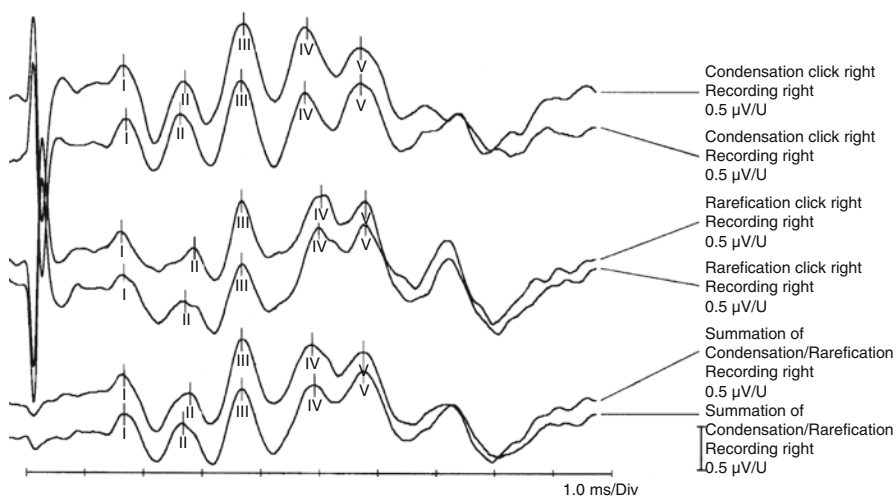


Fig. 2.29 Normal EAEP finding

This prevents stimulus conduction across the cranial bone to the non-stimulated ear.

When the waves are not readily definable, stimulation strength should either be increased or decreased. While decreasing stimulus strength leads to reduced amplitudes at increased latencies, inter-peak latencies remain unaffected.

Recording

The potentials are mostly recorded bilaterally. The electrodes are placed on the mastoids or earlobes and are interconnected at Cz. The Cz electrode is the “different” electrode in EAEP applications and the electrode placed on the mastoid or earlobe represents the “indifferent” electrode, because as far-field potentials, EAEPs have their largest amplitude above the vertex. Employed are needle and surface electrodes, as there are no differences between these regarding latency and amplitude. The transition impedance must not be greater than 5,000 Ω . A filter setting of 100–3,000 Hz is recommended. Measured are the first 10 ms after stimulation. 1,000–2,000 stimulation trains are usually averaged. A second measurement is requisite to ensure reproducibility.

2.3.3.3 Physiologic Variability of EAEP and Abnormal Findings

With increasing age, latencies of waves I and V are found to be increased in men only.

Conversely, interpeak latencies (IPL) remain largely unchanged (Lopez-Escamez et al. 1999).

Body temperature has a pronounced influence on EAEP latencies: latencies are decreased at lower temperatures.

Women show slightly shorter waves III and V, as well as shorter IPLs I–III and I–V (Lopez-Escamez et al. 1999), which may be attributable to a higher mean body temperature in women.

With increasing (senile) **hearing loss** – even when it is not yet of clinical significance – a decrease in amplitudes is observed, principally for wave I, but also for all subsequent waves. When wave I is so low that its latency can not be determined with certainty, determination of the IPL should also be dispensed with.

Wave I is included in the stimulation-ipsilateral recording only. Wave II may also be absent in healthy subjects or be lost in the descending arm of wave I or in the ascending arm of wave III. Wave II is frequently better identifiable on stimulation-contralateral recording. A further variation is the merger of waves IV and V to a common entity. In certain conditions waves IV and V may be better differentiated on suction than on pressure stimulation.

A decisive factor in the neurologic applicability of EAEPs is the differentiability of wave I.

In some cases a normal click-auditory threshold may be identified, despite the absence of wave I. This may be an indication of high tone deafness, since wave I is generated by the high-frequency components of the click. Findings reported in the literature demonstrate that in these cases wave I can be shown in approximately 75% of patients with the application of needle electrodes in the outer auditory canal (Chiappa 1997).

2.3.3.4 Evaluation

Evaluation parameters comprise latencies of waves I, III and V. From these, the more informative IPLs I–III, III–V, and I–V are calculated, because they are not as substantially influenced by biologic factors (sex, age, auditory disturbances, etc.) (Markand 1994). In addition to the absolute latencies of the individual waves and IPLs, side differences can be used in establishing a diagnosis. In view of the fact that amplitudes of the EAEPs are subject to a relatively wide fluctuation range, the absolute values are not suitable for diagnostic purposes. Only the quotient of wave V and I amplitudes is of diagnostic value. The amplitudes from the peak of the wave to the following negative minimum are measured for this purpose. In some instances abnormal findings are detected only on pressure or suction stimulation (Maurer 1985; Hammond et al. 1986). The separate evaluation of both stimulation types is therefore recommended.

The mean value plus 2.5-fold standard deviation is usually defined as the maximum permissible value. Normative values have been described in the literature (e.g. Chiappa 1997), and should be tested for transferability in an own patient collective.

IPL I–V represents the pathway from the distal vestibulocochlear nerve through the pons to the mid-brain, which can be pathologically prolonged due to a lesion along the entire peripheral and central segment. Isolated high tone deafness may lead to a paradoxical shortening of IPL I–V. Because only the low frequency components of the cochlea are present in these circumstances, the latency of wave I is delayed, although this does not apply to the latencies of the following waves.

IPL I–III represents the pathway from the distal vestibulocochlear nerve to the lower pons. A delayed IPL I–III may therefore be generated by a lesion in the cerebellopontine angle (e.g. acoustic neurinoma), meningitis, neoplastic meningitis, Guillain-Barré syndrome, HMSN I, III, and pontomedullary lesions.

IPL III–V represents the pathway from the lower pons to the tegmental pontomesencephalic region.

The **V/I amplitude quotient** should be within a range from 0.5 to 3 (Pratt et al. 1999). This signifies that, as a rule, the amplitude of wave V is larger than that of wave I. At a V/I quotient <0.5, wave V is thus too low, which lends support to the presence of a central lesion.

At a V/I quotient >3 , wave I is too low; this finding serves as an indication of a peripheral lesion or hearing disturbance.

Central Lesions

The following constellations serve as an indication of a central lesion in the brainstem:

- Normal waves I, II and III with absence or delayed and/or amplitude reduced waves IV and V, or wave V alone. The probability of a central lesion is increased if not only the V/I amplitude quotient is <0.5 , but wave V is simultaneously also delayed (Figs. 2.30–2.33).
- Pathologically prolonged IPL III–V, on condition that the V/I amplitude quotient is <0.5 and waves I and II are within the normal range. In clinical practice an extension of IPL III–V is only rarely observed. A prolonged latency of wave V at a still normal IPL III–V is detected more frequently.

- Pathologically prolonged IPL I–III with an V/I amplitude quotient <0.5 and normal waves I and II. This constellation may, however, also be observed in the presence of proximal lesions of the cochlear nerve. Indicative of a central lesion is a simultaneously prolonged IPL III–V, while IPL III–V is normal for peripheral lesions.

Multiple Sclerosis

Conflicting results have been reported regarding the incidence of pathologic EAEP findings in multiple sclerosis (MS). This is due to the different examination techniques, the size of the patient collectives, duration of the disease, and assessment criteria used. The more parameters as, e.g. absolute latency of individual waves as well as their right–left differences (and not only the IPL and V/I amplitude quotient), are used in the evaluation, and the narrower the limits of the upper norm are

Fig. 2.30 Arnold–Chiari-II-malformation. Loss of waves III–V. Upper two traces: condensation clicks; middle two traces: rarefaction clicks; lower two traces: summation of condensation and rarefaction clicks

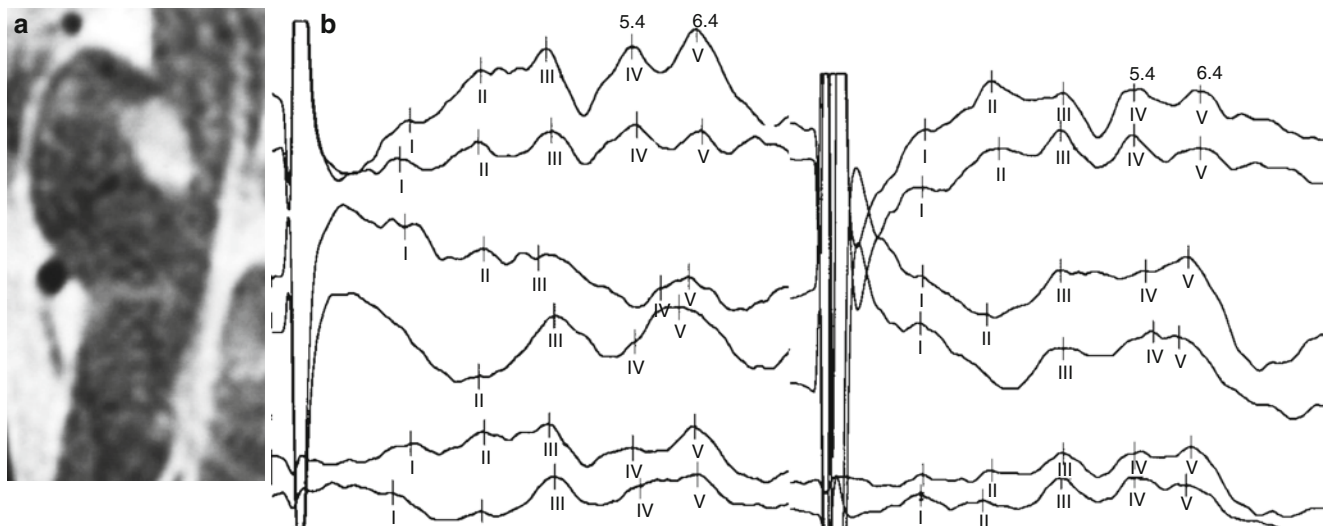
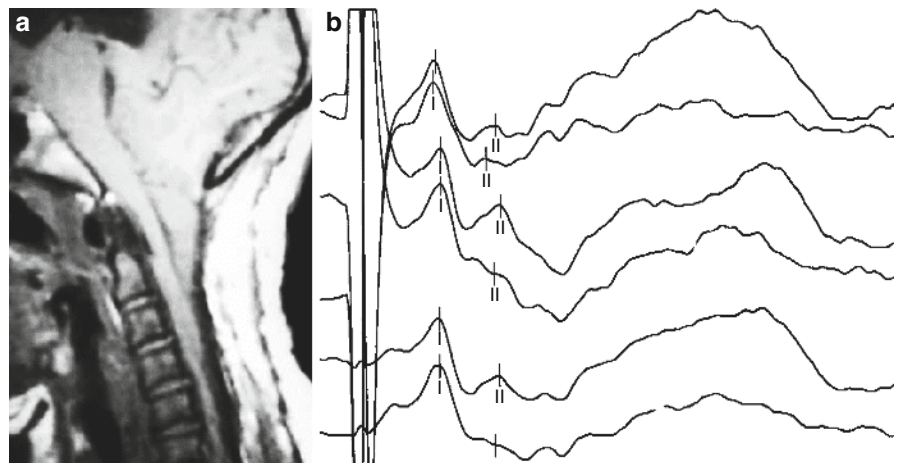


Fig. 2.31 Pons infarction right. Delayed latencies of waves IV and V bilateral. Description of curves see Fig. 2.30

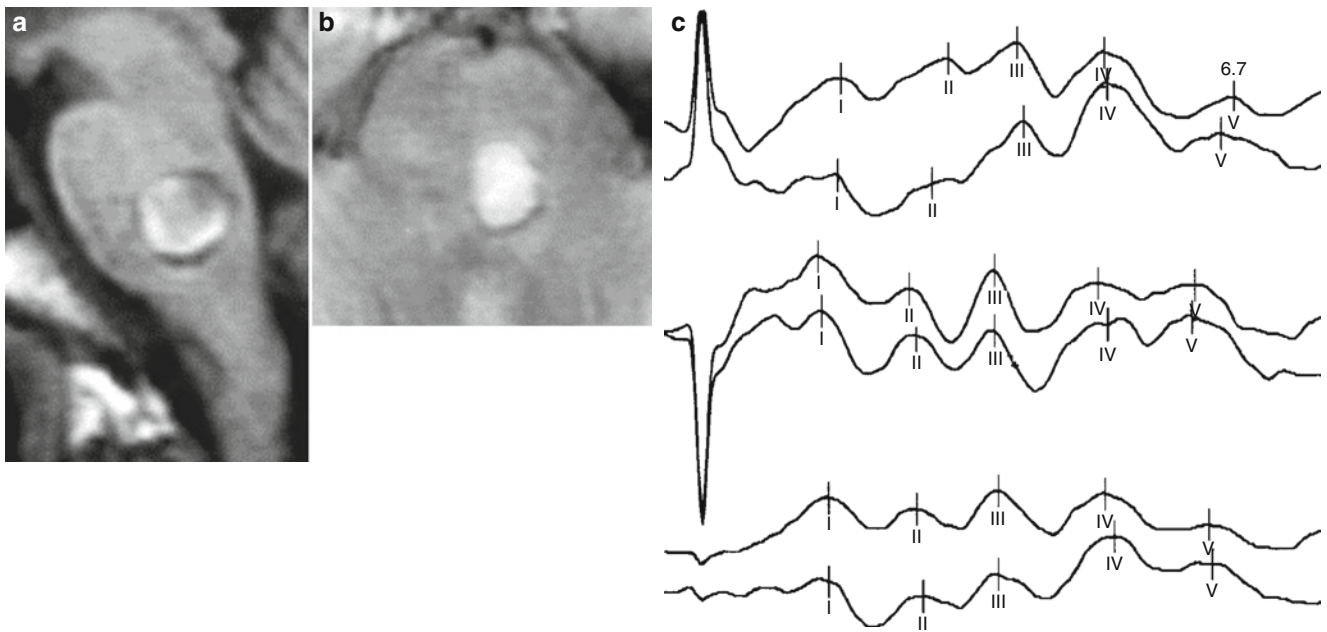


Fig. 2.32 Cavernoma left pontine. Delay of wave V. Description of curves see Fig. 2.30

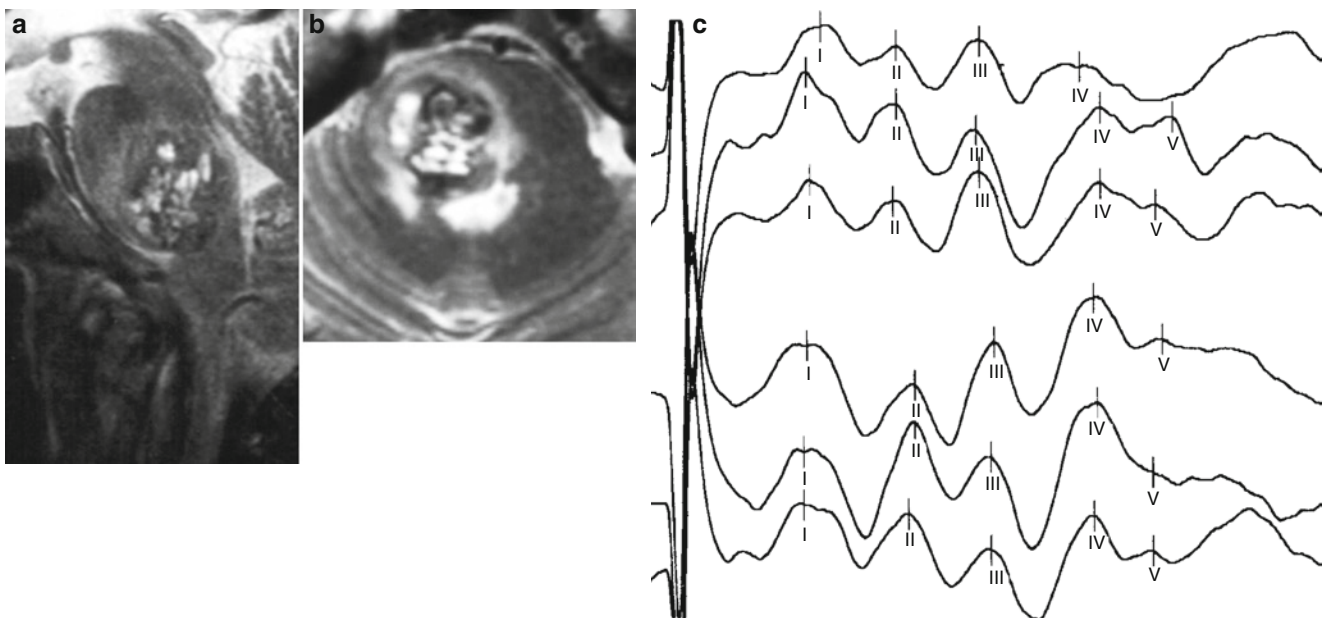


Fig. 2.33 Cavernoma right pontine. Amplitude-ratio wave V/I < 0.5. Delay of wave V. Description of curves see Fig. 2.30

determined, the higher is the proportion of pathologic findings. The cumulative incidence rate of pathologic EAEP findings ranges from 30% to 60% for clinically confirmed (Friedli and Fuhr 1990; Chiappa 1997), and from 20% to 40% (Chiappa 1997; Buchner 2000) for clinically possible or probable MS. Although the incidence rate of pathologic EAEP findings is substantially lower than that for other evoked potentials (VEP, SEP and MEP), a pathologic EAEP finding

may, in individual cases, indicate the presence of a clinically silent lesion and increase the probability of the diagnosis.

The EAEP patterns in MS correspond to the findings of a central lesion. Although patients with a central lesion do not have a hearing disorder in spite of distinct EAEP changes, MS patients with sudden unilateral hearing disturbance have been described, who showed demyelinating lesions in the pontomedullary junction, or in the dorsolateral caudal pons

on MRI. These patients had an ipsilateral loss of waves II–V or IV and V on EAEP (Drulovic et al. 1993). In approximately 50% of all MS patients with pathologic EAEPs, this is abnormal on unilateral stimulation alone (Chiappa 1997).

IPL III–V is generally only rarely pathologically prolonged, while this is very often observed for waves IV and V in the presence of normal waves I–III.

Brainstem Ischemia/Bleeding

Unilateral brainstem lesions in the region of the lateral lemniscus and the inferior colliculus ordinarily do not lead to clinically observable hearing disturbances, despite the fact that differentiated investigations on interaural time discrimination have identified abnormalities (Levine et al. 1993). Bilateral lesions of the trapezoid body, the lateral lemniscus, and the inferior colliculus may, however, be causal factors of central bilateral hearing loss (Hoistad and Hain 2003). The correlation between the occurrence of hearing disturbances and EAEPs is, nevertheless, very limited with brainstem lesions. Pathologic EAEPs are most often detected in patients with clinically normal auditory function. On the other hand, normal EAEPs have been described for brainstem lesions on different levels, even in the presence of central hearing loss (Egan et al. 1996; Vitte et al. 2002; Lee et al. 2004). EAEP patterns in ischemia or bleeding in the brainstem correspond to the findings of a central lesion.

EAEPs with monaural stimulation in patients with rostral brainstem lesions with involvement of the lateral lemniscus and the inferior colliculus have until now detected pathologic findings only on contralateral, but not on respective stimulation-ipsilateral recordings (Fischer et al. 1995; Cho et al. 2005). More caudally located unilateral lesions in the region of the superior olivary complex, the

region of the cochlear nucleus, or the entrance site of the vestibulocochlear nerve can, however, represent the cause of ipsilateral hearing disturbances and pathologic EAEPs (Häusler and Levine 2000; Fig. 2.34).

Infarctions of the dorsolateral medulla oblongata (Wallenberg's syndrome) seldom cause changes in EAEPs (Chia and Shen 1993). In cases with maintained tegmental function, ventral infarctions of the base of the pons, ranging in severity to the clinical picture of locked-in syndrome are associated with normal EAEPs (Bassetti et al. 1994). An analysis of pontine hemorrhages did not show a correlation between clinical and EAEP findings, while a bilateral loss of waves III, IV and V was associated with a poor prognosis (Ferber et al. 1990). EAEPs further provide prognostic information on the presence of brainstem compression in patients with space-occupying cerebellar infarctions (Krieger et al. 1993).

Brain Death

The following EAEP patterns show the irreversibility of clinical defunctionalization symptoms in primary supratentorial and in secondary brain damage:

- Progressive consecutive loss of waves with eventual bilateral loss of all components
- Progressive consecutive loss of waves III–V at unilateral or bilateral preservation of waves I or I and II
- Isolated preservation of waves I or I and II

According to guidelines for brain death diagnosis issued by the Federal German Chamber of Physicians (BÄK) (Scientific Committee BÄK 1997) can “in primary supratentorial and in secondary brain damage under specified conditions the silence of EAEP confirm the irreversibility of clinical defunctionalization and substitute the observation period.”

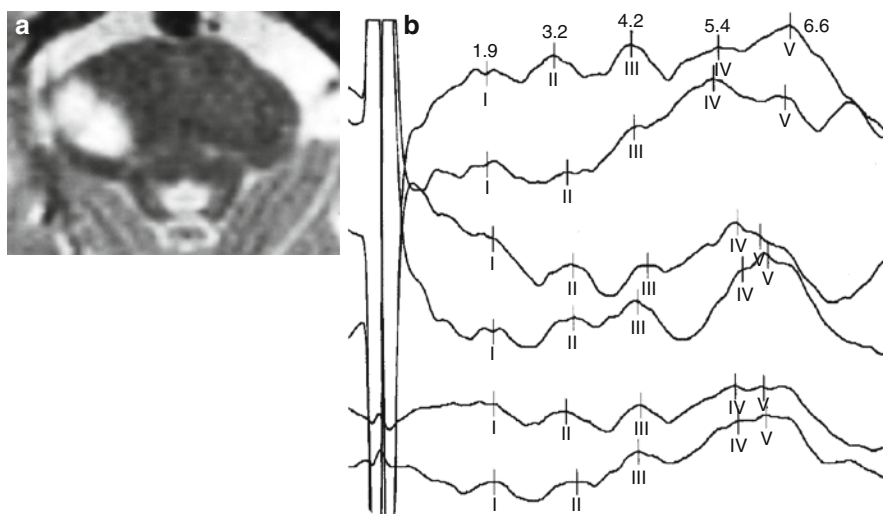


Fig. 2.34 Acute decrease in hearing on the right. Infarction in the territory of the anterior inferior cerebellar artery (AICA). Delayed latencies of waves I–V. Description of curves see Fig. 2.30

2.3.4 Vestibulocollic Reflex

Sandra Bense and Marianne Dieterich

2.3.4.1 Anatomic and Physiologic Principles

In recording the vestibulocollic reflex, also named “vestibular-evoked myogenic potentials” (VEMP), the vibration sensitivity of the sacculus is used to test the reflex arc from the otoliths to the neck musculature (Colebatch and Halmagyi 2000). The reflex arc of the vestibulocollic reflex (VCR) courses from the sacculus via the inferior segment of the vestibular nerve, the vestibular nucleus region in the brainstem, interneurons, and α -motoneurons of the vestibulospinal tract to the sternocleidomastoid muscle.

2.3.4.2 Application

In clinical diagnostics the VCR represents a readily performed screening test for side-related otolith function of the sacculus. It is usually evoked by a loud click sound markedly above the auditory threshold (in healthy subjects approximately 95–105 dB SPL [sound pressure level]), and is applied via earphones monoaurally with a repetition frequency between 3 and 5 Hz. The stimulation elicits brief inhibition and subsequent excitation of a small number of motoneurons in the neck musculature. The reflex potential is recorded by surface EMG from the neck musculature, preferably from the sternocleidomastoid muscle. For registration, electrodes are affixed bilaterally above the middle of the muscle belly and the sternal line. An additional electrode placed on the forehead serves as the ground electrode. From 50 to 100 stimulations per side are averaged for the recording. The study subject is placed in a supine position. Pretensing of the sternocleidomastoid muscles should be ensured, as the resulting reflex muscle movement can be better recorded (Lim et al. 1995). This is achieved by slight lifting of the subject’s head (Fig. 2.35). Middle ear function of the study subject must be intact, although this does not apply to the auditory function.

2.3.4.3 Evaluation and Reference Values

In a healthy subject, a biphasic potential with a positive wave is recorded ipsilateral to stimulation after approximately 14 ms (P14), and a negative wave after about 21 ms (N21) (Fig. 2.36). The absence of these waves, or a decrease in amplitude are useful diagnostic criteria. Later components are not of vestibular, but of possible cochlear origin. Contralateral reflex responses are usually not recorded. The VCR can be obtained



Fig. 2.35 Experimental recording procedure of the click-evoked myogenic potential or vestibulocollic reflex (VCR) from the sternocleidomastoid muscle

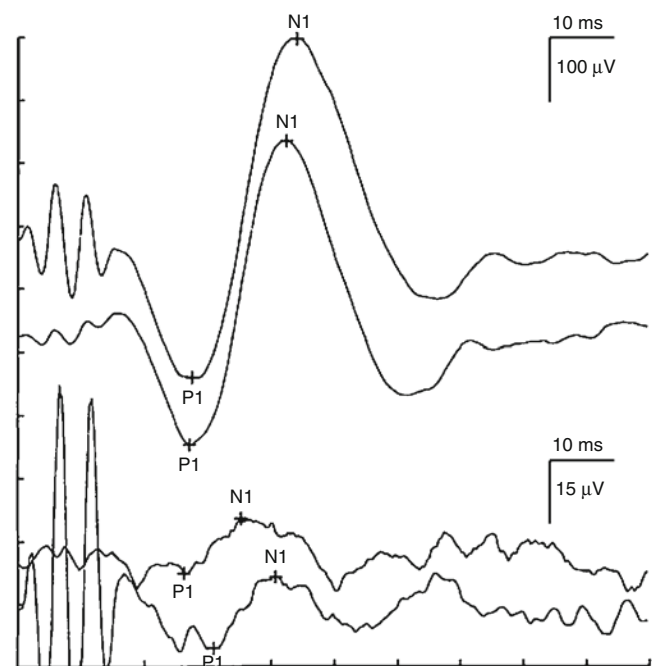


Fig. 2.36 Vestibulocollic reflex (VCR) in a healthy volunteer. A biphasic potential with a positive wave can be recorded ipsilateral to stimulation after approximately 14 ms (P14), and a negative wave after approximately 21 ms (N21)

in all persons under 60 years, although the amplitudes are lower with increasing age. Amplitudes further vary significantly interindividually, so that side differences greater than 35% or 50% have been shown to be more sensitive than absolute values (Welgampola and Colebatch 2001). Alternatively, the peak-to-peak amplitudes of the two recordable components

(p14 – n24) can be used as a measure for the response; an amplitude of 100 μV should be reached in individuals younger than 60 years. The assessment of latencies is possible only on the basis of normative values under the respective stimulation and recording conditions (Basta et al. 2005), and is therefore primarily subject to the scientific objectives.

2.3.4.4 Interpretation

In the past few years pathologic changes in the VCR have been described for a number of different central and peripheral vestibular disturbances (vestibular neuritis, otic zoster, Ménière's disease or vestibular schwannoma) (Welgampola and Colebatch 2005). In approximately 35–54% of patients with advanced Ménière's disease (De Waele et al. 1999), and in up to 80% of patients with vestibular schwannoma, pathologically changed or absent VCRs have been identified (Patko et al. 2003). The proportion of cases ranging from 12% to 39% in vestibular neuritis is substantially lower, and may be explained by the fact that vestibular neuritis affects primarily the superior segments of the vestibular nerve and spares the sacculus projections of the inferior segment (Murofushi et al. 1996; Chen et al. 2000; Ochi et al. 2003). In the rare Tullio's phenomenon caused by an inner perilymph fistula (superior canal dehiscence syndrome), reduced stimulation thresholds and increased amplitudes may be found on the affected side (Watson et al. 2000; Minor et al. 2001).

The VCR can be used as a rapid screening test in bilateral vestibulopathy, the bilateral loss of peripheral vestibular organ function of different etiology. However, in these patients sacculus function appears to be less frequently impaired than semicircular canal function on caloric testing (Zingler et al. 2008). Comparable to findings in patients with Ménière's disease, in patients with vestibular migraine the amplitude is often found to be reduced bilaterally (in 68%) while latencies are normal (Baier and Dieterich 2009; Baier et al. 2009).

As may be expected, the VCR in pontomesencephalic lesions above the vestibular nuclear region remains unaffected (Heide et al. 1999; Itoh et al. 2001). Abnormal VCRs, in particular latency delays have been described for pontomedullary lesions of different etiology (e.g. ischemic infarction, bleeding, compression) (Chen and Young 2003; Murofushi et al. 2001), and in lesions involving the vestibulospinal pathways (e.g. in disseminated encephalomyelitis) (Murofushi et al. 2001; Sartucci and Logi 2002; Versino et al. 2002; Bandini et al. 2004). Overall, the VCR is of secondary importance in the diagnosis of central-vestibular disturbances. Pathologic findings should be interpreted

with caution in individuals older than 60 years, or under difficult recording conditions with inconstant muscle preinnervation.

2.3.5 Exteroceptive Suppression of Masticatory Muscle Activity

Peter P. Urban

Inhibition of masticatory muscle activity through the application of painful stimuli to the trigeminal-innervated buccal mucous membrane or the periglottis is an antinociceptive defense reflex that synapses in the brainstem and is not clinically verifiable. The electromyographically demonstrated inhibition of masticatory muscle activity by electrical stimulation of the trigeminal-innervated periglottis or other trigeminal-innervated areas has been described in the literature as the jaw-tongue reflex, the jaw-opening reflex, the masseter inhibiting reflex, or the masseter silent period.

Electric stimulation of facial areas innervated by the sensory trigeminal nerve represents a readily standardized and widely available stimulation modality that has become an accepted technique for diagnostic purposes. The finding that in contrast to mechanical excitation, electrical stimulation activates only cutaneous afferences, lead (Godeaux and Desmedt 1975) to introduce the term "exteroceptive suppression" (ES) of masticatory muscle activity, which will be used in the following discussion.

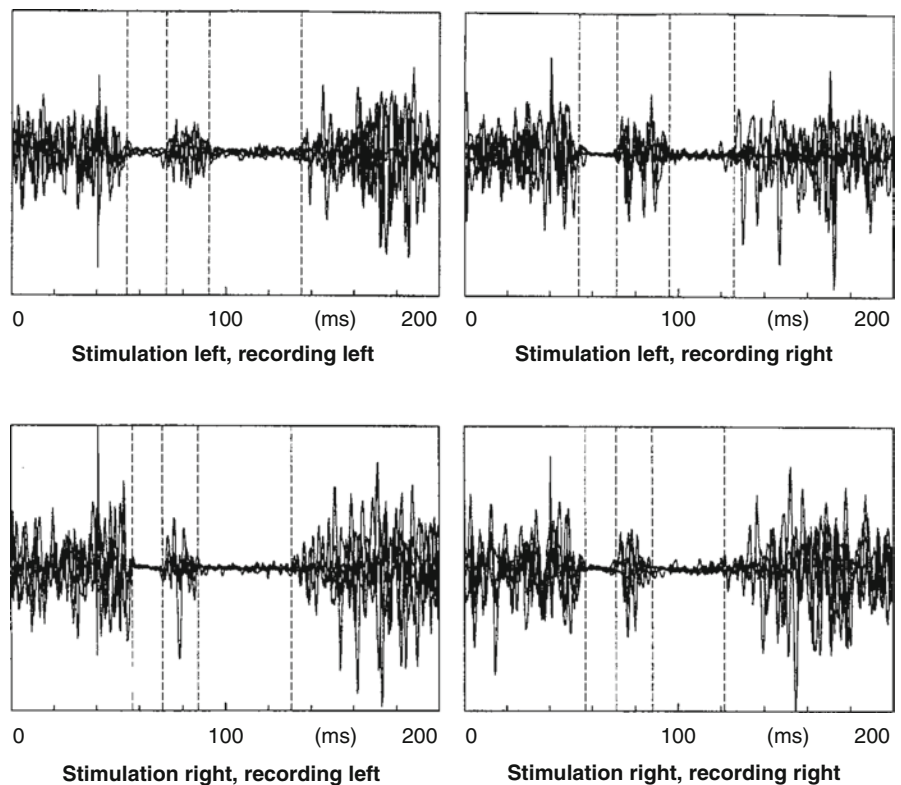
The diagnostic field of application for exteroceptive suppression of masticatory muscle activity comprises the functional assessment of sensory trigeminal afferents, of the reflex arc in the pontomedullary brainstem, and of motor trigeminal efferents to the masticatory musculature.

2.3.5.1 Anatomic and Physiologic Principles

Afferences of Exteroceptive Suppression

In an experimental setting one or two phases of suppression (ES1 and ES2) of the voluntarily preinnervated masticatory musculature can be evoked mechanically with reflex hammer tap, electric stimulation (e.g. of the mental nerve), or with selective stimulation of nociceptive or non-nociceptive fibers of skin areas innervated by the trigeminal nerve (Ellrich et al. 1997; Fig. 2.37). While inhibition of masticatory muscle activity can also be achieved with the application of acoustic (Meier-Ewert et al. 1974) and electric stimulation to the upper extremities (Erb's point, median nerve) (Urban and

Fig. 2.37 ES1 and ES2 of a healthy subject. EMG recording bilateral, electrical stimulation at the mental foramen right



Hopf 1992), this is not possible for the lower extremities. The multimodal and multitopic elicitation confirms a convergence of different afferent influences on the motor neuron pool of the masticatory musculature located in the midpontine segment.

Interconnection of ES1

The findings obtained by experimental animal studies provide conclusive evidence of a disynaptic interconnection of ES1. Impulses from the primary afferents (pseudounipolar trigeminal neurons in the trigeminal ganglion Gasseri) are initially transferred to an inhibitory interneuron in the supratrigeminal nucleus, which is located immediately dorsomedial to the midpontine motor nucleus of the trigeminal nerve (Mizuno and Konishi 1975). The inhibitory interneurons are directly interconnected with the ipsilateral and contralateral motor neurons of the motor nucleus of the trigeminal nerve. Experimental or clinical tegmental midpontine lesions therefore lead to changes in the ES1 only (Goldberg 1972; Ongerboer de Visser et al. 1989; Ongerboer de Visser and Cruccu 1993; Fig. 2.38).

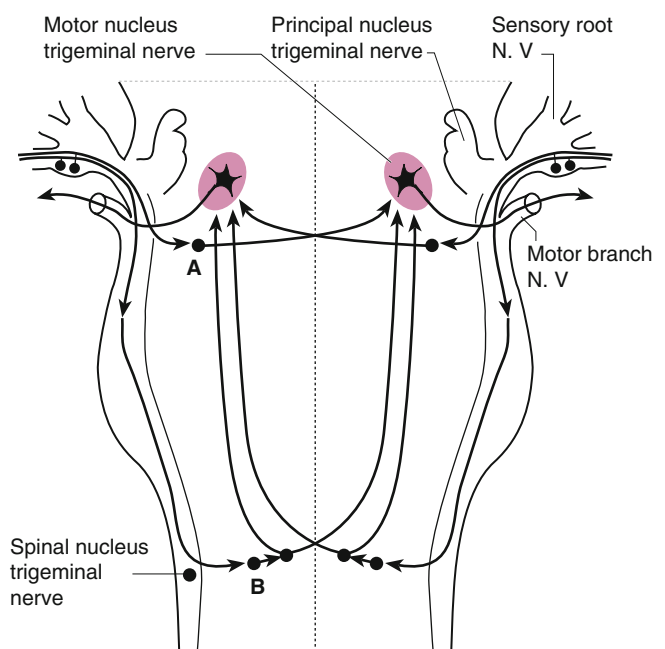


Fig. 2.38 Schematic drawing of the central pathways of the exteroceptive suppression of masticatory muscle activity (Modified according to Ongerboer de Visser 1983)

Interconnection of ES2

The reflex path of the ES2 is significantly less well documented. The ES2 latency of 30–60 ms lends support to the assumption of a polysynaptic interconnection. The selective loss of ES2 in the presence of experimental lesions near the midline at the level of the obex confirmed a course of the reflex path extending to the medulla oblongata (Nakamura et al. 1973). Correlative with this finding, lesions of the upper and middle dorsolateral medulla oblongata showed changes in the ES2 alone (Ongerboer de Visser et al. 1989; Valls-Solé et al. 1996). Changes in the ES2 after acute supratentorial lesions speak in favor of an influence exerted on the ES2 by structures located in the rostral brainstem (Cruccu et al. 1988; Liepert et al. 1993).

2.3.5.2 Clinical Application

Stimulation

Proven and tested stimulation sites include, in dependence on the clinical problem (e.g. peripheral nerve lesions) the exit sites of the mental and infraorbital nerves (Cruccu et al. 1987). Two suppression periods can generally be distinguished on stimulation of the mental nerve. Suppression on stimulation of the supraorbital nerve is not observed in all healthy study subjects. Electric stimulation is applied using a bipolar stimulation electrode, with the cathode being placed above the nerve exit site. Stimulation time is 0.2 ms (rectangular stimulation). The stimulation frequency should not exceed 0.1 Hz in order to avoid habituation (Göbel and Schoenen 1993). The stimulation strength has an influence on the duration and degree of EMG suppression. The increase in stimulation strength mediates shortening of ES1 latency, an increase in ES1 duration, fusion of ES1 and ES2 latency into a long suppression phase, and a higher degree of suppression. The application of a constant stimulation strength of 20 mA is proposed for all individuals, with the aim of standardizing the elicitation of exteroceptive suppression. In order to account for differences in the perception of stimulation strength, it has alternatively been recommended to initially determine the perception threshold (= lowest stimulation strength, at which the study subject perceives the stimulation), before setting the definitive stimulation strength at a previously determined multiple (Kimura et al. 1994).

Suppression is further influenced by the degree of preactivation of the masticatory musculature. A specified minimum of preactivation is required to enable suppression of EMG activity. At increasing strength of preactivation, the duration of suppression is shortened, and the occurrence of ES1 and ES2 fusion is reduced. A standardized preactivation (e.g. maximum masticatory force) is therefore indispensable (Connemann et al. 1997).

Recording

Electromyographic recording of the reflex response is carried out with Ag/AgCl surface electrodes bilaterally from the masseter muscle (stimulation electrode: above the muscle belly; indifferent electrode: above the cheekbone), or from the temporal muscle (stimulation electrode: in the middle of the temporal muscle directly below the hairline; indifferent electrode before the tragus). Registration is done at an amplitude of 200–1,000 $\mu\text{V}/\text{cm}$ and a sweep of 20 ms/div, at a lower/upper threshold frequency of 20/2,500 Hz. Recorded are a minimum of five applications.

2.3.5.3 Evaluation

Included in the evaluation are latencies to the onset of EMG suppression and the duration of suppression. As suppression neither begins nor ends abruptly, it is essential to define the reduction degree of the initial activity, which determines the presence of suppression as well as its onset and end. Because the mean amplitude of the inference pattern over a period from 20 to 40 ms prior to the stimulus is frequently determined as the reference value, a delay circuit should be applied. The degree of the required reduction in initial activity has not yet been standardized and varies from 50% to 95% (Schoenen et al. 1987; Göbel et al. 1992, 1994; Bendtsen et al. 1996; Connemann et al. 1997). The raw or the rectified EMG signal can be used in the evaluation. A number of studies have evaluated every individual recording, and calculated the mean value and standard deviation. Other authors have averaged or superimposed the curves and based the determination of the presence of suppression on the resulting “sum-curve.” In view of the fact that the established values vary in dependence on the respective evaluation method, individual researchers need to determine their own reference ranges.

2.3.5.4 Reference Values/Normal Variants and Pathologic ES Criteria

Reference values have been established for the latency and duration of ES1 and ES2, as well as for the duration of voluntary activity occurring between ES1 and ES2 (Keidel et al. 1994; Göbel and Dworschak 1996). A number of additional factors with an influence on the obtained measurements should be considered (recording site, stimulation site, duration and frequency of recording, recording electrode and strength, degree of

preactivation, definition of ES, evaluation technique). The ES1 latency ranges from 10 to 15 ms, and from 35 to 60 ms for ES2. As a rule, ES1 and ES2 are separated by a voluntary activity phase. The interposed activation phase is described as “breakthrough voluntary activity” or “interposed EMG activity.” In particular in the presence of higher stimulation strengths and/or lower preactivation the facilitation period is absent, which leads to the merger of ES1 and ES2. Further variants observed in healthy subjects include, at decreasing frequency: absence of ES2, absence of ES1, absence of ES1 and ES2, or the occurrence of an ES3 (Göbel 1996). These variants can be confirmed with certainty as variants when they are found to be bilaterally symmetric.

Unilateral changes in suppression may be an indication of the presence of a brainstem lesion (Ongerboer de Visser and Cruccu 1993). In addition to the absence of an ES, the finding of reduced suppression intensity can be assessed as pathologic. Prerequisites for the described evaluation include well standardized stimulation and recording techniques, as well as the quantitative assessment of the degree of suppression (Connemann et al. 1997). Further criteria for the presence of a pathologically changed ES are increased (onset of suppression) ES1 and ES2 latencies, as well as a shorter duration of ES2 (at normal latency).

2.3.5.5 Interpretation of Findings

Circumscribed brainstem lesions in the pontine and medullary tegmentum can induce changes in the ES pattern (Ongerboer de Visser et al. 1989; Ongerboer de Visser and Cruccu 1993; Valls-Solé et al. 1996) and thus contribute to the topodiagnosis. Afferent disturbances lead to a loss of ipsilateral and contralateral responses after stimulation of the affected side. Efferent disturbances are the cause of diminished or absent masseter activity on the affected side with ES1 and ES2 loss on both left and right stimulation.

Pontine lesions: Isolated changes in ES1 can develop in the presence of a small ipsilateral lesion in the mid- to lower pons (Urban et al. 1999a; Figs. 2.39 and 2.40).

Medullary lesions: Isolated changes in ES2 can be observed in the presence of medullary lesions (Urban et al. 1999). However, ES2 may also be delayed or absent in the presence of supramedullary lesions. Changes in ES2 after acute supratentorial lesions may be evidence of an influence on ES2 by structures located rostral to the brainstem. A shortened duration of ES2 has been reported for acute supratentorial lesions with hemiparesis (Figs. 2.41 and 2.42).

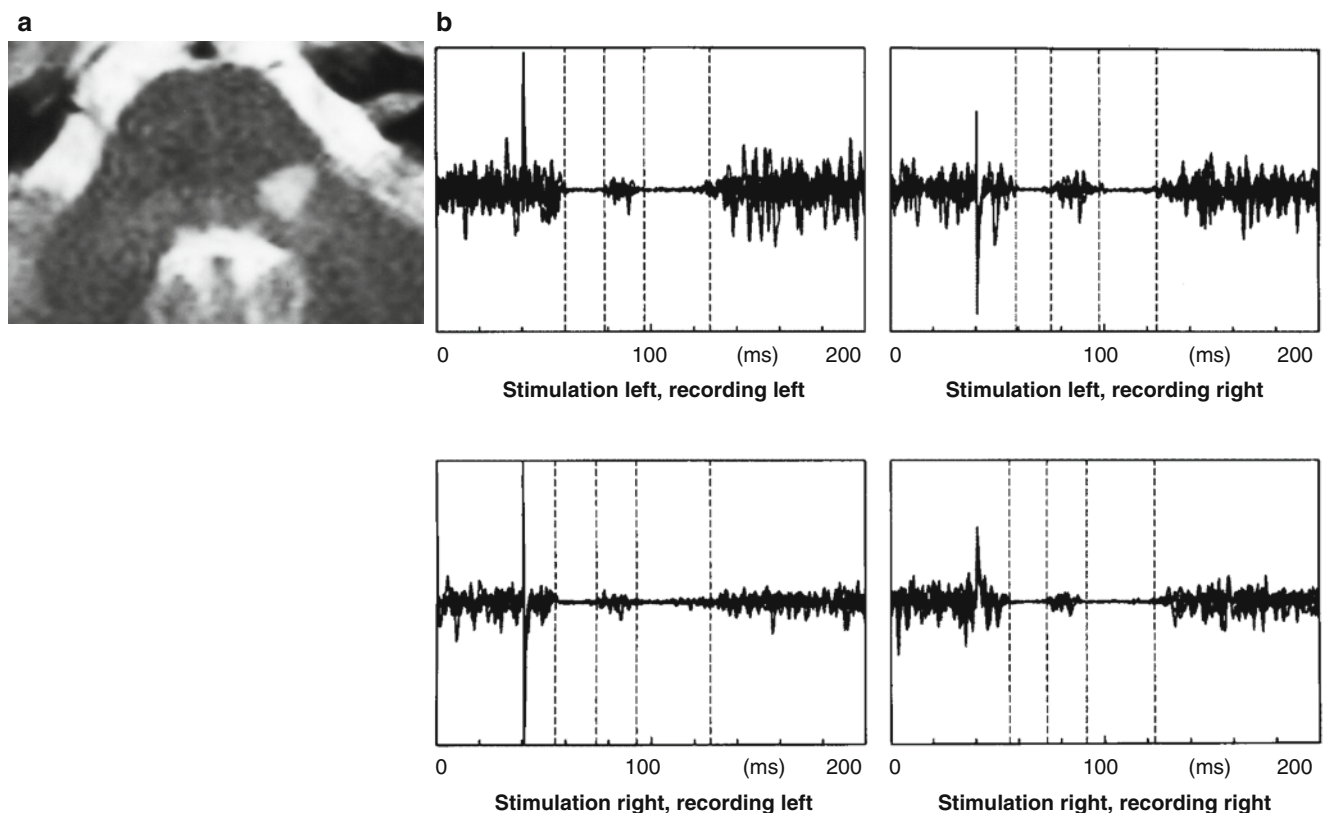


Fig. 2.39 Multiple sclerosis. (a) Demyelinating lesion in the tegmentum of the left pons. (b) ES1 latency delay on stimulation left (ES1 – stimulation left, recording masseter right: 19.0 ms, masseter left: 20.0 ms. ES1 – stimulation right, recording masseter right: 15.8 ms, masseter left: 15.2 ms) at normal ES2 bilaterally

20.0 ms. ES1 – stimulation right, recording masseter right: 15.8 ms, masseter left: 15.2 ms) at normal ES2 bilaterally

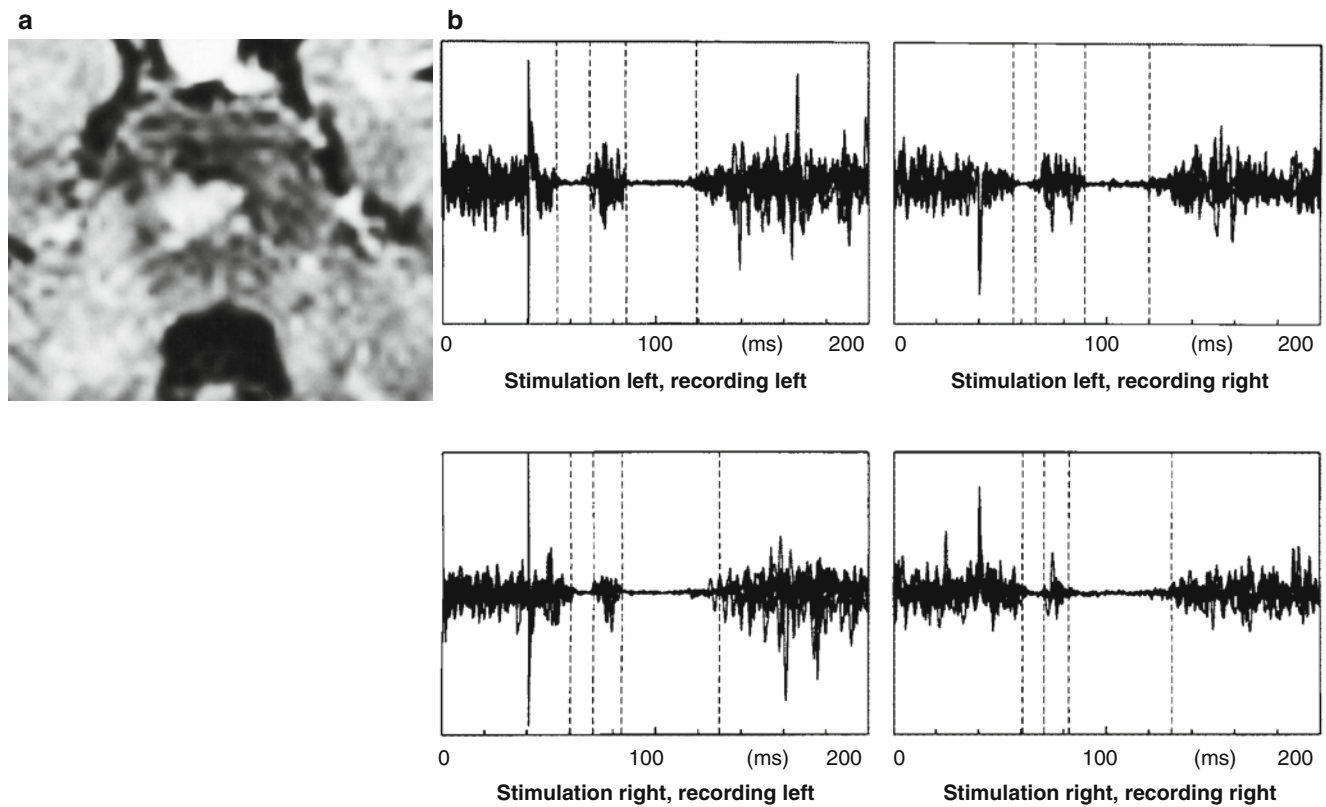


Fig. 2.40 Multiple sclerosis. (a) Demyelinating lesion in the tegmentum of the right pons. (b) ES1 latency delay on stimulation right (ES1 – stimulation right, recording masseter right: 20.8 ms, masseter left: 20.2 ms. ES1 – stimulation left, recording masseter right: 16.2 ms, masseter left: 13.8 ms) at normal ES2 bilaterally

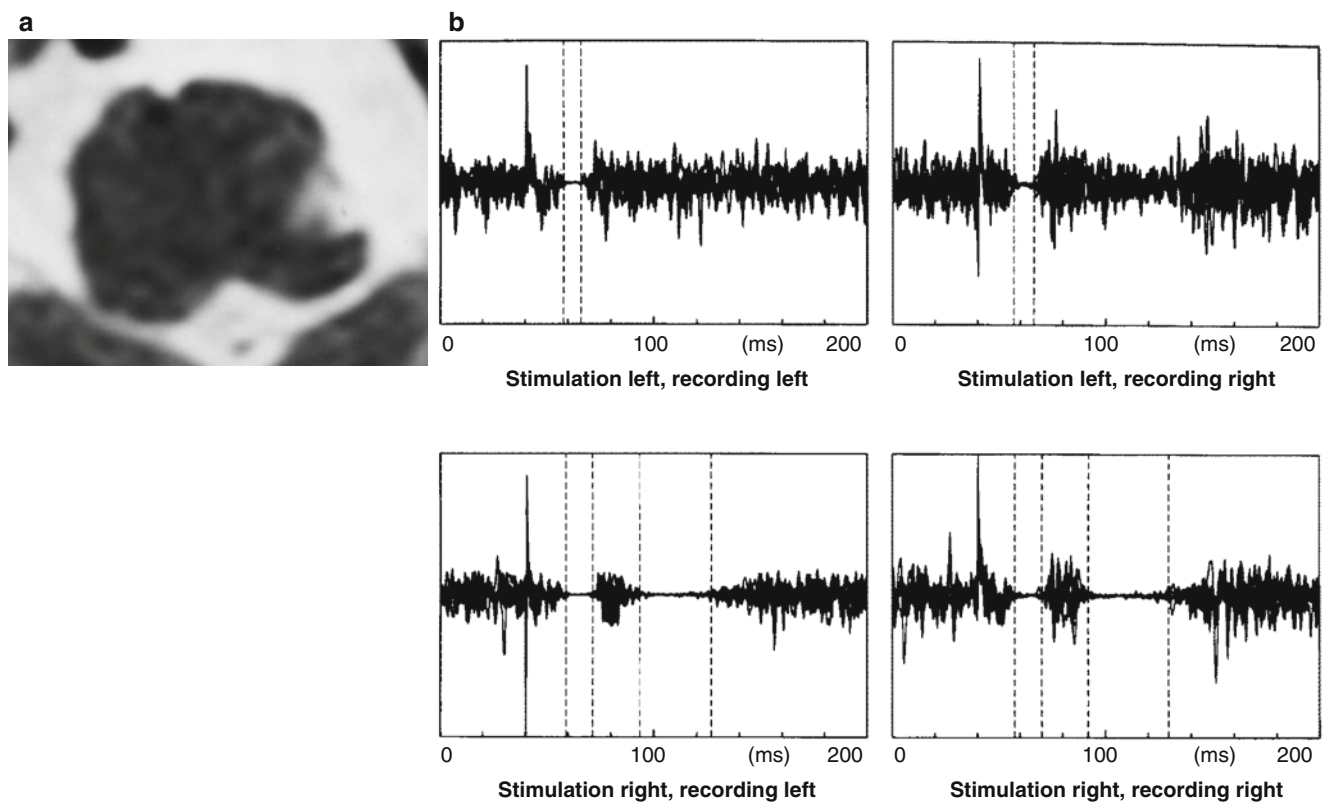


Fig. 2.41 Mediolateral medulla oblongata infarction left. (a) MRI. (b) Absence of ES2 on stimulation left at normal contralateral ES2 and normal ES1 bilaterally

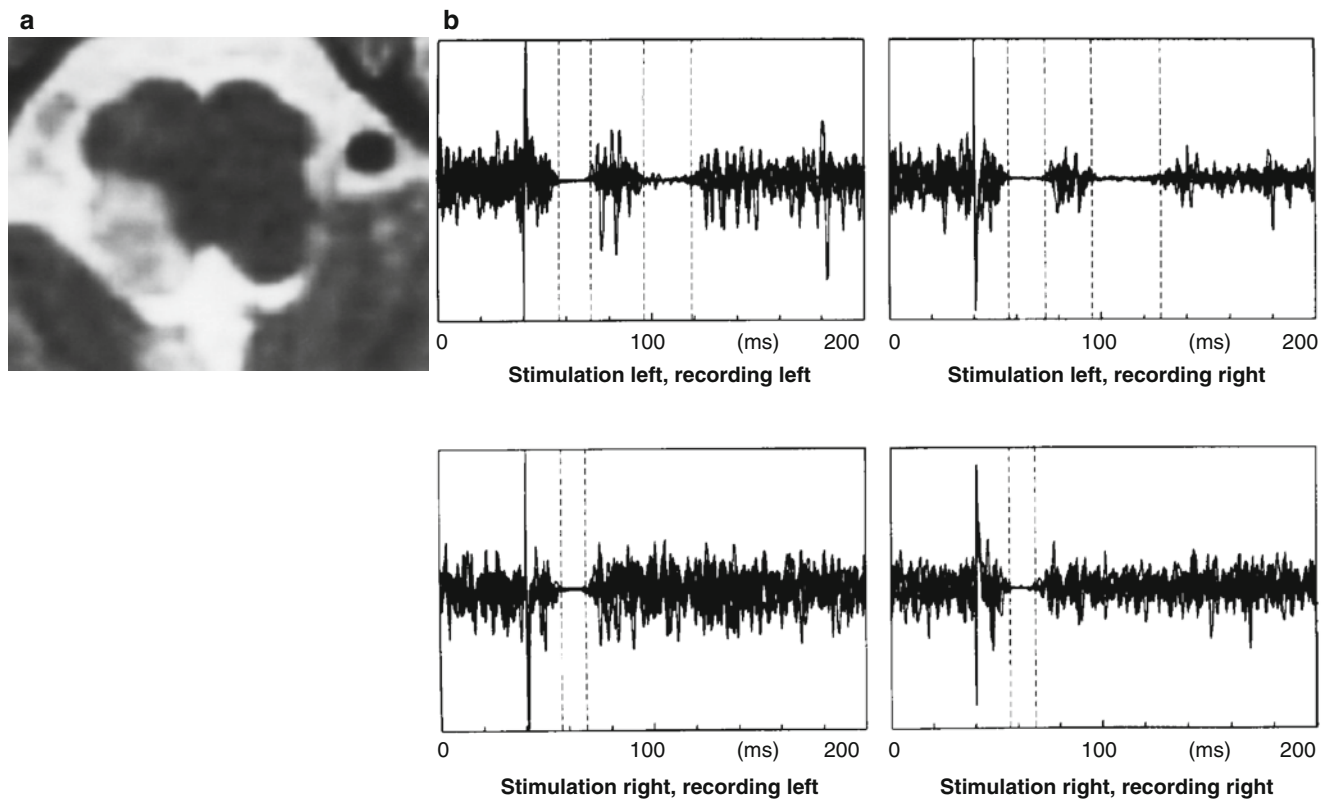


Fig. 2.42 Dorsolateral medulla oblongata infarction right. (a) MRI; (b) absence of ES2 on stimulation right at normal contralateral ES2 and normal ES1 bilaterally

2.3.6 Somatosensory Evoked Potentials

Peter P. Urban

Somatosensory evoked potentials (SEP) are changes in potentials resulting from electric stimulation of sensory peripheral nerves, and can be recorded with electrodes from the scalp, the cervical region or, in dependence on the stimulation site, from the extremities.

Due to the anatomic course of the central somatosensory projections, median SEPs (stimulation of the median nerve) are suitable for the detection of circumscribed brainstem lesions, affecting the rostral segments of the dorsal columns and the medial lemniscus.

In addition to median SEPs, stimulation of the trigeminal nerve is used in some instances to assess the integrity of the sensory afferents in this innervated region (Stöhr et al. 1981). The validity of trigeminal SEPs has, however, been questioned and is used by only a small number of laboratories in view of a pronounced stimulation artefact and inconstant reproducibility (Tackmann 2000). The median SEPs will therefore be discussed in this chapter.

2.3.6.1 Anatomic and Physiologic Principles

The SEP examination represents an objective function test of the somatosensory system. The early components of

somatosensory evoked potentials consist of changes in amplitudes generated along the peripheral pathways (peripheral nerve, plexus and posterior root) and the central projections (dorsal columns, dorsal column nuclei, medial lemniscus, thalamus and sensory cortex) by repeated stimulation of sensory peripheral nerves. Activation of the A β fibers of the peripheral nerves that are capable of fast impulse conduction is chiefly responsible for the generation of the primary cortical SEP complex. Normal SEP consists of a complex wave formation, whose components are named in relation to polarity and peak latency. The polarity and latency of individual components is dependent upon

- **Individual variables:** gender, height and age
- **Stimulation conditions:** stimulation strength and stimulation frequency
- **Recording conditions:** filter settings, electrode placement and interconnection

2.3.6.2 Application

Stimulation

Electrical stimulation of the median nerve is applied at the volar surface of the wrist above the nerve. Stimulation strength is set at 4 mA above the motor threshold (for mixed nerves),

or at the threefold to fourfold sensory threshold (for purely sensory nerves) with a proximally positioned cathode.

The duration of stimulation ranges from 0.1 to 0.2 ms at stimulation strengths from 3–5 Hz.

Between 500 and 2,000 stimulation trains are averaged for an analysis time of 50 ms. The filter should be set at 10 Hz–2 kHz; recommended amplification is 50 μ V per unit, and electrode impedance should be below 5 k Ω .

Recording

The potentials are recorded using thin subcutaneously placed steel needle electrodes or adhesive electrodes affixed above Erb's point (N10), spinal process C7 (N13a), spinal process C2 (N13b) and sensory cortex C3'/C4' (N20), against a reference electrode placed over Fz (10/20 system) (Fig. 2.43).

An additional recording from C3'/C4' and Fz (stimulation electrode) against a non-cephalic reference is required for assessment of brainstem potentials P14 and N18a, as well as for the peripherally generated P9 potential (Fig. 2.44).

2.3.6.3 Evaluation

Latencies, amplitudes, as well as the waveform of the respective potentials are evaluated and compared with the reference values established by the individual laboratory. Latencies outside the 2.5-fold standard deviation of the age- and size-corrected mean value, and amplitude asymmetries $\geq 60\%$ on bilateral comparison are rated as pathologic (Maugière et al. 1999).

The Generator Question and the Interconnection of SEPs

The N10 potential of the brachial plexus in the region adjacent to the root is recorded above Erb's point, following

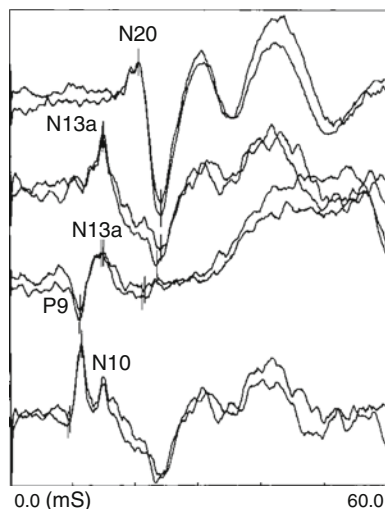


Fig. 2.43 Median nerve SEP – normal finding

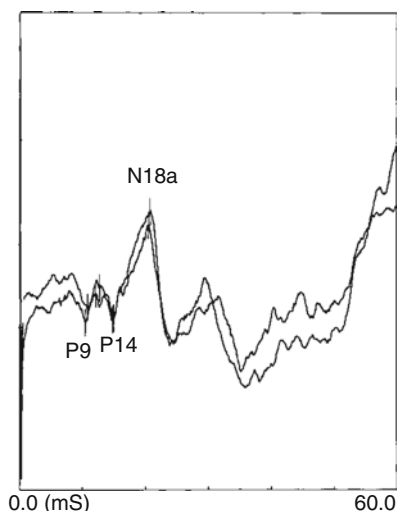


Fig. 2.44 Median nerve far-field potentials – normal finding

stimulation of the median nerve and recording against Fz as reference. A negative potential can be recorded after 13 ms over C7. This so-called N13a potential originates from a horizontal dipole in the dorsal horn at the level of segment C6 and represents the first centrally generated potential. An N13b potential can also be recorded above C2, although its exact site of origin has not been conclusively identified. In addition to a postsynaptic response in the region of the cuneate nucleus, a presynaptic impulse in the region of the dorsal columns in the vicinity of the cuneate nucleus has been discussed as a possible generator. Results obtained by investigations in brain dead patients suggest, however, that the negative potentials recorded after 13 ms above C2 and C7 represent two different generator potentials (Besser et al. 1988). The principal cortical potential (N20) originates from gyrus 3b in the postcentral region. The latency difference between the N20 and the N13a potential constitutes the central conduction time.

Far-Field Potentials

Far-field potentials are generated on stimulation of the median nerve and recording against a non-cephalic reference (e.g. the contralateral shoulder). The initially recorded potential is P9 in the brachial plexus of the axillary region. Several authors have described a location in the region of the medial lemniscus for the subsequent P14 potential (Jacobson and Tew 1988; Dillmann et al. 1990), namely in the region between the cervicomedullary junction and the lower pons (Claß and Buettner 1993). P14 has, however, also been recorded in patients after brain death (Wagner 1996; Sonoo et al. 1999), which lends support to the hypothesis of a more caudal origin (Lueders et al. 1983). The N18a potential is a further brainstem potential whose precise point of origin has not yet been definitely defined; it can be determined on recording from Fz against a non-cephalic reference. The N18a potential represents a sub-component of a broad-based N18 complex that can be

optimally recorded above C3' or C4'. A mesencephalic origin has nevertheless been suggested by findings obtained by brainstem and intraarterial recordings (Koehler et al. 2000). The N18 potential is generated in the medulla at the level of the cuneate nucleus and should not be confused with the N18a potential (Sonoo et al. 1992; Noel et al. 1996; Maudière et al. 1999).

2.3.6.4 Interpretation of Findings

Brainstem lesions that include the medial lemniscus induce changes in the N20 potential and/or a prolongation of the central conduction time at a normal N13b potential above C2. Even though a diagnostic assessment of the lesion level in the longitudinal axis is not possible on the basis of this finding, it nonetheless permits assignment of the lesion to the transverse level. Further conclusions may be drawn following consideration of the far-field potentials.

2.3.6.5 Brainstem Lesions

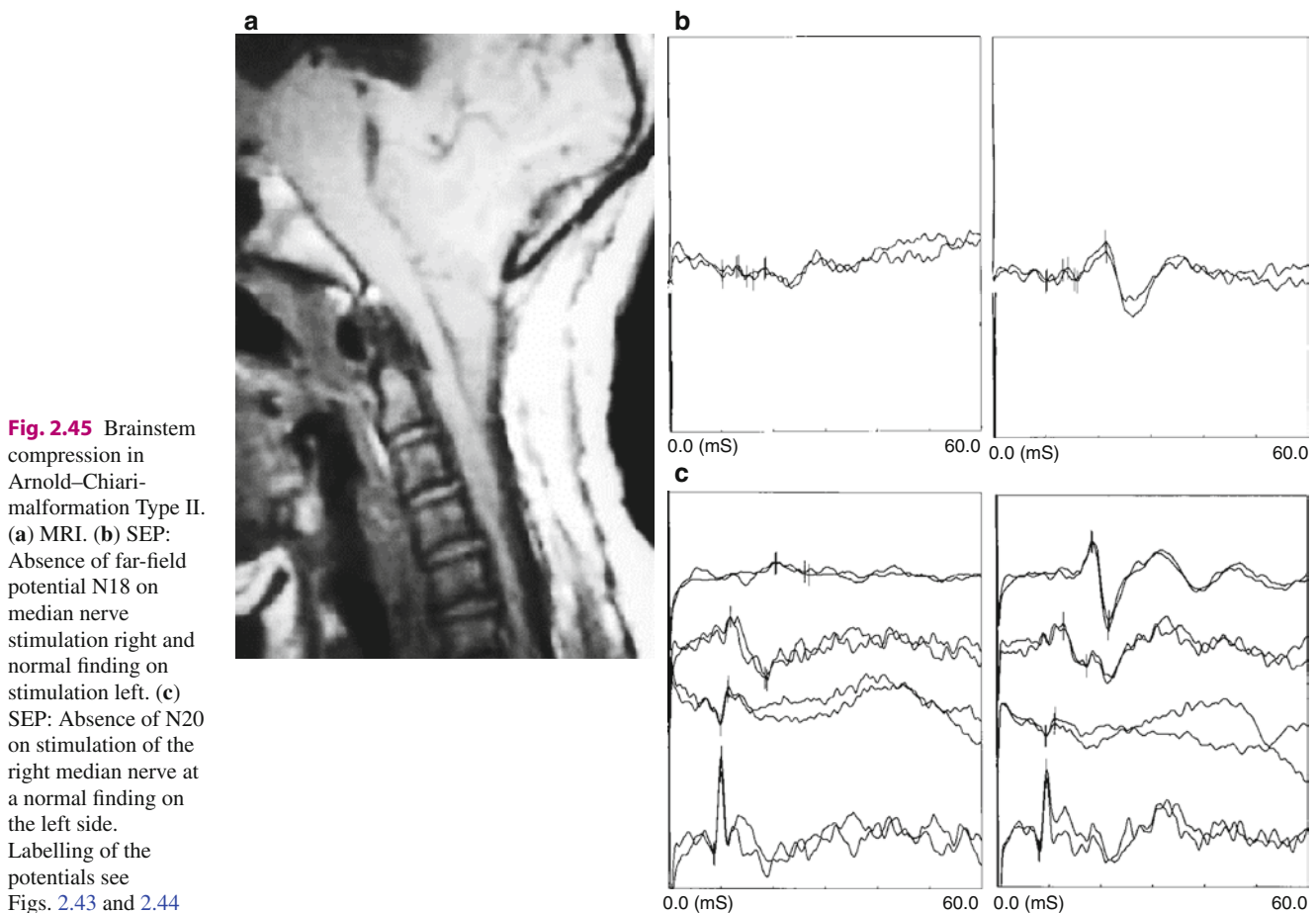
Only a small number of studies have reported reliable findings regarding a correlation between singular brainstem

lesions and SEPs. The most promising approach appears to be the inclusion of far field potentials. Although the exact diagnosis on the height of the lesion based on SEPs alone is generally not possible. In the presence of certain constellations SEPs can nevertheless provide topodiagnostic information. The cervical potentials N13a and N13b are preserved in all brainstem lesions with involvement of the medial lemniscus, while N20 is pathologically changed. This finding does, however, not permit any conclusions as to the topography of the lesion, which may be located between the cervical region of the spinal cord and the post-central gyrus.

Pontine lesions: The far field potentials P14 (Claß and Buettner 1993) and N18 (Sonoo et al. 1991; Raroque et al. 1994) are preserved in the presence of pontine lesions, while pathologic changes are manifested in N20.

Medullary lesions: Lesions in the rostral aspect of the medulla are characterized by a preserved N18 at an absent P14 potential, which lends support to the assumption of an origin of P14 in the caudal medulla oblongata (Sonoo et al. 1996; Manzano et al. 1999). N18 may also be absent in cases with a high medullary lesion (Fig. 2.45).

SEPs provide prognostic information on brainstem hemorrhage, basilar artery thrombosis and traumatic brainstem lesions: the bilateral absence of N20 potentials is always



associated with a poor prognosis, although not with a unilateral extinction of the potentials (Ferbert et al. 1988, 1990; Christophis 2004).

Brain Death

A typical initial finding in brain death on recording against a Fz reference is the absence of a cortical response at the concurrent demonstration of an N13b potential above C2 (Besser et al. 1988). The N13b potential is subsequently also lost (Stöhr et al. 1987). According to guidelines for brain death determination (Third update 1997, Scientific Committee, Federal German Chamber of Physicians) the extinction of N13b represents a criterion in the diagnosis of brain death, as it correlates with intact posterior column nuclei and is thus associated with the brainstem. In the further course, the N13a potential generated at the level of C6 may also be lost due to ischemic spinal cord injury with spinal vessel supply via the vertebral arteries.

Primary supratentorial or secondary brain damage is a further precondition of SEP assisted brain death diagnosis. Additional diagnostic investigations (EEG, cerebral circulation) must be carried out in patients with primary infratentorial lesions. SEP diagnosis as the only diagnostic procedure is not permissible for suspected lesions in the cervical part of the medulla. Four channel recording is obligatory to identify peripheral lesions (e.g. polytrauma with brachial plexus injury) and to provide evidence of the preservation of peripheral potentials (N10).

2.3.7 Transcranial Magnetic Stimulation

Peter P. Urban

2.3.7.1 Anatomic and Physiologic Principles

Evaluation of motor evoked potentials (MEP) with the use of transcranial magnetic stimulation (TMS) permits the functional, non-invasive assessment of pyramidal pathway function. A capacitor discharges a very brief pulse of current which flows through a copper coil and initially induces a pulse-shaped magnetic field that passes through the skull cap without significant discomfort to the subject. The magnetic field in turn induces an electric field in the brain, which synchronously activates primarily presynaptic neurons of the motor cortex, thus triggering a series of descending action potentials, while the peripheral nerves are directly polarized. Individual segments of the corticobulbar and corticospinal tract can be examined by recording the compound muscle action potentials (CMAPs) from different target muscles. In the cranial nerve region these comprise mainly the facial nerve innervated mimic musculature and the tongue. In addition to the corticomuscular latency, the peripheral motor

latency is determined with stimulation of the proximal nerve segments or roots; the difference between these latencies corresponds to the so-called central motor conduction time (CMCT). The central motor conduction time reflects the function of the pyramidal pathway segments which project to the motor neurons of the target muscle used for the recording.

The **corticofacial projections** descend from the primary motor cortex to the contralateral facial nucleus, while the facial neurons supplying the forehead muscles also receive projections from other, premotor areas (Morecraft et al. 2001). The corticofacial projections in the brainstem are located at the mesencephalic level in the middle segment of the cerebral peduncle; in the mid-pontine region they are, however, distributed across the entire base of the pons. The fibers cross the midline in the most caudal part of the pons, at the level of the facial nucleus region. Variations of the described course have, however, been described. Some individuals are characterized by so-called aberrant fiber bundles of the pyramidal pathway; they leave the pyramidal pathway at the level of the pontomesencephalic junction, and travel caudally along the border of the tegmentum before reaching the facial nucleus (Yamashita and Yamamoto 2001). In other subjects it may be assumed that corticofacial projections travel with the largest part of the pyramidal pathway through the ventral base of the pons, which they leave in the region of the ventral medulla oblongata only, to cross the midline at the level of the upper medulla oblongata, and continue rostrally to the facial nucleus located in the lower pontine dorsolateral tegmentum (Urban et al. 2001). A lesion location after decussation of the projections in the lateral medulla, and before arrival at the facial nucleus serves to explain the clinical picture of an ipsilaterally located central facial paresis (Urban et al. 1998, 1999; Urban and Hopf 2002).

The **corticolingual projections** descend, by and large symmetrically, from the primary motor cortex to both hypoglossal nuclei; this can be documented electrophysiologically with the use of transcranial magnetic stimulation, which enables the demonstration of bilaterally symmetrical CMAPs on cortical stimulation (Urban et al. 1996, 1997). Due to the bilaterally symmetrical excitation of the tongue, a unilateral lesion of the cortical projections does not in all cases lead to a lateral deviation of the tongue, but is routinely associated with dysarthrophonia, caused by a disturbance of the highly complex fine motor requirements of the tongue motor system in the context of articulation (Urban et al. 1997, 1999, 2001). Comparable to corticofacial projections, corticolingual projections course through the middle segment of the cerebral peduncle, subdivide in the base of the pons and cross the midline in the region of the ventromedial segment of the base of the pons. Location variability has also been described for corticolingual projections in the brainstem with “aberrant bundles” in the paralemniscal tegmental position (Urban et al. 1996).

2.3.7.2 Application

Recordings in the cranial nerve region are obtained from the masticatory musculature (trigeminal nerve), the facial mimic musculature (facial nerve), the sternocleidomastoid and trapezius muscle (accessory nerve), and the tongue (hypoglossal nerve). Of clinical importance are thus far principally recordings from the facial mimic musculature and the tongue, which also enable a fractional assessment of the corticomuscular segments.

Corticofacial Projections

For stimulation of the motor cortex a circular coil (mean diameter: 90 mm) or a double coil (mean diameter of each coil half: 70 mm) is placed 2 cm lateral to the vertex. In view of the variability of the CMAPs, a minimum of four MEPs are recorded and the shortest latency and largest amplitude are assessed. Recordings of the CMAPs are taken simultaneously, side-related from a facial muscle. A number of different facial muscles have been described as possible recording sites. A systematic comparison of the validity of different target muscles regarding evokability of a response potential, stimulus artefacts, interference with the R1 component of the blink reflex, cross-talk with registration of contralateral side activity, side differences between amplitudes on right-left comparison, and intraindividual reproducibility demonstrated distinct advantages of the buccinator and triangular muscles over other muscles when electrical or magnetic stimulation of the facial nerve is used, and of the buccinator and levator labii superioris muscles when magnetic stimulation of the motor cortex alone is applied (Urban 2002). This correlates with findings of anatomic studies, showing that only the lateral region of the facial nerve nucleus, where the orofacial musculature is represented, receives almost exclusively contralateral projections from the primary motor cortex, while the upper facial muscles are supplied by bilateral projections from the supplementary motor cortex and the rostral segment of the cingulate gyrus (Morecraft et al. 2001). Recordings from the orofacial musculature, most notably from the buccinator muscle via an enoral approach, are therefore particularly suitable for the examination of corticofacial projections (Urban et al. 1997). In addition to cortical stimulation, magnetic stimulation of the proximal, peripheral segment of the facial nerve is applied and enables determination of the peripheral motor conduction time (PMCT).

Comparative studies investigating the surgically exposed facial nerve during surgical interventions in the cerebellopontine angle showed the superiority of a stimulation site located in the most proximal segment of the facial canal, approximately 10–15 mm after entry of the nerve into the internal acoustic meatus (Rösler et al. 1989; Schmid et al. 1991). This requires a

parietotemporal coil placement and relatively low stimulation strength (as a rule 30–50% of the maximum stimulator performance). Attention should be paid that the PMCT is approximately 1–1.5 ms longer than with supramaximal electric stimulation at the stylomastoid foramen. Careful monitoring is required here to avoid accidental magnetic stimulation of the facial nerve at its exit point from the petrous canal. The conduction time difference between corticomuscular conduction time (CCT) and PMCT corresponds to the so-called central motor conduction time (CMCT), which also comprises the infranuclear segment of the facial nerve up to its entry into the petrous canal. The conduction time difference between magnetic stimulation of the proximal segment and electric stimulation at the stylomastoid foramen (= distal motor latency [DML]) corresponds to the transsossal conduction time, which has not gained significant diagnostic importance thus far. Electric stimulation at the stylomastoid foramen corresponds to the classical facial excitability test (FET), although this is used principally in CMAP evaluations.

Corticolingual Projections

TMS of the motor cortex is applied with a circular or a double coil, placed 4–6 cm lateral to the vertex. Recordings of the CMAPs are taken from each side of the tongue, using a spoon-shaped electrode device made of plastic material, into which two pairs of Ag/AgCl electrodes are embedded (Schmid et al. 1991; Meyer 1992). Light preactivation is achieved by slight pressure of the tongue against the electrode device, with the hard palate serving as a counterpressor. Synchronous with cortical stimulation, magnetic stimulation of the proximal hypoglossal nerve is applied in the hypoglossal canal, with coil placement in a deep occipital position. Due to both the deep anatomic location of the hypoglossal canal at the caudal end of the base of the skull and low magnetic field intensity, at this site the hypoglossal nerve can be reached and PMCT or CMCT determined in only 75% of all healthy subjects (Urban et al. 1997). No further conclusions can be drawn in cases of an unavailable MEP. More distal in the course of the nerve, electric stimulation can be applied to the mandibular angle (Redmond and Di Benedetto 1988).

2.3.7.3 Evaluation

TMS of Corticofacial Projections

Since even in healthy subjects merely inconstant ipsilateral responses can be achieved after cortical stimulation (Urban et al. 1997; Fischer et al. 2005), only contralateral responses are considered in patients. A lesion of the supranuclear projections is presumed:

- When no CMAP is evoked on cortical stimulation (absence of potential is defined as no reproducible response on four consecutive stimulations and amplification of 200 $\mu\text{V}/\text{div}$) (Rösler et al. 1989; Fig. 2.46).
- At an amplitude quotient (amplitude on cortical stimulation: amplitude on electric stimulation of the facial nerve at the stylomastoid foramen) $\leq 10\%$.
- In the presence of an abnormally delayed central motor conduction time or a pathologic side difference for the CMCT.

An infranuclear facial nerve lesion can be assumed at an amplitude reduction of $\leq 50\%$ compared to the healthy side (Urban 2002), approximately 10 days after the acute lesion with onset of axonal degeneration. Reference values for the buccinator muscle have been published (Urban et al. 1994, 1997).

TMS of Corticolingual Projections

In healthy subjects, bilaterally symmetric muscle responses can be evoked on cortical stimulation at both sides of the tongue (Urban et al. 1994). A lesion of the supranuclear projections is presumed:

- When no CMAP is evoked on cortical stimulation (absence of potential is defined as no reproducible response on four consecutive stimulations and amplification of 200 $\mu\text{V}/\text{div}$) (Rösler et al. 1989; Fig. 2.47).
- At an amplitude quotient (amplitude on cortical stimulation: amplitude on electric stimulation of the hypoglossal nerve at the mandibular angle) $\leq 10\%$.
- In the presence of an abnormally delayed central motor conduction time or a pathologic side difference for the CMCT. Reference values have been published elsewhere (Urban et al. 1994, 1997).

2.3.7.4 Interpretation of Findings

Brainstem Ischemia

Prognostic Significance of MEPs

Typical characteristics of MEPs after cerebral ischemias comprise a reduced amplitude quotient, in some instances even the absence of CMAPs on cortical stimulation, an increased motor stimulation threshold, and an only slightly delayed CMCT (Weber and Eisen 2002). Only a small number of studies have analyzed TMS for vascular

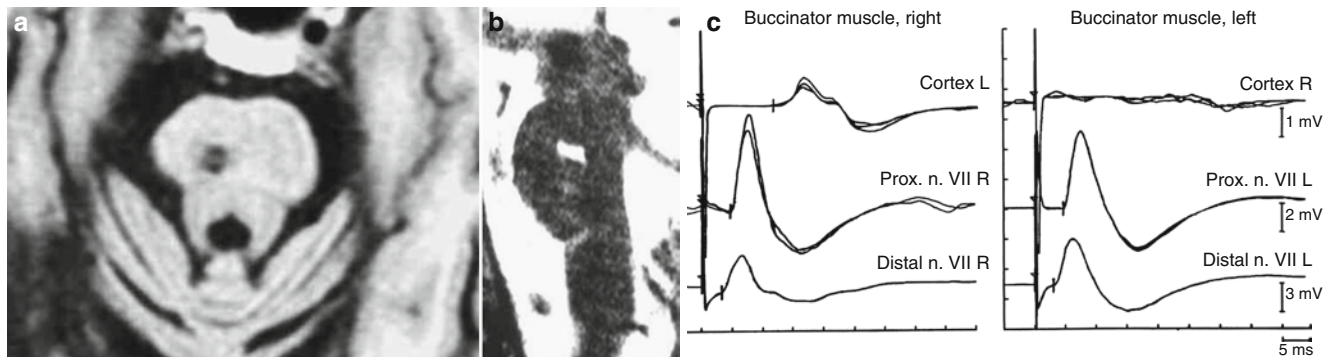


Fig. 2.46 Infarction in the dorsal base of the pons right near the medial lemniscus with central facial paresis left. TMS of the motor cortex right does not evoke a contralateral CMAP in the buccinator muscle

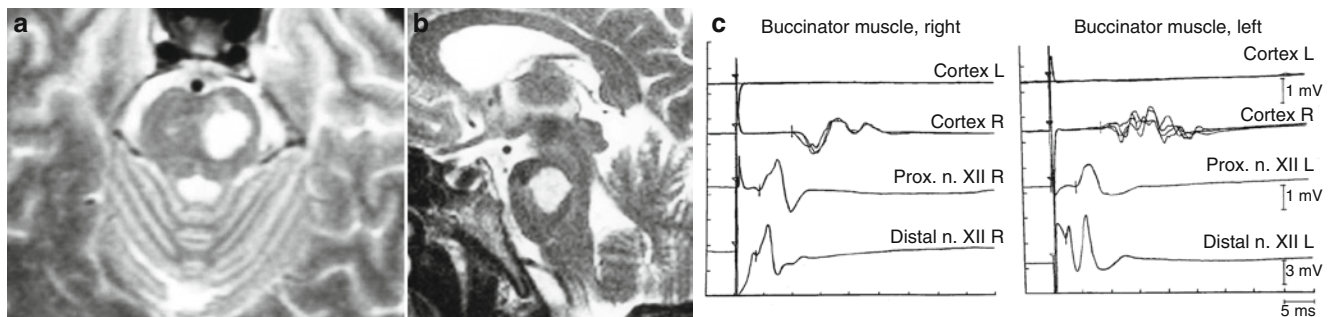


Fig. 2.47 Infarction of the left base of the pons, presenting with dysarthria and central facial paresis right. TMS of the motor cortex left does not evoke a CMAP across the two sides of the tongue

brainstem ischemias. In the largest series, 30 intensive care patients with acute brainstem lesions were investigated 12 h after termination of sedation and muscle relaxation (Schwarz et al. 2000). The causal factor was a brainstem infarction in 15 patients, and a space-occupying cerebellar infarction in five cases. Causes in the remaining patients included brainstem and cerebellar hemorrhages, brainstem contusion, encephalitis and basilar aneurysm, respectively. It was found that the absence of MEPs to the abductor pollicis brevis muscle in the acute phase correlated significantly ($p < 0.0001$) with a motor deficit persisting after 3 months. Bassetti et al. (1994) reported on six patients with locked-in-syndrome and recording of MEPs from the upper and lower extremities. Four patients with an initial absence of MEP did not show clinical motor recovery, while two patients with still obtainable muscle responses had a nearly complete regression of paresis. Ferbert et al. (1992) investigated MEPs to the abductor pollicis brevis muscle in 20 patients with hemiparesis due to a circumscribed pontine infarction. TMS in the acute phase was, however, carried out in only seven patients, and was used in the chronic infarction study of 13 patients. CMCT was pathologically prolonged in patients with moderate to severe pareses, while the amplitude quotient between cortical and electric stimulation of the peripheral nerves did not permit differentiation between the paretic and non-affected side. From these studies it can be concluded that MEPs in the acute phase of brainstem infarctions are of prognostic significance with respect to paretic regression. This finding is in accordance with reports on investigations of MEPs at other infarct locations (Escudero et al. 1998; Trompetto et al. 2000).

Topodiagnostic Significance of MEPs

On principle, the findings reported by TMS studies permit only tentative conclusions regarding the height of the lesion. In all cases the lesion has to be located rostral to the body segment showing pathologically changed MEPs. The possibility of level diagnostics arises only in the presence of a pathologic finding, since a normal MEP does not permit the exclusion of a partial lesion, e.g. of the slow conducting fiber segments. The investigation of MEPs does, however, permit a statement with respect to a lesion location at the axial level (Urban et al. 1996, 1997).

Multiple Sclerosis

Typical changes in MEP characteristics in multiple sclerosis (MS) include a markedly prolonged CMCT,

potential dispersion on cortical stimulation, and a reduction in the amplitude quotient. MS lesions located in the brainstem, as well as ischemias, can mediate functional impairment of corticobulbar and corticospinal projections. Singular lesions exist only rarely in the brainstem, chiefly at the onset of the disease, which qualifies the utility of TMS for topodiagnostic mapping. Of greater importance for meeting the diagnostic criterion of topical dissemination is the possibility of identifying clinically silent lesions by means of TMS. The examination of corticospinal and corticobulbar projections can make a valuable contribution to this procedure (Riepe and Ludolph 1993; Urban et al. 1994). In individual cases, the investigation of corticofacial projections with TMS can also provide topodiagnostic information. The occurrence of incomplete peripheral facial paresis with preserved excitability of the proximal facial nerve on magnetic stimulation, and prolonged CMCT suggests the presence of an infranuclear, but more proximally located, e.g. intra-axial, lesion, for example a demyelinating lesion of the dorsolateral pons (Fig. 2.48).

Amyotrophic Lateral Sclerosis

Typical changes in MEP characteristics in amyotrophic lateral sclerosis (ALS) comprise a reduction in the amplitude quotient, frequently in form of an absent potential on cortical stimulation, and in some instances a slightly prolonged CMCT. In ALS, corticobulbar functions are often affected early in the course of the disease. In 51 patients with different clinical courses of ALS, a lesion of the corticolingual projections was detected in 53% of cases, of the corticofacial projections in 47%, and of the corticospinal projections to the upper or lower extremities in 25% and 43% of patients, respectively (Urban et al. 1998, 2001). Similar incidences of function disturbances of the corticobulbar projections have been reported for recordings from the masseter muscle (Trompetto et al. 2000) and from the trapezius muscle (Truffert et al. 2000). Additional examination of the corticobulbar projections can be helpful, in particular in the differential diagnosis of cervical myelopathy (Truffert et al. 2000).

Hereditary Spastic Spinal Paralysis

In patients with hereditary spastic spinal paralysis, in particular MEPs to the lower extremities are absent or amplitude-reduced, while, depending on the clinical findings, the upper extremities are less often and less severely affected. The corticobulbar projections may, however, also be affected in the absence of a clinical correlate (Visbeck et al. 2000).

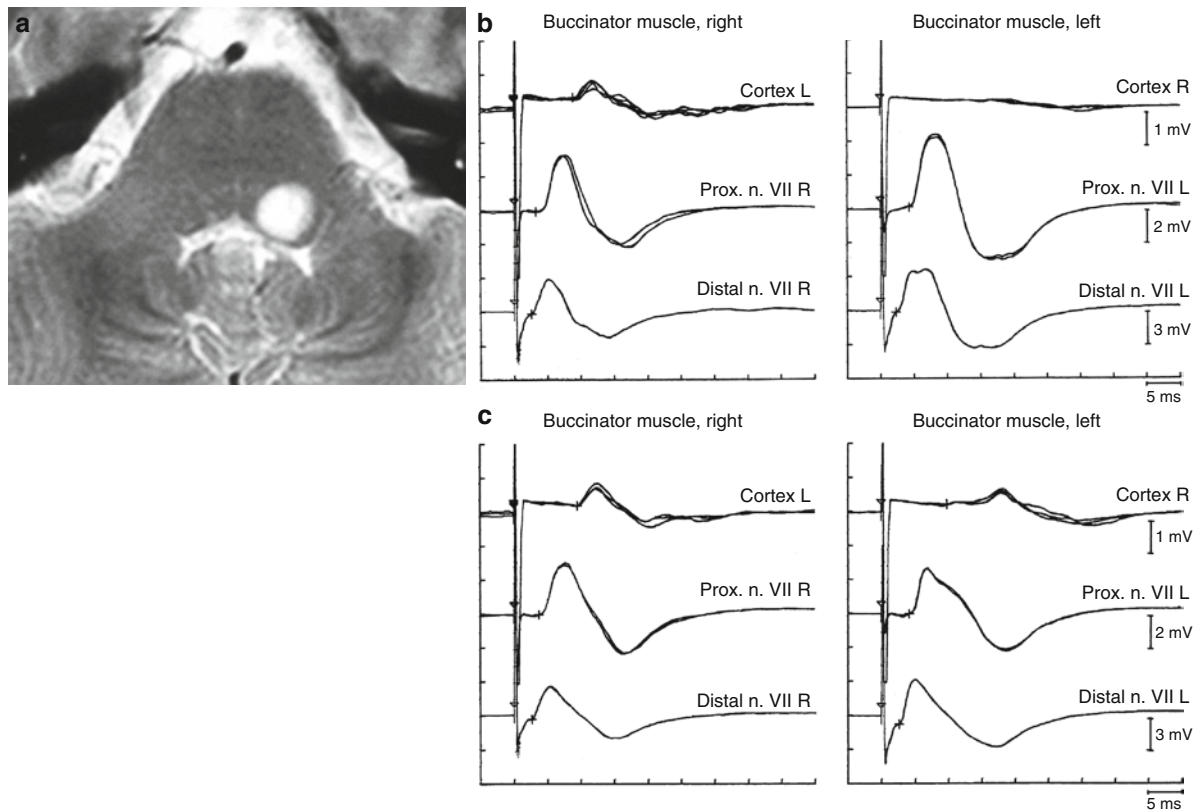


Fig. 2.48 Multiple sclerosis. MRJ: Demyelinating lesion in the region of the dorsolateral pons left, presenting with peripheral facial paresis left. TMS (upper right figure) On day 2 absence of CMAP on cortical stimulation of the right motor cortex and recording from the left buc-

cinator muscle. The peripheral facial nerve showed a normal excitability at canalicular stimulation. Lower right figure: Corresponding to clinical improvement, CMAP reappeared following cortical stimulation on day 14

2.3.8 Laser Evoked Potentials

Peter P. Urban

2.3.8.1 Anatomic and Physiologic Principles

A number of similarities exist between the method of laser evoked potentials (LEP) and somatosensory evoked potentials, but only the LEPs enable an objective examination of nociceptive pathways. The term nociceptive pathway refers to the entire distance from the peripheral receptor to the cortex. The peripheral **pain receptors** (nociceptors) are so-called free nerve endings of A δ - and C-fibers. These fibers enter the dorsal horn via the dorsal root and synapse in the dorsal horn upon the second neuron. The second neuron crosses at the spinal level through the anterior commissure to the contralateral side and courses within the spinothalamic tract in the anterior part of the spinal cord to cranial.

2.3.8.2 Application

Stimulation

Stimulation is applied with short repeated heat impulses generated by a CO₂ laser (wavelength 10.6 μ m, stimulation time

20–100 ms) or a thulium (Tm) laser (wavelength 2.01 μ m, stimulation time 3 ms). Stimulation strength is 1.5- to two-fold the pain threshold (Treede et al. 2003). These pulses are conducted via a glass fiber where they can be directed to any user-defined skin surface area by means of a mirror handpiece. The laser beams do not cause skin damage. Strong laser stimulation may lead to some transitory reddening of the skin. The interval between two stimulations applied in a random order ranges from 8 to 12 s. Forty laser stimulations are applied per train.

Recording

The LEPs are recorded using Ag/AgCl cup electrodes and electrode impedances below 5 k Ω . A minimum of two channels is required for the assembly: vertex (Cz) against connected earlobes, and a vertical oculogram for the identification of eye movements and blinking. The amplifier sensitivity is 100 μ V for the oculography and 25 μ V for the remaining channels. At a bandpass of 0.2–70 Hz, the recording rate is set at 200 Hz and the time window at 1 s before and up to 3.5 s after onset of the stimulation. To increase the amplitude of LEPs, the attention of the study subject is directed toward the stimulations (e.g. by counting of stimulations, etc.).

In patients, two areas are examined by left-right comparison (e.g. both hands or both feet), only one of which has pathologic change. Both areas are subjected to two stimulations each, applied in balanced succession to compensate for habituation effects.

2.3.8.3 Evaluation

The principal LEP component used for evaluation in view of its good reproducibility is a negative-positive complex within a latency range of approximately 200–400 ms, derived from stimulation to the dorsum of the hand. On application of the Tm laser, negativity (N2) occurs at a latency of 210 ms, positivity (P2) occurs at a latency of 330 ms, and the peak-to-peak amplitude ranges from 10 to 60 μ V. The long latency of LEPs is attributable to the slow nerve conduction velocity of nociceptive fibers (A δ : 15 m/s), and the fact that these are late potentials which are not generated in the primary sensorimotor cortex. Positivity represents the LEP component with the most reliable reproducibility, making it the most frequently assessed factor in the evaluation process.

Absolute amplitude values are not considered for diagnostic purposes because of their high interindividual variability and numerous influential factors (subjective pain sensation following laser stimulation, vigilance, age, etc.). A complete absence of the cortical potential constitutes the only factor for evaluation (Treede 1996). Side-to-side differences in amplitudes $\geq 35\%$ have been described as pathologic (Beydoun et al. 1993). The absolute latencies are only rarely prolonged; a 2.5-fold excess of the standard deviation from the mean values in a normal collective documents evidence of pathology (Treede 1996). The latency delay following stimulation of the dorsal foot ranges from 30 to 70 ms compared to stimulation to the dorsum of the hand. Maximum amplitudes are observed above the vertex.

2.3.8.4 Interpretation of Findings

While pathologic latency delays, reduced amplitudes on right–left comparison, or the absence of a potential document the presence of a lesion involving the nociceptive pathways, they do not initially enable the differentiation between a lesion of the peripheral and the central nervous system.

Central Lesions

The first application of LEPs was described in patients with syringomyelia (Kakigi et al. 1991; Treede et al. 1991). These patients had the typical symptoms of sensory dissociation, i.e. the absence of pain and temperature perception at preserved tactile sensitivity. LEPs showed pathologic latency delays, amplitude reductions, or the absence of potentials.

Brainstem Ischemia/Hemorrhage

In patients with brainstem infarction and absent or diminished pain perception owing to a lesion of the spinothalamic tract, good correlation has been found between clinical and electrophysiologic findings, which also reflect the clinical course (Hansen et al. 1996). Patients with a lesion of the lateral spinothalamic tract due to a dorsolateral medullary brainstem infarction (Kanda et al. 1996), or a distinctly lateral caudal medullary infarction (Urban et al. 1999) are characterized by contralateral sensory dissociation that can be objectified with LEPs. The absence of LEPs on stimulation to the ipsilateral side of the face has been reported in patients with dorsolateral medulla oblongata infarction and the clinical picture of Wallenberg's Syndrome (Cruccu et al. 2003; Figs. 2.49 and 2.50).

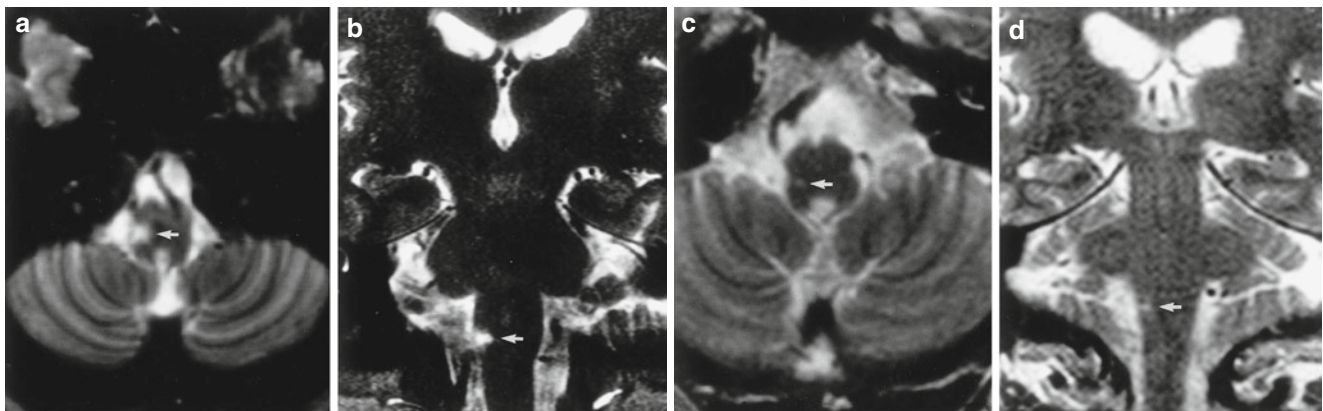
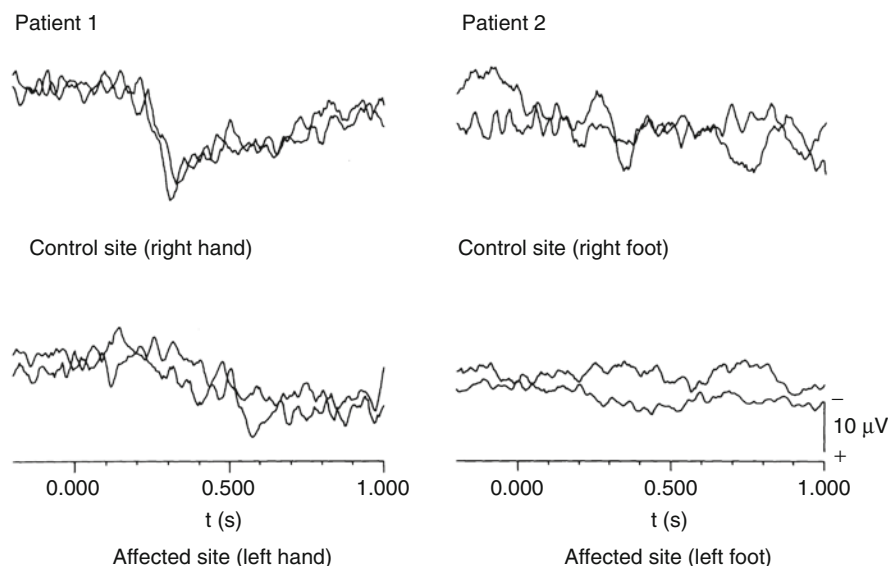


Fig. 2.49 MRIs of two patients with an infarction of the right lateral medulla oblongata. (a, b) Patient 1 presented with dissociated sensory deficits on the left side of the body caudal to C3. (c, d) Patient 2 presented with dissociated sensory deficits of the left half of the body caudal to Th4

Fig. 2.50 Laser evoked potentials of the patients from Fig. 2.49 with dissociated sensory deficits caudal to C3 (patient 1) and caudal to Th4 (patient 2). LEPs were absent from the affected sides, but could be obtained on the control side



2.3.9 Recording of Eye Movements

Frank Thömke

Electrooculography enables quantitative, accurate recording of different types of eye movements. A number of different, more or less complex, methods are available for this purpose, whose advantages and disadvantages are discussed below. The cooperation of the patient is a basic requirement of all electrooculographic methods. In an inattentive or tired patient, disturbances of smooth pursuit eye movements may occur, and saccades may be characterized by varying degrees of target inaccuracies, or they may be slowed. These irregularities can, on principle, also occur through the influence of centrally acting substances.

2.3.9.1 Direct Current Recording

Direct current electrooculography is the longest known (and probably most widely used) method for recording different types of eye movements. It enables quantitative, relatively accurate recording, and is capable of providing sufficient information to answer most clinical questions. The method is based on the so-called corneoretinal potential, a difference of potential between the cornea and the retina, with a positive cornea against a negative retinal potential. On movements in the direction of the electrode, a positive deflection is observed (the positive cornea is located closer to the electrode than the negative cornea); on movements away from the electrode a negative deflection is noted (the negative retina lies closer to the electrode than the positive cornea). The eye thus functions as a flexible dipole, so that every eye movement mediates changes in the electric field, which can

be recorded as changes of potentials between two surface electrodes. This can be achieved with the subject's eyes either open or closed. Adhesive electrodes for recording of horizontal eye movements are placed at the lateral and the medial corner of the eye, respectively; for recording of vertical eye movements, the electrodes are affixed above or below the respective eye (Fig. 2.51).

There is a linear correlation between the amplitudes of these deflections and those of eye movements for amplitudes of up to 40° . Within this range ($\pm 40^\circ$ from the primary position), direct current electrooculography permits evaluation of different eye movements with a resolution of about 1° . Due to the fact that eye movements can be recorded from closed eyes, investigations of the vestibular system, e.g. caloric excitability of the horizontal semicircular canals on warm and cold water stimulation, or rotational testing may be performed and followed by quantitative evaluation of the recorded caloric and postrotatory nystagmus (Table 2.7).

2.3.9.2 Infrared Reflective Oculography

Infrared reflective oculography is based on the finding that the intensity of light reflection of the white sclera is greater than that of the darker iris, which, in turn, is greater than light reflection of the pupil. Movements of the eye exposed to invisible infrared light cause the iris-sclera border and the iris-pupil border to shift in the direction of the eye movement, i.e. the positions of areas with strong, moderate, and mild reflection of the infrared light change commensurate with the eye movement. The infrared light reflected from the eyes and changes over time, which are proportional to the respective eye movement, are measured during this process. Modern systems comprise more than 1,700 photosensitive

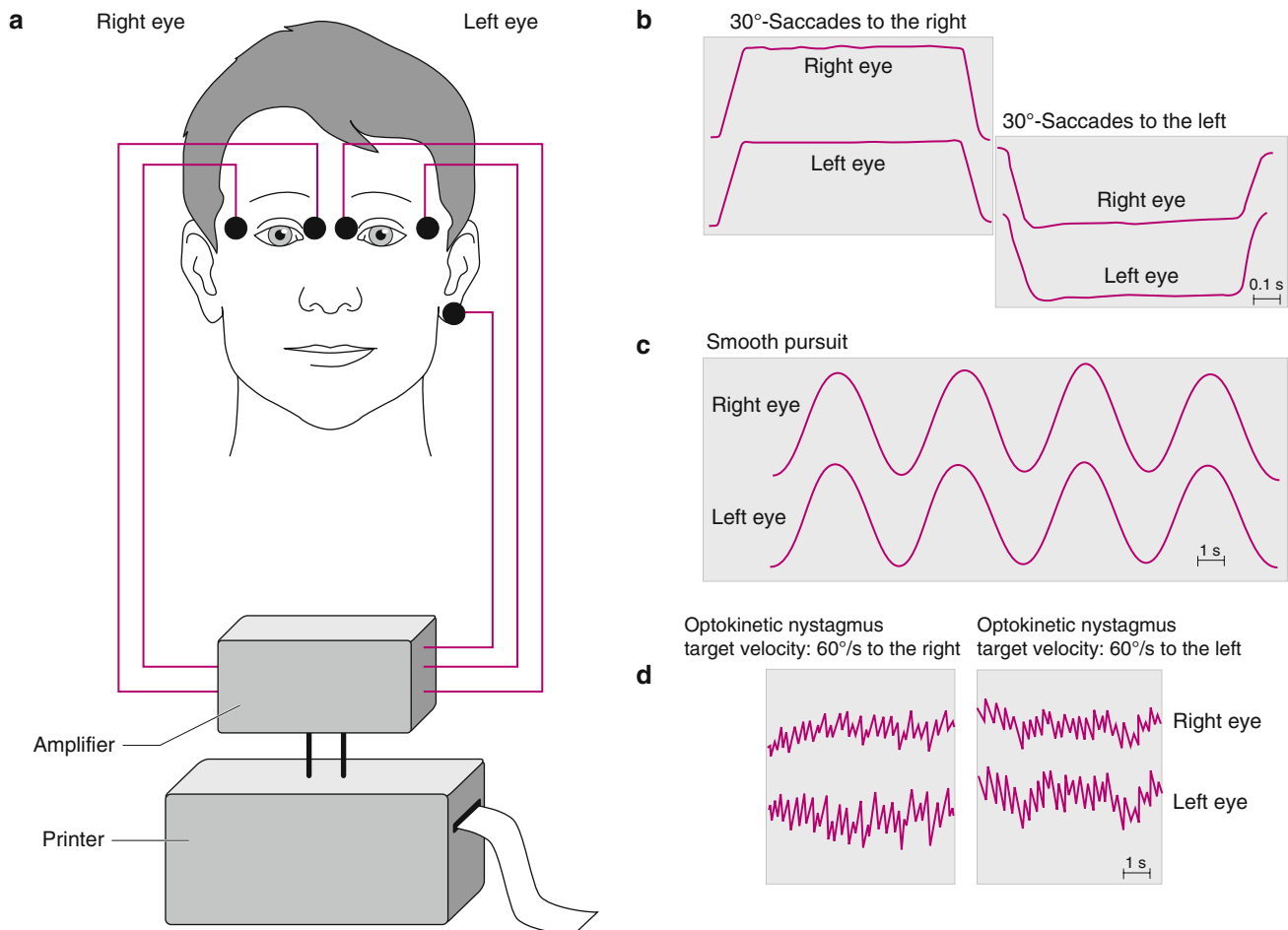


Fig. 2.51 Direct current recording of eye movements. (a) The eye functions as a flexible dipole, with the cornea relating to the positive and the retina relating to the negative pole. Eye movements function as “dipole movements” and mediate changes in the electric field which are

recorded as changes of potentials between two surface electrodes. (b–d) Different types of eye movements: saccades (b); smooth pursuit eye movements (c); optokinetic nystagmus (d) (see Thömke: Eye movement disturbances. Stuttgart: Thieme 2001)

diodes (e.g. AMTech Eyetracker E.T.3: 1,728 diodes, height 13 μm , distance 10 μm) arranged in a linear array opposite each eye. The mode of operation of this diode array is comparable to that of a television camera recording only a single image line, while here the reflection of infrared light is determined by what may be imagined as a line proceeding across the eye. From these data the computer calculates the changes in infrared light reflection recorded during the respective eye movement. The infrared light sources and photosensitive diodes can be integrated into a helmet or a ring mounted on the head. They may also be installed in a frame furnished with a head and chin support for the patient.

Eye movement recordings obtained with this method can only be done with open eyes and are within a range of approximately $\pm 20^\circ$ proportional to the eye position and have a resolution of less than 0.5° . Comparable to direct current recording, infrared reflective oculography does not permit recording of rotational eye movements (Table 2.7).

2.3.9.3 Videoculography

Videoculography uses video cameras to record eye movements, in addition to a system for computer-based data evaluation. The study subject wears head-mounted goggles with an integrated camera system and semi-translucent mirrors, weighing less than 500 g (progressively lighter models are becoming available). The eyes are illuminated with infrared light emitted by diodes integrated into the goggle frame. Horizontal and vertical eye positions are calculated by back-transformation after the respective image processing system has mapped the pixel coordinates of the pupil center and calibration of the system. The torsional components are determined based on individual characteristic iris patterns in a selected segment of the iris (alternatively, a mark is made on the iris using a tissue-compatible make-up pencil). The degree of torsion and the eye speed are again calculated by back-transformation of the achieved eye position with consideration of the time domain. The spatial resolution of

Table 2.7 Advantages and disadvantages of different eye movement recording methods

Method	Characteristics	Advantages	Disadvantages
Direct current recording	Recording area: approximately $\pm 40^\circ$ Spatial resolution about 1° Temporal resolution about 40 Hz	Non-invasive Low patient discomfort Recording from open and closed eyes possible	Prone to artefacts (muscle artefacts, blink artefacts, baseline fluctuations) Lower reliability in recording of vertical eye movements Recording of torsional eye movements not possible
Infrared reflective oculography	Recording area: approximately $\pm 20^\circ$ Spatial resolution below 0.5° Temporal resolution about 100 Hz	Non-invasive Low patient discomfort Reliable recording of horizontal and vertical eye movements	Recording possible from open eyes only Limited recording area ($\pm 20^\circ$) Recording of torsional eye movements not possible
Videoculography	Recording area: approximately $\pm 25^\circ$ horizontal and \pm approximately 20° vertical Spatial resolution up to 0.02° Temporal resolution 500 Hz	Non-invasive Low patient discomfort Reliable recording of horizontal, vertical and torsional eye movements	Recording possible from open eye, only (influence of fixation as a result of recording in complete darkness is assessable) Limited recording area ($\pm 25^\circ$ horizontal or $\pm 20^\circ$ vertical)
Scleral search coil technique	Recording area: always $\pm 180^\circ$ Spatial resolution up to 0.01° Temporal resolution 500 Hz	Recording possible from open and closed eyes Reliable recording of horizontal, vertical and torsional eye movements	The cornea must be anesthetized A contact lens with an opening at the center and an integrated coil must be affixed Very cost-intensive and complex technology

currently available systems are within a range of 0.02° horizontal, 0.03° vertical and 0.1° torsional; temporal resolution ranges up to 500 Hz (Table 2.7).

2.3.9.4 Scleral Search Coil Technique

The scleral search coil technique is by far the most precise and accurate technique for eye movement recordings in a three-dimensional space, which also permits recording of rotational eye movements. It is based on the principle that voltage is induced in an electrically conductive material while this conductor moves within a magnetic field (or the strength of the magnetic field changes). A contact lens with a small opening at its center and an embedded coil of very thin wire is fixed on the anesthetized cornea (instead of the described contact lens, older systems based on the method developed by Robinson (1963) used a flat metal ring fixed to the cornea). The head of the patient is placed in the center of a strong magnetic field elicited by large magnetic coils. During eye movements in the magnetic field, a voltage is induced in the metal ring, which is proportional to the amplitude of the eye movement. The method is not widely available and employed predominantly in scientific experimentation. It enables three-dimensional recording of horizontal, vertical and rotational eye movements from open and closed eyes at a very high resolution of up to 1 min of angle (0.01°) (Table 2.7).

2.3.10 Other Electrophysiologic Methods for the Investigation of Brainstem Reflexes

Peter P. Urban

2.3.10.1 Stapedius Reflex

The stapedius reflex (Fig. 2.52) is an acousticofacial reflex with the cochlear part of the vestibulocochlear nerve functioning as the afferent, and the facial nerve as the efferent branch. Proceeding from the cochlear nucleus, the neurons to the stapedius muscle in both facial nuclei are accessed,

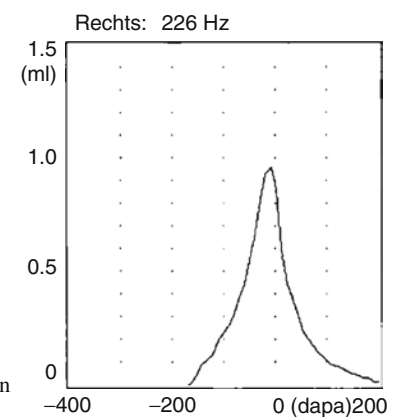


Fig. 2.52 Stapedius reflex in a healthy subject

inducing bilateral contraction of the stapedius muscle after unilateral stimulation. Synapsing occurs at the pontomedullary level. The stapedius reflex is used primarily by ENT clinicians as an objective audiometric test method. While the examination of the stapedius reflex permits a qualitative assessment, a quantitative evaluation of latencies or amplitudes is not possible. Pathologic findings of the stapedius reflex may, on principle, be expected in the presence of tegmental pontomedullary lesions; an inference as to the lesion topography may be drawn from the pattern of the pathologic findings (ipsilateral/contralateral) (Lehnhardt 1993). However, other important influences also need to be considered in the interpretation of abnormal findings. Mechanical damage to the auditory ossicle chain, e.g. as a result of stapes ankylosis, or peripheral facial paresis are further possible pathologies responsible for the absence of a reflex response.

2.3.10.2 Trigemino-Cervical Reflex

The trigeminocervical reflex (head retraction reflex) was first described as a clinical reflex by (Wartenberg 1941). In a positive case, a light tap with the reflex hammer to the region below the nose elicits a brief head jerking reaction in the seated patient. The reflex may also be examined neurophysiologically. With the patient in a seated position, the exit sites of the supraorbital or intraorbital nerves are stimulated electrically at the pain threshold and the reflex response is recorded from the sternocleidomastoid and/or semispinalis capitis muscle, using surface or needle electrodes (Ertekin et al. 2001; Serrao et al. 2003). The trigeminocervical reflex is a polysynaptic interconnected nociceptive protective reflex between the sensory trigeminal and the accessory nucleus, or the cervical motor neurons. At low stimulation strengths, inconstant stimulus responses with

latencies of about 40 ms are elicited in the spinal musculature (Ertekin et al. 2001). Conversely, several reflex responses with different latencies can be recorded at higher stimulation strengths. Short latency responses are obtained after approximately 10 ms, while later response latencies of about 40 ms are associated with the mechanical reflex response (Sartucci et al. 1986; Di Lazzaro et al. 1996; Serrao et al. 2003).

Absent or abnormally prolonged reflex responses have been described in patients with tegmental medullary infarctions, cervical myelopathy, and multiple sclerosis (Rossi et al. 1989; Di Lazzaro et al. 1996).

2.3.10.3 Trigemino-Hypoglossal Silent Period

Inhibitory connections between sensory trigeminal afferents and hypoglossal neurons have been described in animal models (Tomioka et al. 1999; Zhang et al. 2003). Similar projections have also been shown in humans (Urban et al. 2005). Analogous to the masseter silent period, the trigeminohypoglossal silent period may be assumed to be an antinociceptive protective reflex.

Examination of the trigeminohypoglossal silent period is performed with a specially prepared enoral stimulation and recording device, which permits right–left unilateral electric stimulation of the trigeminal (V2) innervated palatine mucosa and simultaneous recording of EMG activity from both sides of the tongue surface (Fig. 2.53). Stimulation is applied to each side of the palate with the fivefold sensory stimulation threshold, while the study subject is asked to maximally activate the tongue muscle. Five trains are recorded and EMG activity is averaged. Filter settings are 20 Hz and 2 kHz, respectively.

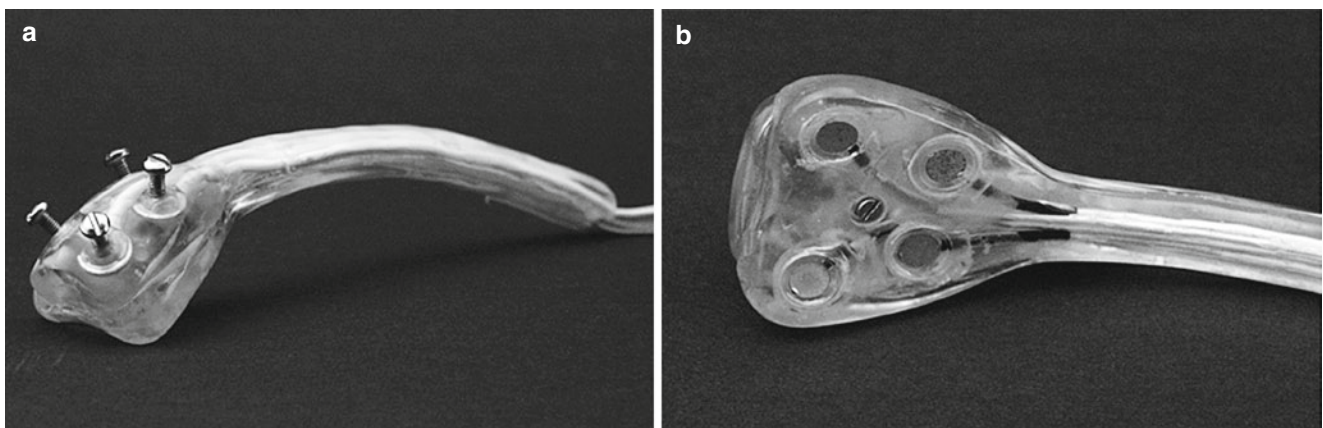


Fig. 2.53 Stimulation and recording device for unilateral electric stimulation of the hard palate. Recording of CMAPs is achieved from surface area of the tongue using Ag/AgCl-electrodes. (a) View from

above showing stimulation electrodes. (b) View from below showing recording electrodes

In 18 of 20 subjects, monophasic bilateral suppression of tongue activity was observed on right-left unilateral stimulation, starting at 41.1 ± 4.7 ms and terminating at 82.4 ± 12.5 ms. Mean duration of the silent period ranged at 41.4 ± 10.2 ms. Tongue muscle activity was not suppressed after bilateral palatal stimulation in two of the subjects (Fig. 2.54).

Initial investigations in individual patients with circumscribed tegmental brainstem lesions of the caudal pons and the dorsolateral medulla oblongata showed the absence of a silent period on the ipsilateral side of the lesion location, although no sensory abnormality was found on clinical examination (Figs. 2.55 and 2.56). In individual patients with multiple sclerosis, a unilateral clinically silent lesion was

Fig. 2.54 Trigeminohypoglossal silent period in a healthy subject. Unilateral electric stimulation of the hard palate induces bilateral suppression of muscle activity at both halves of the tongue

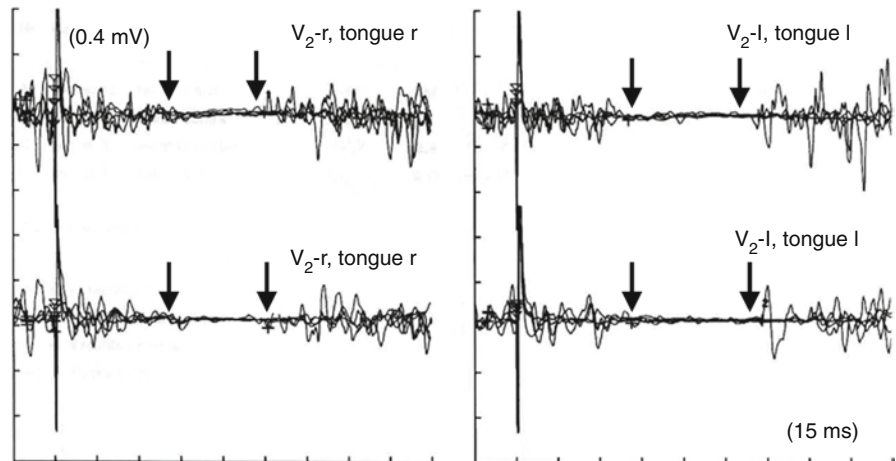


Fig. 2.55 Patient with dorsolateral infarction involving the right medulla oblongata. (a) Axial MRI. (b) Sagittal MRI. (c) Electrical stimulation of the hard palate at the right side shows no suppression of muscle activity at both halves of the tongue, while stimulation to the left side of the palate leads to bilateral suppression of tongue muscle activity

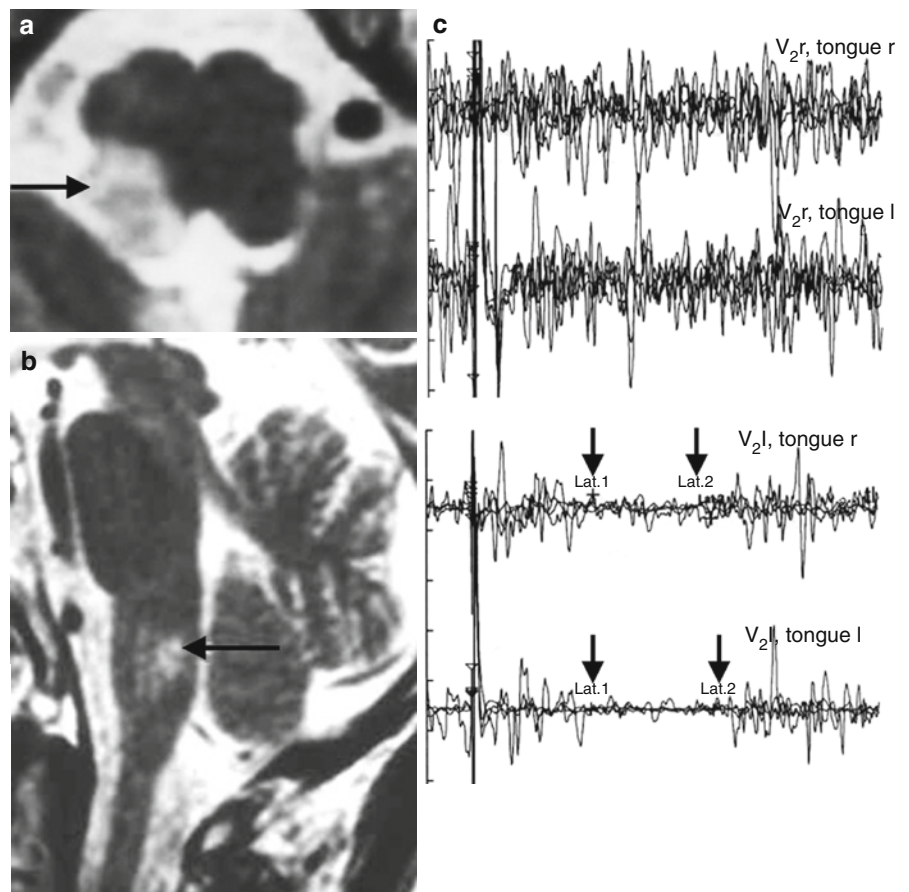
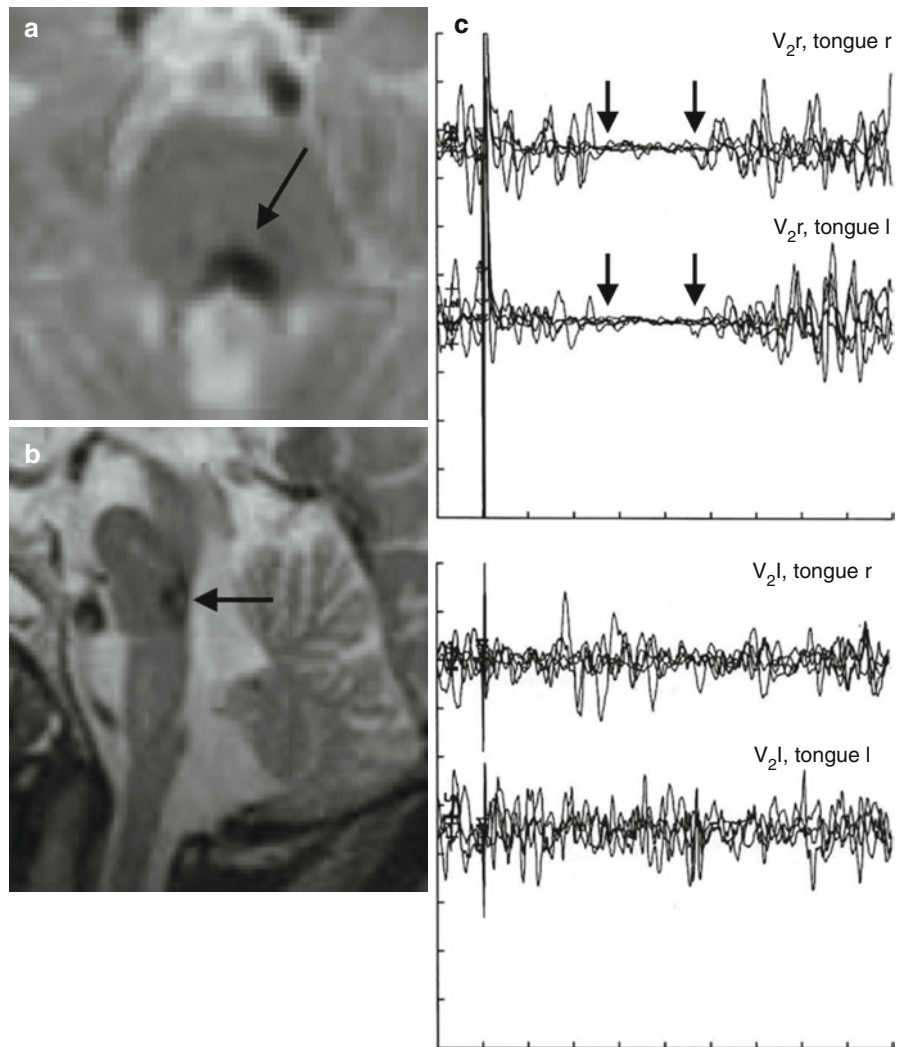


Fig. 2.56 Patient with hemorrhage into a cavernoma in the left pontine tegmentum. (a) Axial MRI. (b) Sagittal MRI. (c) Electrical stimulation of the hard palate at the left side shows no suppression of muscle activity at both halves of the tongue, while stimulation of the right side of the palate leads to bilateral suppression of tongue muscle activity



detected. Further studies in a larger patient population and in patients with circumscribed brainstem lesions will be conducted to determine the diagnostic validity of this method.

Literature

2.1 “Neuroradiology”

- Bendszus M, Koltzenburg M, Bartsch AJ, Goldbrunner R, Günthner-Lengsfeld T, Weillbach FX, Roosen K, Toyka KV, Solymosi L (2004) Heparin and air filters reduce embolic events caused by intra-arterial cerebral angiography. A prospective, randomized trial. *Circulation* 110:2210–2215
- Berkefeld J, du Mesnil de Rochemont R, Zanella FE (2004) Endovaskuläre Behandlung intrakranieller Aneurysmen. *Dtsch Arztebl* 101:A 260–A 267
- Boor S, Maurer J, Mann W, Stoeter P (2000) Virtual endoscopy of the inner ear and the auditory canal. *Neuroradiology* 42:543–547
- Dammert S, Krings T, Möller-Hartmann W, Ueffing E, Hans FJ, Willmes K, Mull M, Thron A (2004) Detection of intracranial aneurysms with multislice CT: comparison with conventional angiography. *Neuroradiology* 46:427–434
- Eckert B, Kucinski T, Pfeiffer G, Groden C, Zeumer H (2002) Endovascular therapy of acute vertebrobasilar occlusion: early treatment onset as the most important factor. *Cerebrovasc Dis* 14: 42–50
- Fitzek C, Tintera J, Müller-Forell W, Urban P, Thömke F, Hopf HC, Stoeter P (1998) Differentiation of recent from old cerebral infarction by diffusion weighted MR imaging (DWI). *Neuroradiology* 40:778–782
- Giacomuzzi SM, Torbica P, Rieger M, Lottersberger C, Peer S, Peer R, Perkmann R, Buchberger W, Bale R, Mallouhi A, Jaschke W (2001) Untersuchungen zur Strahlenexposition bei der Einzelschicht- und Mehrschicht-Spiral-CT (eine Phantom-Studie). *Fortschr Röntgenstr* 173:643–649
- Hounsfield G (1973b) Computerized transverse axial scanning (tomography, part 1). Description of the system. *Br J Radiol* 45: 1010–1022
- Hirai T, Korogi Y, Arimura H, Katsuragawa S, Kitajima M, Yamura M, Yamashita Y, Doi K (2005) Intracranial aneurysms at MR angiography: effect of computer-aided diagnosis on radiologists’ detection performance. *Radiology* 237:605–610
- Kachel R, Basche S, Heerklotz I, Grossmann K, Endler S (1991) Percutaneous transluminal angioplasty (PTA) of supra-aortic arteries especially the internal carotid artery. *Neuroradiology* 33:191–194
- Kurre W, Berkefeld J, Brassel F, Brüning R, Eckert B, Kamek S, Klein GE, Knauth M, Liebig T, Maskova J, Mucha D,

- Neumann-Haefelin T, Pilgram-Pastor S, Sitzler M, Sonnberger M, Tietke M, Trenkler J, Turowski B, INTRASTENT Study Group (2010 March) In-hospital complication rates after stent treatment of 388 symptomatic intracranial stenoses: results from the INTRASTENT multicentric registry. *Stroke* 41(3):494–498, Epub 2010 Jan 14
- Weber W, Mayer TE, Henkes H, Kis B, Hamann GF, Schulte-Altdorneburg G, Brückmann H, Kuehne D (2005a) Stent-angioplasty of intracranial vertebral and basilar artery stenoses in symptomatic patients. *Eur J Radiol* 55:231–236
- Lauterbur PC (1973) Image formation by induced local interactions: examples employing nuclear magnetic resonance. *Nature* 242:190–191
- Liu HM, Wang YH, Chen YF, Tu YK, Huang KM (2003) Endovascular treatment of brainstem arteriovenous malformations: safety and efficacy. *Neuroradiology* 45:644–649
- Livingstone RS, Raghuram L, Korah IP, Raj DV (2003) Evaluation of radiation risk and work practices dural cerebral interventions. *J Radiol Prot* 23:327–336
- Loewy J, Loewy A, Kendall EJ (2004) Reconsideration of pacemakers and MR imaging. *Radiographics* 24:1257–1267
- MacLennan AC, Hadley DM (1995) Radiation dose to the lens from computed tomography scanning in a neuroradiology department. *Br J Radiol* 68:19–22
- Molyneux A, Kerr R, Stratton I, Sandercock P, Clarke M, Shrimpton J, Holman R (2002) International subarachnoid aneurysm trial (ISAT) on neurosurgical clipping versus endovascular coiling in 2143 patients with ruptured intracranial aneurysms: a randomized trial. *Lancet* 360:1267–1274
- Pfefferkorn T, Mayer TE, Schulte-Altdorneburg G, Brückmann H, Hamann GF, Dichgans M (2006) Diagnosis and therapy of basilar artery occlusion. *Nervenarzt* 77:416–422
- Saatci I, Cekirge HS, Ozturk MH, Arat A, Ergungor F, Sekerci Z, Senveli E, Er U, Turkoglu S, Ozcan OE, Ozgen T (2004) Treatment of internal carotid artery aneurysms with a covered stent: experience in 24 patients with mid-term follow-up results. *Am J Neuroradiol* 25:1742–1749
- Saigal G, Bhatia R, Bhatia S, Wakhloo AK (2004) MR findings of cortical blindness following cerebral angiography: Is this entity related to posterior reversible leukoencephalopathy? *Am J Neuroradiol* 25:252–256
- Schonewille WJ, Algra A, Serena J, Molina CA, Kappelle LJ (2005) Outcome in patients with basilar artery occlusion treated conventionally. *J Neurol Neurosurg Psychiatry* 76:1238–1241
- Schonewille WJ, Wijman CA, Michel P, Rueckert CM, Weimar C, Mattle HP, Engelter ST, Tanne D, Muir KW, Molina CA, Thijs V, Audebert H, Pfefferkorn T, Szabo K, Lindsberg PJ, de Freitas G, Kappelle LJ, Algra A, BASICS study group (2009 Aug) Treatment and outcomes of acute basilar artery occlusion in the Basilar Artery International Cooperation Study (BASICS): a prospective registry study. *Lancet Neurol* 8(8):724–730, Epub 2009 Jul 3
- SSYLVA Study Investigators (2004) Stenting of symptomatic atherosclerotic lesions in the vertebral or intracranial arteries (SSYLVA). Study results. *Stroke* 35:1388–13392
- Szikora I (2004) Dural arteriovenous malformations. In: Forsting M (ed) *Intracranial vascular malformations and aneurysms. From diagnostic work-up to endovascular therapy*. Springer, Berlin, pp 101–141
- Schulte-Altdorneburg G, Liebig T, Brückmann H, Jansen O (2009 Dec) Treatment of basilar artery occlusion: a prospective randomised therapeutic study is needed. *Lancet Neurol* 8(12):1084–1085
- Pfefferkorn T, Mayer TE, Schulte-Altdorneburg G, Brückmann H, Hamann GF, Dichgans M (2005) Diagnostik und Therapie der Basilaristhrombose (Epub ahead of print)
- Tintera J, Gawehn J, Bauermann T, Vucurevic G, Stoeter P (2004) New partially parallel acquisition technique in cerebral imaging: preliminary findings. *Eur J Radiol* 14:2273–2281
- Vindlacheruvu RR, Mendelow AD, Mitchell P (2005) Risk-benefit analysis of the treatment of unruptured intracranial aneurysms. *J Neurol Neurosurg Psychiatry* 76:234–249
- Weber W, Mayer TE, Henkes H, Kis B, Hamann GF, Schulte-Altdorneburg G, Brückmann H, Kuehne D (2005) Stent-angioplasty of intracranial vertebral and basilar artery stenoses in symptomatic patients. *Eur J Radiol* 55:231–236
- Willinsky RA, Taylor S, terBrugge K, Farb RI, Tomlinson G, Montanera W (2003) Neurologic complications of cerebral angiography: prospective analysis of 2899 procedures and review of the literature. *Radiology* 227:522–528

2.2 “Ultrasound Diagnostics”

- Bartels E (1991) Duplexsonographie der Vertebralarterien, 1. Teil. Praktische Durchführung, Möglichkeiten und Grenzen der Methode, 2. Teil. Klinische Anwendungen. *Ultraschall Med* 12:54–69
- Becker G, Seufert J, Bogdahn U, Reichmann H, Reiners K (1995a) Degeneration of substantia nigra in chronic Parkinson's disease visualized by transcranial color-coded real-time sonography. *Neurology* 45:182–184
- Becker G, Becker T, Struck M, Lindner A, Burzer K, Retz W, Bogdahn U, Beckmann H (1995b) Reduced echogenicity of brainstem raphe specific to unipolar depression: a transcranial color-coded real-time sonography study. *Biol Psychiatry* 38:180–184
- Berg D, Supprian T, Hofmann E, Zeiler B, Jager A, Lange KW, Reiners K, Becker T, Becker G (1999a) Depression in Parkinson's disease: brainstem midline alteration on transcranial sonography and magnetic resonance imaging. *J Neurol* 246:1186–1193
- Berg D, Becker G, Zeiler B, Tucha O, Hofmann E, Preier M, Benz P, Jost W, Reiners K, Lange KW (1999b) Vulnerability of the nigrostriatal system as detected by transcranial ultrasound. *Neurology* 53:1026–1031
- Berg D, Siefker C, Ruprecht-Dorfler P, Becker G (2001a) Relationship of substantia nigra echogenicity and motor function in elderly subjects. *Neurology* 56:13–17
- Berg D, Siefker C, Becker G (2001b) Echogenicity of the substantia nigra in Parkinson's disease and its relation to clinical findings. *J Neurol* 8:684–689
- Brunner-Beeg F, von Reutern GM (1999) Farbduplexsonographie des intrakraniellen vertebrobasilären Systems: Verbesserung der Darstellung durch Echosignalverstärkung. *Ultraschall Med* 20:83–86
- Igleseder B, Huemer M, Staffen W, Ladurner G (2000) Imaging the basilar artery by contrast-enhanced color-coded ultrasound. *J Neuroimaging* 10:195–199
- Netuka D, Benes V, Mikulik R, Kuba R (2005) Symptomatic rotational occlusion of the vertebral artery. Case report and review of the literature. *Zentralbl Neurochir* 66:217–222
- Ringelstein EB, Koschorke B, Niggemeyer E, Otis SM (1990) Transcranial Doppler sonography: anatomical landmarks and normal velocity values. *Ultrasound Med Biol* 16:745–761
- Schweitzer K, Hilker R, Walter U, Burghaus L, Berg D (2006) Substantia nigra hyperechogenicity as a marker of predisposition and slower progression in Parkinson's disease. *Mov Disord* 21:94–98
- von Büdingen HJ, Staudacher T (1987) Die Identifizierung der Arteria basilaris mit der transkraniellen Doppler-Sonographie. *Ultraschall* 8:95–101
- Walter U, Niehaus L, Probst T, Benecke R, Meyer BU, Dressler D (2003) Brain parenchyma sonography discriminates Parkinson's disease and atypical parkinsonian syndromes. *Neurology* 60:74–77
- Walter U, Dressler D, Benecke R (2004) Hirnparenchym-Sonographie zur Früh- und Differenzialdiagnostik der Parkinson-Krankheit. *Akt Neurol* 31:325–332

- Walter U, Dressler D, Wolters A, Wittstock M, Greim B, Benecke R (2006a) Sonographic discrimination of dementia with Lewy bodies and Parkinson's disease with dementia. *J Neurol* 253:448–454
- Walter U, Morrissey L, Herpert S, Benecke R, Höppner J (2006b) Brainstem raphe echogenicity predicts response to selective serotonin reuptake inhibitors in depressive states: a transcranial sonography study. *Klin Neurophysiol* 37:97
- Widder B (1999) Verschlussprozesse im vertebrobasilären Gefäßsystem. In: Widder B (ed) *Doppler- und Duplexsonographie der hirnvorsorgenden Gefäße*. 5. Aufl. Springer, Berlin/Heidelberg/New York, pp 265–289
- Bremer T (1993) Der Eigenreflex des Musculus masseter: Erstellung der Normwerttabelle. Thesis, Mainz
- Cruccu G, Inghileri M, Fraioli B, Guidetti B, Manfredi M (1987a) Neurophysiologic assessment of trigeminal function after surgery for trigeminal neuralgia. *Neurology* 37:631–638
- Ferguson IT (1978) Electrical study of jaw and orbicularis oculi reflexes after trigeminal nerve surgery. *J Neurol Neurosurg Psychiatry* 41:819–823
- Fitzek S, Fitzek C, Hopf HC (2001) The masseter reflex: postprocessing methods and influence of age and gender. *Eur Neurol* 46:202–205
- Goodwill CJ (1968) The normal jaw reflex: measurement of the action potential in the masseter muscles. *Ann Phys Med* 9:183–188
- Görömbey Z, Csecsei G, Klug N (1986) Veränderungen des Masseter-Reflexes bei primären und sekundären Hirnstammschädigungen. In: Lowitzsch (Hrsg) *Hirnstammreflexe. Methodik und klinische Anwendung*. Thieme, Stuttgart, pp 204–210
- Hassler O (1967) Arterial pattern of human brainstem. Normal appearance and deformation in expanding supratentorial conditions. *Neurology* 17:368–375
- Hopf HC (1994) Topodiagnostic value of brainstem reflexes. *Muscle Nerve* 17:475–484
- Hopf HC, Gutmann L (1990) Diabetic 3rd nerve palsy: evidence for a mesencephalic lesion. *Neurology* 40:1041–1045
- Hopf HC, Hinrichs C, Stoeter P, Urban PP, Marx J, Thömke F (2000) Masseter reflex latencies and amplitudes are not influenced by supratentorial and cerebellar lesions. *Muscle Nerve* 23:86–89
- Kimura J, Rodnitzky RL, Van Allen MW (1970) Electrodiagnostic study of trigeminal nerve. Orbicularis oculi reflex and masseter reflex in trigeminal neuralgia, paratrigeminal syndrome, and other lesions of the trigeminal nerve. *Neurology* 20:574–583
- Koehler J, Schwarz M, Urban PP, Voth D, Hölker C, Hopf HC (2001) Masseter reflex and blink reflex abnormalities in Chiari II malformation. *Muscle Nerve* 24:425–427
- Krämer G, Bremer T, Hubrich P, Lüder G, Hopf HC (1992) Altersabhängige Normwerte des Masseter Reflexes. *Akt Neurol* 19: XVIII
- Lowitzsch K, Marzi I (1986) Multimodale Hirnstammreflexe in der Prognose des Koma. In: Lowitzsch (Hrsg) *Hirnstammreflexe. Methodik und klinische Anwendung*. Thieme, Stuttgart, pp 237–251
- Marx JJ, Mika-Grüttner A, Thömke F, Fitzek S, Fitzek C, Vucurevic G, Urban PP, Stoeter P, Hopf HC (2002) Electrophysiological brainstem testing in the diagnosis of reversible brainstem ischemia. *J Neurol* 249:1041–1047
- Mika-Grüttner A, Marx J, Thömke F, Fitzek S, Fitzek C, Urban PP, Stoeter P, Hopf HC (2001) Wertigkeit der Elektrophysiologie bei Hirnstammischämien und normalem diffusionsgewichteten und hochauflösenden MRT. *Klin Neurophysiol* 32:135–140
- Mika-Grüttner A, Thömke F, Marx JJ, Urban PP, Ringel K, Hopf HC (2002) Magnetic resonance imaging versus electrophysiological testing in internuclear ophthalmoplegia. *Mov Disord* 17:S92
- Nieuwenhuys R, Voogd J, van Huijzen C (1989) *The human central nervous system*, 3rd edn. Springer, Berlin
- Ongerboer de Visser BW, Goor C (1974) Electromyographic and reflex study in idiopathic and symptomatic trigeminal neuralgias: latency of the jaw and blink reflexes. *J Neurol Neurosurg Psychiatry* 37:1225–1230
- Thömke F (1999) Isolated cranial nerve palsies due to brainstem lesions. *Muscle Nerve* 22:1168–1176
- Thömke F (2003) Die elektrophysiologische Untersuchung des Masseter-Reflexes. Ableittechnik, klinischer Einsatz und topodiagnostische Bedeutung. *Klin Neurophysiol* 34:1–6
- Thömke F, Hopf HC (1999) Pontine lesions mimicking acute peripheral vestibulopathy. *J Neurol Neurosurg Psychiatry* 66: 340–349

2.3 “Electrophysiologic Diagnostics”

2.3.1 “Blink Reflex”

- Aramideh M, Ongerboer de Visser BW, Koelman JH, Majoie CB, Holstege G (1997) Late blink reflex response abnormality due to lesion of the lateral tegmental field. *Brain* 120:1685–1692
- Cruccu G, Iannetti GD, Marx JJ, Thömke F, Truini A, Fitzek S, Galeotti F, Urban PP, Romaniello A, Stoeter P, Manfredi M, Hopf HC (2005) Brainstem reflex circuits revisited. *Brain* 128:386–394
- Hopf HC (1994a) Topodiagnostic value of brainstem reflexes. *Muscle Nerve* 17:475–484
- Hopf HC, Thömke F, Gutman L (1991) Midbrain versus pontine medial longitudinal fasciculus lesions: the utilization of masseter and blink reflexes. *Muscle Nerve* 14:326–330
- Hopf HC, Ellrich J, Hundemer H (1992) The pterygoid reflex in man and its clinical application. *Muscle Nerve* 15:1278–1283
- Kimura J (1975) Electrically elicited blink reflex in diagnosis of multiple sclerosis. *Brain* 98:413–426
- Kimura J (1989) *Electrodiagnosis in diseases of nerve and muscle: principles and practices*. 2. Aufl. F.A. Davis, Philadelphia, pp 307–331
- Kugelberg E (1952) Facial reflexes. *Brain* 75:385–396
- Marx JJ, Thömke F, Fitzek S, Vucurevic G, Fitzek C, Mika-Grüttner A, Urban PP, Stoeter P, Hopf HC (2001) Topodiagnostic value of blink reflex R1 changes – a digital postprocessing MRI correlation study. *Muscle Nerve* 24:1327–1331
- Metha AJ, Seshia SS (1976) Orbicularis oculi reflex in brain death. *J Neurol Neurosurg Psychiatry* 39:784–787
- Ongerboer de Visser BW (1983) Anatomical and functional organisation of reflexes involving the trigeminal system in man: Jaw reflex, blink reflex, corneal reflex and exteroceptive suppression. *Adv Neurol* 39:729–738
- Rossi B, Pasca SL, Sartucci F, Siciliano G, Murri L (1989) Trigemino-cervical reflex in pathology of the brain stem and of the first cervical cord segments. *Electromyogr Clin Neurophysiol* 29:67–71
- Tackmann W, Ettlin T, Barth R (1982) Blink reflexes elicited by electrical, acoustic and visual stimuli. *Eur Neurol* 21:210–216
- Valls-Solé J, Graus F, Font J, Pou A, Tolosa ES (1990) Normal proprioceptive afferents in patients with Sjögren's syndrome and sensory neuropathy. *Ann Neurol* 28:786–790

2.3.2 “Masseter Reflex”

- Ben Ghezala K, Hundemer HP, Koehler J, Urban PP, Connemann B, Hopf HC (1996) The variance of masseter reflex (MassR) latencies and amplitudes with different recording techniques and follow-up with weekly intervals. *Electroencephal Clin Neurophysiol* 99:334

- Thömke F, Gutmann L, Stoeter P, Hopf HC (2002) Cerebrovascular brainstem diseases with isolated cranial nerve palsies. *Cerebrovasc Dis* 13:147–155
- Yates SK, Brown WF (1981) The human jaw jerk: electrophysiologic methods to measure latency, normal values and changes in multiple sclerosis. *Neurology* 31:632–634

2.3.3 “Early Acoustic Evoked Potentials”

- Bassetti C, Mathis J, Hess CW (1994a) Multimodal electrophysiological studies including motor evoked potentials in patients with locked-in syndrome: report of six patients. *J Neurol Neurosurg Psychiatry* 57:1403–1406
- Buchner H (2000) Frühe akustisch evozierte Potentiale (FAEP). In: Lowitzsch K, Hopf HC, Buchner H, Claus D, Jörg J, Rappelsberger P, Tackmann W (eds) *Das EP-Buch*. Thieme, Stuttgart
- Chia L-G, Shen W-C (1993) Wallenberg’s lateral medullary syndrome with loss of pain and temperature sensation on the contralateral face: clinical, MRI and electrophysiological studies. *J Neurol* 240:462–467
- Chiappa KH (ed) (1997) *Evoked potentials in clinical medicine*, 3rd edn. Lippincott-Raven, Philadelphia
- Cho T-H, Fischer C, Nighoghossian N, Hermier M, Sindou M, Maugière F (2005) Auditory and electrophysiological patterns of a unilateral lesion of the lateral lemniscus. *Audiol Neurotol* 10:153–158
- Druilovic B, Ribaric-Jankes K, Kostic VS, Sternic N (1993) Sudden hearing loss as the initial monosymptom of multiple sclerosis. *Neurology* 43:2703–2705
- Egan CA, Davies L, Halmagyi GM (1996) Bilateral total deafness due to pontine haematoma. *J Neurol Neurosurg Psychiatry* 61:628–631
- Ferber A, Buchner H, Brückmann H (1990a) Brainstem auditory evoked potentials and somatosensory evoked potentials in pontine haemorrhage. *Brain* 113:49–63
- Fischer C, Bognar L, Turjman F, Lapras C (1995) Auditory evoked potentials in a patient with a unilateral lesion of the inferior colliculus and medial geniculate body. *Electroencephal Clin Neurophysiol* 96:261–267
- Friedli WG, Fuhr P (1990) Electrocutaneous reflexes and multimodality evoked potentials in multiple sclerosis. *J Neurol Neurosurg Psych* 53:391–397
- Hammond SR, Yiannikas C, Chan YW (1986) A comparison of brainstem auditory evoked responses evoked by rarefaction and condensation stimulation in control subjects and in patients with Wernicke-Korsakoff syndrome and multiple sclerosis. *J Neurol Sci* 74:177–190
- Häusler R, Levine RA (2000) Auditory dysfunction in stroke. *Acta Oto-Laryngol* 120:689–703
- Hoistad DL, Hain TC (2003) Central hearing loss with a bilateral inferior colliculus lesion. *Audiol Neurotol* 8:111–113
- Kaga K, Shinoda Y, Suzuki JI (1997) Origin of auditory brainstem responses in cats: whole brainstem mapping, and a lesion and HRP study of the inferior colliculus. *Acta Otolaryngol* 117:197–201
- Krieger D, Adams H-P, Rieke K, Hacke W (1993) Monitoring therapeutic efficacy of decompressive craniotomy in space occupying cerebellar infarcts using brainstem auditory evoked potentials. *Electroencephal Clin Neurophysiol* 88:261–270
- Lee H, Ahn B-H, Baloh RW (2004) Sudden deafness with vertigo as a sole manifestation of anterior inferior cerebellar artery infarction. *J Neurol Sci* 222:105–107
- Levine RA, Gardner JC, Fullerton BC, Stufferbeam SM, Carlisle EW, Furst M, Rosen BR, Kiang NYS (1993) Effects of multiple sclerosis brainstem lesions on sound lateralization and brainstem auditory evoked potentials. *Hear Res* 68:73–88

- Lopez-Escamez JA, Salguero G, Salinero J (1999) Age and sex differences in latencies of waves I, III and V in auditory brainstem responses of normal hearing subjects. *Acta Otorhinolaryngol Belg* 53:109–115
- Markand ON (1994) Brainstem auditory evoked potentials. *J Clin Neurophysiol* 11: 319–342
- Martin WH, Pratt H, Schwegler JW (1995) The origin of the human auditory brainstem response wave II. *Electroencephal Clin Neurophysiol* 96:357–370
- Maurer K (1985) Uncertainties of topodiagnosis of auditory nerve and brainstem auditory evoked potentials due to rarefaction and condensation stimuli. *Electroencephal Clin Neurophysiol* 62: 135–140
- Pratt H, Aminoff M, Nuwer MR, Starr A (1999) Short-latency auditory evoked potentials. *Electroencephal Clin Neurophysiol* 52:69–77
- Scientific committee BÄK (1998) Richtlinien zur Feststellung des Hirntodes. Dritte Fortschreibung 1997. *Dtsch Ärztebl* 95: 1509–1516
- Vitte E, Tankere F, Bernat I, Zouaoui A, Lamas G, Soudant J (2002) Midbrain deafness with normal brainstem auditory evoked potentials. *Neurology* 58:970–973

2.3.4 “Vestibulocollic Reflex”

- Baier B, Dieterich M (2009) Vestibular-evoked myogenic potentials in “vestibular migraine” and Menière’s Disease. A sign of an electrophysiological link? *Ann NY Acad Sci* 1164:324–327
- Baier B, Stieber N, Dieterich M (2009) Vestibular evoked myogenic potentials in “vestibular” migraine. *J Neurol* (256; 1447–54)
- Bandini F, Beronio A, Ghiglione E, Solaro C, Parodi RC, Mazzella L (2004) The diagnostic value of vestibular evoked myogenic potentials in multiple sclerosis. *J Neurol* 251:621–671
- Basta D, Todt I, Ernst A (2005) Normative data for P1/N1-latencies of vestibular evoked myogenic potentials induced by air- or bone-conducted tone bursts. *Clin Neurophysiol* 116: 2216–2219
- Chen CH, Young YH (2003) Vestibular evoked myogenic potentials in brainstem stroke. *Laryngoscope* 113:990–993
- Chen CW, Young YH, Wu CH (2000) Vestibular neuritis: three-dimensional videonystagmography and vestibular evoked potential results. *Acta Otolaryngol* 120:845–848
- Colebatch JG, Halmagyi GM (2000) Vestibular evoked myogenic potentials in humans. *Acta Otolaryngol* 120:12
- De Waele C, Tran Ba Huy P, Diard JP, Freyss G, Vidal PP (1999) Saccular dysfunction in Menière’s patients. A vestibular-evoked myogenic potential study. *Ann NY Acad Sci* 871:205–208
- Heide G, Freitag S, Wollenberg I, Ivo H, Schimrigk K, Dillmann U (1999) Click evoked myogenic potentials in the differential diagnosis of vertigo. *J Neurol Neurosurg Psychiatry* 66: 787–790
- Itoh A, Kim YS, Yoshioka K, Yoshioka K, Kanaya M, Enomoto H, Hiraiwa F, Mizuno M (2001) Clinical study of vestibular-evoked myogenic potentials and auditory brainstem responses in patients with brainstem lesions. *Acta Otolaryngol* 545(Suppl): 116–119
- Lim CL, Clouston P, Sheean G, Yiannikas C (1995) The influence of voluntary EMG activity and click intensity on the vestibular click evoked potential. *Muscle Nerve* 18:1210–1213
- Minor LB, Cremer PD, Carey JP, Della Santana CC, Streubel SO, Weg N (2001) Symptoms and signs in superior canal dehiscence syndrome. *Ann NY Acad Sci* 942:259–273
- Murofushi T, Halmagyi GM, Yavor RA, Colebatch JG (1996) Absent vestibular evoked myogenic potentials in vestibular

- neurlabyrinthitis. An indicator of inferior vestibular nerve involvement? *Arch Otolaryngol Head Neck Surg* 122:845–818
- Murofushi T, Shimizu K, Takegoshi H, Cheng PW (2001) Diagnostic value of prolonged latencies in the vestibular evoked myogenic potential. *Arch Otolaryngol Head Neck Surg* 127: 1069–1072
- Ochi K, Ohashi T, Watanabe S (2003) Vestibular-evoked myogenic potential in patients with unilateral vestibular neuritis: abnormal VEMP and ist recovery. *J Laryngol Otol* 117:104–108
- Patko T, Vidal PP, Vibert N, Tran Ba Huy P, de Waele C (2003) Vestibular evoked myogenic potentials in patients suffering from an unilateral acoustic neurinoma: a study of 170 patients. *Clin Neurophysiol* 114:1344–1350
- Sartucci F, Logi F (2002) Vestibular-evoked myogenic potentials: a method to assess vestibulo-spinal conduction in multiple sclerosis. *Brain Res Bull* 59:59–63
- Versino M, Colnaghi S, Callieco R, Bergamaschi R, Romani A, Cosi V (2002) Vestibular evoked myogenic potential in multiple sclerosis patients. *Clin Neurophysiol* 113:1464–1469
- Watson SR, Halmagyi GM, Colebatch JG (2000) Vestibular hypersensitivity to sound (Tullio phenomenon): structural and functional assessment. *Neurology* 54:722–728
- Welgampola MS, Colebatch JG (2001) Vestibulocollic reflexes: normal values and the effect of age. *Clin Neurophysiol* 112: 1971–1979
- Welgampola MS, Colebatch JG (2005) Characteristics and application of vestibular-evoked myogenic potentials. *Neurology* 64: 1682–1688
- Zingler V, Weintz E, Jahn K, Bötzel K, Wagner J, Huppert D, Mike A, Brandt T, Strupp M (2008) Sacular function less affected than canal function in bilateral vestibulopathy. *J Neurol* 255: 1332–1336
- Göbel H, Krapat S, Dworschak M, Heuss D, Ensink FBM, Soyka D (1994) Exteroceptive suppression of temporalis muscle activity during migraine attack and migraine interval before and after treatment with sumatriptan. *Cephalalgia* 14:143–148
- Godeaux E, Desmedt JE (1975) Exteroceptive suppression and motor control of the masseter and temporalis muscles in normal man. *Brain Res* 85:447–458
- Goldberg LJ (1972) Excitatory and inhibitory effects of lingual nerve stimulation on reflexes controlling the activity of masseteric motoneurons. *Brain Res* 39:95–108
- Keidel M, Rieschke P, Jüptner M, Diener HC (1994) Pathologischer Kieferöffnungsreflex nach HWS-Beschleunigungsverletzung. *Nervenarzt* 65:241–249
- Kimura J, Daube J, Burke D, Hallett M, Cruccu G, de Visser BW, Ongerboer, Yanagisawa N, Shimamura M, Rothwell J (1994) Human reflexes and late responses. Report of an IFCN committee. *Electroencephal Clin Neurophysiol* 90:393–403
- Liepert J, Tegenthoff M, Malin J-P (1993) Die exteropezeptive Suppression der Aktivität des M. temporalis bei Hemiparesen nach akuten vaskulären Insulten. *Z EEG-EMG* 24:174–177
- Meier-Ewert K, Gleitsmann K, Reiter F (1974) Acoustic jaw reflex in man: its relationship to other brain-stem and microreflexes. *Electroencephal Clin Neurophysiol* 36:629–637
- Mizuno N, Konishi A (1975) An electron microscope study of supratrigeminal fibers to two motor nucleus of the trigeminal nerve. *Anat Rec* 181:538
- Nakamura Y, Mori S, Nagashima H (1973) Origin and central pathways of crossed inhibitory effects of afferents from the masseteric muscle on the masseteric motoneuron of the cat. *Brain Res* 57:29–42
- Ongerboer de Visser BE, Cruccu G (1993) The masseter inhibitory reflex in pontine lesions. In: Caplan LR, Hopf HC (eds) *Brainstem localization and function*. Springer, Berlin/Heidelberg, pp 199–206
- Ongerboer de Visser BW, Cruccu G, Manfredi M, Koelman JHTM (1989) Effects of brainstem lesions on the masseter inhibitory reflex. *Brain* 113:781–792
- Schoenen J, Jamart B, Gerard P, Lenarduzzi P, Delwaide PJ (1987) Exteroceptive suppression of temporalis muscle activity in chronic headache. *Neurology* 37:1834–1836
- Urban PP, Hopf HC (1992) Masseter-Innervationspausen (silent periods) nach Stimulation des N. medianus, Plexus cervicalis und N. mentalis. *Z EEG-EMG* 23:48–52
- Urban PP, Lüttkopf V, Hopf HC (1999a) Methodische Aspekte und diagnostische Anwendungen der exterozeptiven Suppression der Kaumuskelaktivität. *EEG-Labor* 21:49–64
- Valls-Solé J, Vila N, Obach V, Alvarez R, González LE, Chamorro A (1996) Brain stem reflexes in patients with Wallenberg's syndrome: correlation with clinical and magnetic resonance imaging (MRI) findings. *Muscle Nerve* 19:1093–1099
- Bendtsen L, Jensen R, Olesen J (1996) Amytrytiline, a combined serotonin and noradrenaline re-uptake inhibitor, reduces exteroceptive suppression of temporal muscle activity in patients with chronic tension-type headache. *Electroencephal Clin Neurophysiol* 101: 418–422
- Connemann BJ, Urban PP, Lüttkopf V, Hopf HC (1997) A fully automated system for the evaluation of masseter silent periods. *Electroencephal Clin Neurophysiol* 105:53–57
- Cruccu G, Inghileri M, Fraioli B, Guidetti B, Manfredi M (1987) Neurophysiologic assessment of trigeminal function after surgery for trigeminal neuralgia. *Neurology* 37: 631–638
- Cruccu G, Fornarelli M, Manfredi M (1988) Impairment of masticatory function in hemiplegia. *Neurology* 38:301–306
- Ellrich J, Hopf HC, Treede R-D (1997) Nociceptive masseter inhibitory reflexes evoked by laser radiant heat and electrical stimuli. *Brain Res* 764:214–220
- Göbel H (1996) *Die Kopfschmerzen. Ursache, Mechanismen, Diagnostik und Therapie in der Praxis*. Springer, Berlin/Heidelberg /New York
- Göbel H, Dworschak M (1996) Die exterozeptive Suppression der Aktivität des M. temporalis. *Nervenarzt* 67:846–859
- Göbel H, Schoenen J (1993) Exteroceptive suppression in headache research. *Cephalalgia* 13:20
- Göbel H, Ernst M, Jeschke J, Weigle L (1992) Acetylsalicylic acid activates antinociceptive brainstem reflex activity in headache patients and in healthy subjects. *Pain* 48:187–195
- Besser R, Dillmann U, Henn M (1988) Somatosensory evoked potentials aiding the diagnosis of brain death. *Neurosurg Rev* 11:171–175
- Buchner H, Ferbert A, Hacke W (1988) Serial recordings of median nerve stimulated subcortical somatosensory evoked potentials (SEPs) in developing brain death. *Electroencephalogr Clin Neurophysiol* 69:14–23
- Christophis P (2004) The prognostic value of somatosensory evoked potentials in traumatic primary and secondary brain stem lesions. *Zentralbl Neurochir* 65:25–31

2.3.5 “Exteroceptive Suppression of Masticatory Muscle Activity”

2.3.6 “Somatosensory Evoked Potentials”

- Claß R, Buettner UW (1993) Correlation of somatosensory evoked potentials and somatosensory findings in patients with brainstem lesions. In: Caplan LR, Hopf HC (eds) *Brainstem localization and function*. Springer, Heidelberg, pp 161–164
- Dillmann U, Besser R, Eghbal R, Koehler J, Ludwig B (1990) SEP and MRI findings in patients with localized brainstem lesions. *Electroencephalogr Clin Neurophysiol* 41:314–319
- Ferbert A, Buchner H, Brückmann H, Zeumer H, Hacke W (1988) Evoked potentials in basilar artery thrombosis: correlation with clinical and angiographic findings. *Electroencephalogr Clin Neurophysiol* 69:136–147
- Ferbert A, Buchner H, Brückmann H (1990) Brainstem auditory evoked potentials and somatosensory evoked potentials in pontine haemorrhage. *Brain* 113:49–63
- Jacobson GP, Tew JM (1988) The origin of the scalp recorded P14 following electrical stimulation of the median nerve: intraoperative observations. *Electroencephalogr Clin Neurophysiol* 71:73–76
- Koehler J, Besser R, Stoeter P, Urban PP, Hopf HC (2000) Scalp, basal epidural and intravascular far field recordings after median nerve stimulation: evidence for a separate N18a potential. *Somatosens Mot Res* 17:239–243
- Lueders H, Lesser R, Hahn J, Little J, Klem G (1983) Subcortical somatosensory evoked potentials to median nerve stimulation. *Brain* 106:341–372
- Manzano GM, Schultz RR, Barsottini OG, Zukerman E, Nobrega JA (1999) Median nerve SEP after a high medullary lesion. Preserved N18 and absent P14 components. *Arq Neuropsiquiatr* 57: 292–295
- Maugière F, Allison T, Babiloni C, Buchner H, Eisen AA, Goodin DS, Jones SJ, Kagigi R, Matsuoka S, Nuwer M, Rossini PM, Shibasaki H (1999) Somatosensory evoked potentials. *Electroencephalogr Clin Neurophysiol (Suppl)*:52
- Noel P, Ozaki I, Desmedt JE (1996) Origin of N18 and P14 far-fields of median nerve somatosensory evoked potentials studied in patients with a brainstem lesion. *Electroencephalogr Clin Neurophysiol* 98:167–170
- Raroque HG, Batjer H, White C, Bell WL, Bowman G, Greenlee R (1994) Lower brainstem origin of the median nerve N18 potential. *Electroencephalogr Clin Neurophysiol* 90:170–172
- Sonoo M, Sakuta M, Shimo T, Genba K, Mannen T (1991) Widespread N18 in median nerve SEP is preserved in a pontine lesion. *Electroencephalogr Clin Neurophysiol* 80:238–240
- Sonoo M, Genba K, Zai W, Iwata M, Mannen T, Kanazawa J (1992) Origin of the widespread N18 in median nerve SEP. *Electroencephalogr Clin Neurophysiol* 84:418–425
- Sonoo M, Hagiwara H, Motoyoshi Y, Shimizu T (1996) Preserved widespread N18 and progressive loss of P13/14 of median nerve SEPs in a patient with unilateral medial medullary syndrome. *Electroencephalogr Clin Neurophysiol* 100:488–492
- Sonoo M, Tsai-Shozawa Y, Aoki M, Nakatani T, Hatanaka Y, Mochizuki A, Sawada M, Kobayashi K, Shimizu T (1999) N18 in median somatosensory evoked potentials: a new indicator of medullary function useful for the diagnosis of brain death. *J Neurol Neurosurg Psychiatry* 67:374–378
- Stöhr M, Petrucci F, Scheglmann K (1981) Somatosensory evoked potentials following trigeminal nerve stimulation in trigeminal neuralgia. *Ann Neurol* 9:63–66
- Stöhr M, Riffel B, Ullrich A (1987) Short latency somatosensory evoked potentials in brain death. *J Neurol* 234:211–214
- Tackmann W (2000) Somatosensorisch evozierte Potentiale. In: Lowitzsch K, Hopf HC, Buchner H, Claus D, Jörg J, Rappelsberger P, Tackmann W (eds) *Das EP-Buch*. Thieme, Stuttgart, pp 127–172
- Wagner W (1996) Scalp, earlobe and nasopharyngeal recordings of the median nerve somatosensory evoked P14 potential in coma and brain death: detailed latency and amplitude analysis in 181 patients. *Brain* 119:1507–1521
- Wissenschaftlicher Beirat der Bundesärztekammer (1998) Richtlinien zur Feststellung des Hirntodes. Dritte Fortschreibung 1997. *Dtsch Arztebl* 95:1509–1516
- ### 2.3.7 “Transcranial Magnetic Stimulation”
- Bassetti C, Mathis J, Hess CW (1994) Multimodal electrophysiological studies including motor evoked potentials in patients with locked-in syndrome: report of six patients. *J Neurol Neurosurg Psychiatry* 57:1403–1406
- Escudero JV, Sancho J, Bautista D, Escudero M, Lopez-Trigo J (1998) Prognostic value of motor evoked potential obtained by transcranial magnetic brain stimulation in motor function recovery in patients with acute ischemic stroke. *Stroke* 29:1854–1859
- Ferbert A, Vielhaber S, Meincke U, Buchner H (1992) Transcranial magnetic stimulation in pontine infarction: correlation to degree of paresis. *J Neurol Neurosurg Psychiatry* 55:294–299
- Fischer U, Hess CW, Rösler KM (2005) Uncrossed cortico-muscular projections in humans are abundant to facial muscles of the upper and lower face, but may differ between sexes. *J Neurol* 252: 21–26
- Meyer BU (ed) (1992) *Die Magnetstimulation des Nervensystems*. Springer, Heidelberg
- Morecraft RJ, Louie JL, Herrick JL, Stilwell-Morecraft KS (2001) Cortical innervation of the facial nucleus in the non-human primate: a new interpretation of the effects of stroke and related subtotal brain trauma on the muscles of facial expression. *Brain* 124: 176–208
- Redmond MD, Di Benedetto M (1988) Hypoglossal nerve conduction in normal subjects. *Muscle Nerve* 11:447–452
- Riepe M, Ludolph AC (1993) Untersuchungen kortikobulbärer Bahnen und peripherer Hirnnerven bei Normalpersonen und Patienten mit multipler Sklerose: Ergebnisse nach nichtinvasiver elektromagnetischer Reizung. *Z EEG EMG* 24:269–273
- Rösler KM, Hess CW, Schmid UD (1989) Investigation of facial motor pathways by electrical and magnetic stimulation: sites and mechanisms of excitation. *J Neurol Neurosurg Psychiatry* 52: 1149–1156
- Schmid UD, Moller AR, Schmid J (1991) Transcranial magnetic stimulation excites the labyrinthine segment of the facial nerve: an intraoperative electrophysiological study in man. *Neurosci Lett* 124:273–276
- Schwarz S, Hacke W, Schwab S (2000) Magnetic evoked potentials in neurocritical care patients with acute brainstem lesions. *J Neurol Sci* 172:30–37
- Trompetto C, Assini A, Buccolieri A, Marchese R, Abbruzzese G (2000) Motor recovery following stroke: a transcranial magnetic stimulation study. *Clin Neurophysiol* 111:1860–1867
- Truffert A, Rösler KM, Magistris MR (2000) Amyotrophic lateral sclerosis versus cervical spondylotic myelopathy: a study using transcranial magnetic stimulation with recordings from the trapezius and limb muscles. *Clin Neurophysiol* 111:1031–1038
- Urban PP (2002) Vergleichende Untersuchung elektrisch und magnetisch evozierter Potentiale aus unterschiedlichen Fazialis-innervierten Muskeln. *Klin Neurophysiol* 33:A27
- Urban PP, Hopf HC (2002) Verlauf kortiko-fazialer und kortikolinguale Projektionen im Hirnstamm des Menschen. In: Bohl J (ed) *Neuropathology*. Shaker, Aachen, pp 1–18
- Urban PP, Heimgärtner I, Hopf HC (1994) Transkranielle Stimulation der Zungenmuskulatur bei Gesunden und Patienten mit Encephalomyelitis disseminata. *Z EEG EMG* 25:254–258
- Urban PP, Hopf HC, Connemann B, Hundemer HP, Koehler J (1996) The course of cortico-hypoglossal projections in the human brainstem. Functional testing using transcranial magnetic stimulation. *Brain* 119:1031–1038
- Urban PP, Beer S, Hopf HC (1997a) Cortico-bulbar fibers to orofacial muscles: recordings with enoral surface electrodes. *Electroencephalogr Clin Neurophysiol* 105:8–14
- Urban PP, Hopf HC, Fleischer S, Zorowka PG, Müller-Forell W (1997b) Impaired cortico-bulbar tract function in dysarthria due to hemispheric stroke. *Brain* 120:1077–1084
- Urban PP, Connemann B, Hundemer HP, Koehler J, Hopf HC (1997c) Technical considerations of electromyographic tongue muscle

- recordings using transcranial magnetic stimulation (letter). *Brain* 120:1911–1914
- Urban PP, Vogt T, Hopf HC (1998a) Corticobulbar tract involvement in amyotrophic lateral sclerosis. A transcranial magnetic stimulation study. *Brain* 121:1099–1108
- Urban PP, Wicht S, Marx J, Mitrovic S, Fitzek C, Hopf HC (1998b) Isolated voluntary facial paresis due to pontine ischemia. *Neurology* 50:1859–1862
- Urban PP, Wicht S, Fitzek S, Marx J, Thömke F, Fitzek C, Hopf HC (1999b) Ipsilateral facial weakness in upper medullary infarction-supranuclear or infranuclear origin? *J Neurol* 246:798–801
- Urban PP, Wicht S, Hopf HC, Fleischer S, Nickel O (1999c) Isolated dysarthria due to extracerebellar lacunar stroke: a central monoparesis of the tongue. *J Neurol Neurosurg Psychiatry* 66:495–501
- Urban PP, Wicht S, Vukurevic G, Fitzek C, Stoeter P, Massinger C, Hopf HC (2001a) Dysarthria in ischemic stroke – Localization and etiology. *Neurology* 56:1021–1027
- Urban PP, Wicht S, Vucorevic G et al (2001b) The course of corticofacial projections in the human brainstem. *Brain* 124:1866–1876
- Urban PP, Wicht S, Hopf HC (2001c) Sensitivity of transcranial magnetic stimulation of cortico-bulbar vs. cortico-spinal tract involvement in amyotrophic lateral sclerosis (ALS). *J Neurol* 248:850–855
- Visbeck A, Urban PP, Klimpe S, Wicht S, Hopf HC (2000) Funktion der kortikobulbären und kortikospinalen Projektionen bei hereditärer spastischer Spinalparalyse. *Klin Neurophysiol* 31: 190
- Weber M, Eisen AA (2002) Magnetic stimulation of the central and peripheral nervous system. *Muscle Nerve* 25:160–175
- Yamashita M, Yamamoto T (2001) Aberrant pyramidal tract in the medial lemniscus of the human brainstem: normal distribution and pathological changes. *Eur Neurol* 45:75–82
- 2.3.8 “Laser-Evoked Potentials”**
- Beydoun A, Morrow TJ, Shen JF, Casey KL (1993) Variability of laser-evoked potentials attention, arousal and lateralized differences. *Electroencephalogr Clin Neurophysiol* 88:173
- Cruccu G, Pennisi E, Truini A, Ianetti GD, Romaniello A, Le Pera D, De Armas L, Leandri M, Manfredi M, Valeriani M (2003) Unmyelinated trigeminal pathways as assessed by laser stimuli in humans. *Brain* 126:2246–2256
- Hansen C, Treede RD (1995) Laser-evozierte Potentiale: eine neue klinisch neurophysiologische Untersuchungsmethode für die Schmerzbahnen. *EEG Labor* 17:76–85
- Hansen HC, Treede RD, Lorenz J, Kunze K, Bromm B (1996) Recovery from brainstem lesions involving the nociceptive pathways: comparison of clinical findings with laser-evoked potentials. *J Clin Neurophysiol* 13:330–338
- Kakigi R, Shibasaki H, Kuroda Y, Neshige R, Endo C, Tabuchi K, Kishikawa T (1991) Pain-related somatosensory evoked potentials in syringomyelia. *Brain* 114:1871–1889
- Kanda M, Mima T, Xu X, Fujiwara N, Shindo K, Nagamine T, Ikeda A, Shibasaki H (1996) Pain-related somatosensory evoked potentials can quantitatively evaluate hypalgesia in Wallenberg’s syndrome. *Acta Neurol Scand* 94:131–136
- Treede RD (1996) Funktionsprüfung nozizeptiver Bahnen durch SEP nach schmerzhaften Laser-Reizen. *Z EEG EMG* 27:16–18
- Treede RD, Lankers J, Frieling A, Zangemeister WH, Kunze K, Bromm B (1991) Cerebral potentials evoked by painful laser stimuli in patients with syringomyelia. *Brain* 114:1595–1607
- Treede RD, Lorenz J, Baumgärtner U (2003) Clinical usefulness of laser-evoked potentials. *Neurophysiol Clin* 33:303–314
- Urban PP, Hansen C, Baumgärtner U, Fitzek S, Marx J, Fitzek C, Treede RD, Hopf HC (1999d) Abolished laser-evoked potentials and normal blink reflex in midlateral medullary infarction. *J Neurol* 246:347–352
- 2.3.9 “Recording of Eye Movements”**
- Leigh RJ, Zee DS (2006) Method available for measuring eye movements. In: *The neurology of eye movements*. Oxford University Press, New York, pp 722–725
- Robinson DA (1963) A new method of measuring eye movement using a scleral search coil in a magnetic field. *IEEE Trans Biomed Engng* 10:137–145
- Rottach K, Heide W (1998) Elektrookulographie. In: Huber A, Kömpf D (eds) *Klinische Neuroophthalmologie*. Thieme, Stuttgart, pp 191–199
- 2.3.10 “Other Electrophysiologic Methods for the Investigation of Brainstem Reflexes”**
- Di Lazzaro V, Restuccia D, Nardone R, Tartaglione T, Quartarone A, Tonali P, Rothwell JC (1996) Preliminary clinical observations on a new trigeminal reflex: the trigemino-cervical reflex. *Neurology* 46:479–485
- Ertekin C, Celebisoy N, Uludag B (2001) Trigemino-cervical reflexes elicited by stimulation of the infraorbital nerve: head retraction reflex. *J Clin Neurophysiol* 18:378–385
- Lehnhardt E (1993) The stapedial reflex in pontine lesions. In: Caplan LR, Hopf HC (eds) *Brainstem localization and function*. Springer, Heidelberg, pp 243–250
- Rossi B, Pasca SL, Sartucci F, Siciliano G, Murri L (1989) Trigemino-cervical reflex in pathology of the brain stem and of the first cervical cord segments. *Electromyogr Clin Neurophysiol* 29:67–71
- Sartucci F, Rossi A, Rossi B (1986) Trigemino cervical reflex in man. *Electromyogr Clin Neurophysiol* 26:123–129
- Serrao M, Rossi P, Parisi L, Perrotta A, Bartolo M, Cardinali P, Amabile G, Pierelli F (2003) Trigemino-cervical-spinal reflexes in humans. *Clin Neurophysiol* 114:1697–1703
- Tomioka S, Nakajo N, Takata M (1999) Inhibition of styloglossus motoneurons during the palatally induced jaw-closing reflex. *Neuroscience* 92:353–360
- Urban PP, Pittermann P, Kirchhoff I, Wahlmann U, Dieterich M (2005) Trigemino-hypoglossal silent period-a new pontomedullary brainstem reflex. *J Neurol* 252:13
- Wartenberg R (1941) Head retraction reflex. *Am J Msc* 201:553
- Zhang J, Pendlebury W, Luo P (2003) Synaptic organization of monosynaptic connections from mesencephalic trigeminal nucleus neurons to hypoglossal motoneurons in the rat. *Synapse* 49:157–169



<http://www.springer.com/978-3-642-04202-7>

Brainstem Disorders

Urban, P.P.; Caplan, L.R. (Eds.)

2011, XII, 363 p., Hardcover

ISBN: 978-3-642-04202-7